Master's thesis

NTNU
Norwegian University of Science and Technology
Faculty of Natural Sciences
Department of Biotechnology and Food Science

Malin Stubban Berg

Bacterial community structures and dynamics in host and built environments of Arctic charr (*Salvelinus alpinus*) aquacultured in RAS and FTS

Master's thesis in Biotechnology (MBIOT5)
Supervisor: Olav Vadstein
Co-supervisor: Deni Ribičić
August 2022

NTNU
Norwegian University of Science and Technology

SINTEF

Malin Stubban Berg

Bacterial community structures and dynamics in host and built environments of Arctic charr (*Salvelinus alpinus*) aquacultured in RAS and FTS

Master's thesis in Biotechnology (MBIOT5)
Supervisor: Olav Vadstein
Co-supervisor: Deni Ribičić
August 2022

Norwegian University of Science and Technology
Faculty of Natural Sciences
Department of Biotechnology and Food Science

NTNU
Norwegian University of
Science and Technology

Abstract

Recirculating aquaculture systems (RAS) are receiving increased attention in the production of salmonids. The water is recirculated in a RAS, compared to flow-through systems (FTS) where constant supply of new water is needed. Farming of Arctic charr (*Salvelinus alpinus*) is still in its infantry, and the prior knowledge of rearing of other salmonids such as Atlantic salmon and rainbow trout is, therefore, crucial. Microbial communities are important determinants of water quality by for example participating in water purification processes. Since the fish is in constant contact with its surrounding water, knowledge of microbes present on mucosal surfaces such as the skin, gill, and gut of the fish is important for maintaining optimal fish health. The mucus is the first line of defense from its surrounding environment, and it can harbor both commensal and/or opportunistic bacteria. However, knowledge on how the bacterial communities in the environment affect the mucosal surfaces in farmed fish is limited.

This study aimed to characterize and monitor the microbial communities in host mucus and the rearing environment of Arctic charr in a commercial land-based aquaculture facility. To study the microbial communities, samples for microbial community analysis were collected monthly over a period of 6 months from the skin, gill, and gut mucus, as well as intake and tank water, biofilm in tank and biofilter. A total of 432 samples, from a facility employing both RAS and FTS, were subjected to DNA-extraction, quantification, quality control and 16S rRNA gene amplicon sequencing employing Illumina methodology. Bioinformatic processing of the sequenced data was performed using QIIME2 and corresponding statistical analyses were executed in R for systematic spatiotemporal microbiome profiling in mucosal surfaces and environments of the farmed fish.

Through investigation of alpha diversity, skin samples were found to have the highest alpha diversity measures of the fish samples throughout the three monitored production systems in the facility. However, the built environment samples displayed overall higher values for observed and estimated richness, and higher Shannon's diversity index than the fish samples. The intake water displayed significantly higher richness and Shannon diversity than both fish and built environment samples. On ASV level, significant differences were found in microbial composition between fish samples, and between environment samples. Furter, there were also found significant differences in microbial composition of fish samples between the two RAS and the FTS. Built environment samples were found to be significantly different in microbial composition between the three systems.

Even though no significant temporal differences were found throughout the sampling period for alpha diversity measures, significant differences in microbial composition were found between sampling months in the fish samples. No significant temporal changes were found for environment samples.

The most prominent taxonomic genus in skin and gill mucus was *Pseudomonas*, whereas *Mycoplasma* was the most prominent genus across gut mucus. *Flavobacterium* was the most dominant genus in tank water and biofilter biofilm, while *Arcicella* dominated in tank biofilm, and *Crenothrix* in the source water. However, individual differences were found between the three different production systems.

This thesis has provided significant knowledge on bacterial communities in farming of Arctic charr, and this knowledge can be used as a basis for new research aiming to further improve land-based seafood production.

Sammendrag

Resirkulerende akvakultursystemer (RAS) øker i popularitet for produksjon av laksefisk. Vannet resirkuleres i et RAS, sammenlignet med gjennomstrømningssystemer (FTS) hvor det er behov for konstant tilførsel av nytt vann. Oppdrett av arktisk røye (*Salvelinus alpinus*) er forsatt i oppstartsfasen, og forkunnskap om oppdrett av andre laksefisk som atlantisk laks og regnbueørret er derfor avgjørende. Mikrobielle samfunn er viktige determinanter for vannkvalitet ved å for eksempel bidra i vannrenseprosesser. Siden fisken er i konstant kontakt med vannet i systemet er kunnskap om mikrober som finnes på mucusoverflater som skinn, gjelle og tarm viktig for å opprettholde optimal fiskehelse. Mucus er den første forsvarslinjen fra det omkringliggende vandige miljøet, og miljøet kan inneholde både kommensale og/eller opportunistiske bakterier. Kunnskapen om hvordan bakteriesamfunnene i miljøet påvirker mucus hos oppdrettsfisk er imidlertid begrenset.

Denne studien hadde som mål å karakterisere og overvåke de mikrobielle samfunnene i vertens mucus og opprettsmiljøet til Arktisk røye i et kommersielt landbasert akvakulturanlegg. For å studere disse mikrobielle samfunnene ble det tatt prøver for mikrobiell samfunnsanalyse månedlig over en periode på seks måneder fra fiskeskinn-, gjelle-, og tarmmucus, samt inntak og tankvann, biofilm i tank- og biofilter. Totalt 432 prøver, fra et anlegg som opererer med både RAS og FTS, ble utsatt for DNA-ekstraksjon, kvantifisering, kvalitetskontroll og 16S rRNA-genamplikonsekvensering ved bruk av Illuminametodikk. Bioinformatisk prosessering av de sekvenserte dataene blr utført ved bruk av QIIME2 og tilsvarende statistiske analyser ble utført i R for systematisk spatiotemporal mikrobiomprofilering av mucusoverflater og miljøet rundt oppdretsfisken.

Gjennom undersøkelse av alfadiversitet, ble skinnprøver funnet å ha de høyeste alfa-diversitetsmålene av fiskeprøvene i alle de tre overvåkede produksjonssystemene i anlegget. Det bygde miljøet viste imidlertid totalt sett høyere verdier for observert og estimert artsmangfold og høyere Shannon diversitetsindeks enn fiskeprøvene. Inntaksvannet viste betydelig høyere artsmangfold og Shannon diversitet enn både fiske- og miljøprøver. På ASV nivå ble det funnet signifikant forskjell i mikrobiell sammensetning mellom fiskeprøver, og mellom miljøprøver. Videre ble det funnet signifikant forskjell i mikrobiell sammensetning av fiskeprøver mellom de to RAS-systemene og FTS. Prøver fra det bygde miljøet ble funnet å være signifikant forskjellige i mikrobiell sammensetning på tvers av de tre systemene.

Selv om det ikke ble funnet signifikante forskjeller over tid for alfadiversitet, ble det funnet signifikant forskjell i mikrobiell sammensetning mellom prøvetakingsmånedene i fiskeprøvene. Ingen signifikante endringer ble funnet over tid for miljøprøvene.

Den mest dominernede taksonomiske slekten i skinn- og gjellemucus var *Pseudomonas*, mens *Mycoplasma* var den mest dominerende taksonomiske slekten i tarmmucus. *Flavobacterium* var den mest dominerende slekten i tankvann og biofilter biofilm, mens *Arcicella* dominerte i tank biofilm og *Crenothrix* i kildevannet. Det ble imidlertid funnet individuelle forskjeller mellom de tre ulike produksjonssystemene.

Denne oppgaven har gitt betydelig kunnskap om bakteriesamfunn i oppdrett av røye, og denne kunnskapen kan brukes som grunnlag for ny forskning som tar sikte på å ytterligere forbedre landbasert sjømatsproduksjon.

Preface

This master's thesis was conducted through BlueBio Cofund's financed project DIGIRAS (project #81), a trans-European multi-partner project aiming to close knowledge gaps on production of different fish species in RAS by the digitalization of parameters and processes ranging from systematic observations to technical developments. The thesis was assigned by SINTEF Ocean together with Norwegian University of Science and Technology (NTNU), and marks the end of my 5-year long master program of Biotechnology.

First, I would like to thank my supervisor at SINTEF Ocean, Deni Ribičić, for your guidance and help throughout the process. Thank you for being patient with me and helping me understand things I could not grasp my head around. I appreciate all the time and effort you have put into helping me.

I also want to express my gratitude to my supervisor at NTNU, Olav Vadstein, for always keeping the door open whenever I had questions. Thank you for letting me be a part of the ACMS group at NTNU. Your knowledge and dedication to your work is truly inspiring!

A most sincere thank you to Roman Netzer at SINTEF Ocean for all guidance during the writing process. Thank you for answering my many questions, and for including me in the DIGIRAS project.

Further, I would like to show my appreciation to Marianne Aas at SINTEF Ocean for all the help and positive spirit in the laboratory. It was greatly appreciated.

I also wish to thank the staff at NFFT for all the help during the sampling process, and for providing me with crucial information when needed.

Last, but not least, I would like to thank my family and friends for the endless support. Thank you for the motivational speeches when they were needed the most, and for always believing in me. I could not have done this without you. To my classmates, thank you for making these five years at NTNU the best. We've had a blast, and we did it!

Trondheim, August 2022 **Malin Stubban Berg**

Table of Contents

List of Figures

List of Tables

List of Abbreviations

ASV	Amplicon Sequence Variants
BB	Biofilter biofilm
CeBiTec	Centre of Biotechnology
DIGIRAS	Digital recirculating aquaculture systems
DNA	Deoxyribonucleic acid
dsDNA	Double stranded DNA
FBBF	Fixed Bed Biofilter
FTS	Flow Through System
GIM	Gill mucus
GUM	Gut mucus
HTS	High throughput sequencing
MBBF	Moving Bed Biofilter
NFFT	Norwegian Fish Farms Tydal
NGS	Next Generation Sequencing
NTNU	Norwegian University of Science and Technology
OTU	Operational Taxonomic Unit
PCR	Polymerase Chain Reaction
QIIME	Quantitative Insights Into Microbial Ecology
RAS	Recirculating Aquaculture Systems
RNA	Ribonucleic acid
rRNA	Ribosomal RNA
SD	Standard deviation
SKM	Skin mucus
SW	Source water
TAN	Total Ammonia Nitrate
TB	Tank biofilm
TW	Tank water
V3	Variable region 3
V4	Variable region 4

1 Introduction

1.1 Background

As the world's population is growing to an expected reach of 9.6 billion by 2050 (Kobayashi et al., 2015), so is the need for food to meet its growing needs. Aquaculture is one of the industries that will grow faster than most others in the near future, not only to meet growing population demands, but also as a result of the health benefits of including fish in the diet (FAO, 2020). The rearing of fish species can also help to lower the impact on wild stocks and hinder overfishing (Tlusty, 2002) and is, therefore, an interesting topic to embark on. Dating back to 1970, the aquaculture industry has had a growth of 7.5% each year showing its crucial role in the world's food production. Norway has since 2004 been the second-largest exporter of fish, only exceeded by China. Despite its small size, Norway is one of the biggest producers of (mariculture) finfish species such as cold-water salmonids (FAO, 2020).

Aquaculture's expansion brings with it the need for technical developments. Comprehensive biological knowledge of different species in combination with technical knowledge is required in order to exploit the full potential of the aquaculture industry (Lekang, 2020). In addition to publicity reasons, the welfare of reared species is receiving increased attention as companies strive to exploit the full production potential and hence their financial gain (Ashley, 2007). The world is also faced with limiting freshwater supplies, where re-use technology will be an important contributor to a growing industry (Lekang, 2020). This is one of the reasons why recirculating aquaculture systems (RAS) are of increased focus, especially in parts of the world where a limiting amount of freshwater is an issue. The investment and start-up costs of such a system are high (Rurangwa and Verdegem, 2015), but a study done by Rosten et al. (2013) revealed that Atlantic Salmon can be produced in land-based systems at the same price as net pen farming systems. The baseline for a well-functioning recirculating system is a well-functioning microbiota. Microbial communities contribute to processes purifying the water, but can also enter the system in the form of unwanted bacteria which is why they need to be monitored (Rurangwa and Verdegem, 2015).

In order to make a RAS profitable, maintaining good water quality is crucial. RAS has a high organic load and hence a high concentration of microorganisms that is an important component for the water quality (Rurangwa and Verdegem, 2015). The fish is continuously exposed to all microbes in the system by being in constant contact with its surrounding water, which is why keeping pathogens at a minimum is important (Xue et al., 2017). For land-based fish farms with the ability to control both the inlet and outlet water, control of the water parameters will serve as an advantage for the total production unit. Even though the fish will still grow in sub-optimal water conditions, maximizing their growth rate will not be possible as well as maintaining the fish' welfare (Lekang, 2020). A RAS consists of microbial communities that participate positively in water purification processes, but the microbiota can also harbor pathogens that will influence the water quality negatively in regard to fish health and welfare. It is, therefore, of importance to monitor the microbial communities and their interactions with each other to operate a successful RAS (Rurangwa and Verdegem, 2015).

Being a closed aquaculture system, RAS minimizes the risk of pathogens being introduced to the system. The microbiome of the fish' mucus works as an important barrier, keeping pathogens from entering. It is, therefore, an important first line of defense, serving as a separator for the fish's external and internal environment. Different species of bacteria, viruses, archaea, and eukaryotic microorganisms, collectively called the microbiome, are found in the mucosal surfaces of the fish and is affected by changes in the surrounding aqueous environment (Merrifield and Rodiles, 2015).

There is limited research on how the surrounding water microbiota affects the skin, gill, and gut microbiota of reared salmonids in RAS despite it influencing the health of the reared fish (Blancheton et al., 2013; Vadstein et al., 2018), especially for Arctic charr. It is, therefore, important to improve the understanding of the bacterial composition of the microbiome in a way that can help improve the health of the reared fish, and hence the production of reared fish. Study of commercial land-based systems is one way to address these limitations.

1.2 Arctic charr *(Salvelinus alpinus)*

Arctic charr *(Salvelinus alpinus)* is a teleost species in the family of Salmonidae occurring in cold rivers in the northern hemisphere, making it an important source of food for natives in the Arctic region (Borgstrøm et al., 2010). It is the fish species occurring northernmost of all anadromous and freshwater species (Johnston, 2008). Its life cycle is similar to those of other salmonids starting in the winter and then spawning in the autumn (Imsland and Gunnarsson, 2011). Arctic charr can occur in both anadromous and resident style. For those individuals who live an anadromous lifestyle, it is common to migrate to the sea each summer season, before migrating back to freshwater to overwinter. This cycle is then repeated throughout the rest of their lives (Jensen et al., 2020). However, resident Arctic charr tend to mature at an earlier age than anadromous charr (Johnston, 2008).

Farming of Arctic charr is still in its infancy compared to for example Atlantic salmon farming but learning from the rearing of other cultures is an advantage. The farming of Atlantic salmon in Norway started in the mid '70s, and the idea of farming Arctic charr in open seawater net-pens came thereafter intending to further expand the marked of farmed salmonids. However, even anadromous charr cannot overwinter in seawater (Johnston, 2008) and resident charr is, therefore, a good choice for rearing. Arctic charr is a species that grows well at high densities (Jørgensen et al., 1993) and low temperatures compared to other salmonid species (Johnston, 2008). This makes for lower operation costs as less energy is required in Nordic countries to heat the water, and the density of fish in the tanks can be higher (Johnston, 2008). For Arctic charr, low rather than high densities can lead to a stressful environment for the fish and hence decreased fish health (Ashley, 2007). The species has also been proposed to be quite resistant to diseases (Johnston, 2008). These are traits that make it optimal for rearing and further commercial potential. However, some challenges around the culturing of Arctic charr in Norway revolve around its size and color. Preferred fish size is around 2-3 kg, but the cultured charr is typically no more than 1 kg when it is slaughtered. The color of the flesh is also paler than the marked demands. This leads to poor marked prices and again high production costs, which is a disadvantage to the farmer (Johnston, 2008). Even though there is still a lot of research needed in the rearing of Arctic charr, one can learn from the rearing of other salmonids species such as Atlantic salmon and rainbow trout. There have been tremendous improvements in the technicalities of aquaculture infrastructure over the last years making it an important area to embark on.

1.3 Recirculating Aquaculture Systems

Recirculating aquaculture systems (RAS) are land-based systems that rear aquaculture species in indoor tanks with controlled environments. The water is re-used after filtration instead of being deposed off after going through the RAS loop. Over the last years, the use of recirculating technology for farmed fish has increased immensely due to improvements in the technology (Fjellheim, 2016). As mentioned, the rearing of Arctic charr started in the mid-1970's, but not in land-based systems (Johnston, 2008).

The precursor to the land-based recirculating systems are so-called flow-through systems (FTS). Traditional FTS need a constant supply of new water compared to RAS, where up to 99% of the water can be reused from the fish tanks. This makes for more sustainable production of farmed species. In FTS, the water is deposed off after leaving the fish tank (Minich et al., 2020). Figure 1-1 shows the basic difference between a traditional FTS versus a RAS. Biosecurity is in theory thought to be better in a RAS than a traditional FTS since one can control and regulate the conditions.

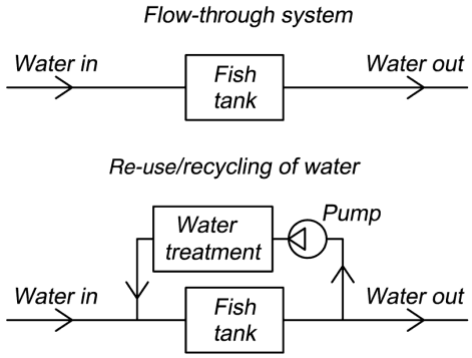

Figure 1-1: A schematic overview of the basic differences between a flow-through system (top) versus a RAS (bottom) (Lekang, 2020). The water goes into the tank before being deposed in an FTS, whereas a pump pushes the water through water treatment before going back into the tanks in a RAS.

RAS are an important future factor in the aquaculture industry because they offer the possibility of higher production rates within these controlled conditions. However, for it to be successful, it is necessary to obtain good water quality as well as optimal welfare for the species (Rurangwa and Verdegem, 2015). The systems use less water since the outlet water is cleaned and reused instead of being disposed of, as mentioned above. The water goes through a loop where different treatment methods will adjust the water quality parameters before it can re-enter the tank. Such water quality parameters include readjustment of gasses such as oxygen (O_2), nitrogen (N_2) and carbon dioxide (CO_2) dissolved in the water, the water pH and temperature, dissolved particles, salinity, and microorganisms (Lekang, 2020). This decreases the need for new water as well as reduces the energy needed to heat the incoming water. Being able to control such parameters (Figure 1-2) and water income makes for better control of the systems than traditional (flow-through) systems, which again leads to the ability of a predictable production plan of the farmed species and all-over better fish health. However, the lack of reliable data on individual parameters, such as those just mentioned, is also what hinders the technology from reaching its full potential.

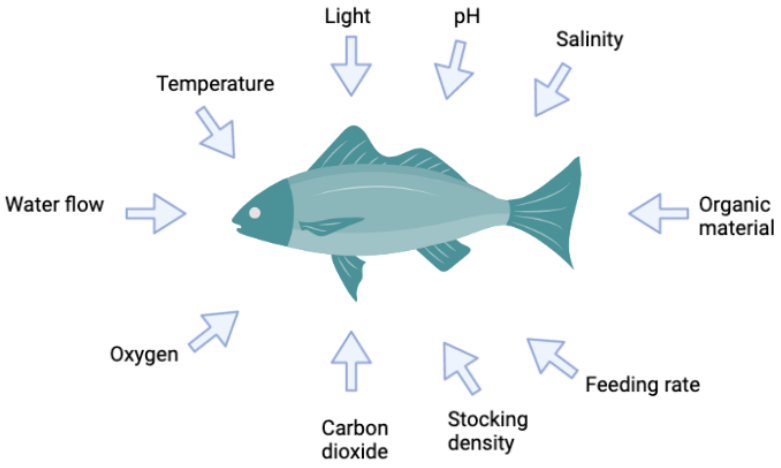

Figure 1-2: Water quality parameters influencing the well-being and growth of fish in a recirculating system. Figure modified from Bregnballe (2015).

The components that are present in a common RAS treatment-loop in addition to the fish tank(s) are filters such as mechanical filters (drum- or belt filter) for removal of larger particles from the water, but also biofilters (moving bed or fixed bed) where nitrifying bacteria work to convert total ammonia nitrogen (TAN) to nitrate via nitrite. Disinfection steps, either ozone or UV, and CO_2 degasser and oxygenation are also common components. New water is added to account for evaporation, and also this water needs to be treated before entering the RAS-loop (Fjellheim, 2016; Bregnballe, 2015). Which components are added to the system can vary between different facilities, but the main function is the same throughout; aiming to optimize the water quality and fish health.

1.4 Microbial Communities

The microbial communities present in RAS facilities are complex and a necessity for both the chemical and microbial water quality, and thus play a crucial role in keeping the reared fish healthy (Vadstein et al., 2018). Hence, a critical factor in operating a successful RAS is the understanding of the microbiota and its interactions. Feed, water, staff, and uncleaned equipment are some of the ways microorganisms are introduced into a RAS facility along with the fish itself (Rurangwa and Verdegem, 2015). Microbial communities present in a fish's mucus system such as the skin, gill, and gut mucus are an important factor in the fish's defense system as the fish is in constant contact with both pathogenic and nonpathogenic microbes in the surrounding aquatic environment (Ángeles Esteban and Cerezuela, 2015). Mucus areas are commonly known as the major pathways of pathogen entry in fish (Merrifield and Rodiles, 2015) which is why study of microbial communities on these surfaces are important. A large change in the bacterial composition in the RAS may cause diseases for the fish in which it is not able to escape since the system is closed. This will further lead to increased mortality, which is unfavorable for the farmer (Xue et al., 2017). One way the mucus interacts with pathogens and unwanted bacteria who have entered the water is to repel and trap them, but the mucus also consists of various antimicrobial factors that work to prevent the pathogens from entering (Castro and Tafalla, 2015). Even with such barriers, bacteria will grow in the system (Derome, 2019).

The microbiota of a RAS is affected by parameters such as feed type and regime, the microflora associated with the fish, make-up water parameters, selection in the biofilter, and management routines (Blancheton et al., 2013; Vadstein et al., 2018). These are factors that need to be monitored at all times to operate a successful RAS seeing as they

can vary in the system over time, and also across systems (Bakke et al., 2017). The bacterial flora of aquaculture systems includes two important groups of bacteria: the autotrophic nitrifiers working in the oxidation of ammonia to nitrate, and the heterotrophs that degrade the organic matter from feces and food. The heterotrophs produce CO_2 and consume O_2, in competition with the autotrophs. They are normally considered to be "neutral microbes" and thus wanted in moderate quantity as they may protect against pathogens (Blancheton et al., 2013). The bacteria will grow in the system in the circulating water, surface and dead zones in the tank, pipes of equipment, and on the fish itself (Derome, 2019; Blancheton et al., 2013). However, it is necessary to direct more focus on how the effects of water treatment influence the rearing tanks since the water and its microbiome are in constant contact with the fish and therefore a direct influence on its health status.

When defining good water quality in an aquaculture system one usually focuses on the absence of pathogens and other bacteria that can be harmful to the fish. As mentioned above, the heterotrophs contribute by degrading organic matter in the water. However, bloom of opportunistic heterotrophic bacteria can be disastrous to fish living in suboptimal rearing conditions (Vadstein et al., 2018). The level of heterotrophs is therefore important to regulate in RAS, and is done by controlling the load of organic matter available (Blancheton et al., 2013). Present in the biofilter, an outer layer of heterotrophs can protect the autotrophic nitrifiers from flow detachment. However, the heterotrophs have a doubling time faster than the autotrophic bacteria and the layer is therefore of essence to keep thin to avoid stop of oxygen flow to the autotrophic nitrifying bacteria present in the biofilter (Blancheton et al., 2013). The mechanisms causing unstable changes in the environment and hence a higher number of opportunistic bacteria leaving the conditions suboptimal for the reared fish (Bakke et al., 2017) are not well-documented for salmonids (Vadstein et al., 2018).

The production of geosmin or MIB (2-methylisoborneol) by microorganisms such as chemotrophic bacteria is known to cause an unwanted off-flavor in food fish reared in RAS. Both compounds can be absorbed by the fish in its flesh, creating a muddy taste when the fish is consumed. One way to remove the off-flavor is by purging the fish prior to slaughtering (Azaria and van Rijn, 2018). Another problem caused by microbes in the water, is formation of hydrogen sulfide (H_2S) by sulphate-reducing bacteria (SRB). H_2S is deadly in low doses to the fish and can therefore cause high mortality in the tanks. The SRB can be located in anoxic zones of the tank, such as in the biofilm, and use sulphate as electron acceptor in the degradation of organic matter (Rojas-Tirado et al., 2021).

1.4.1 Fish immunology

Microorganisms are present on every mucosal surface of teleost fish and have been studied over time using variety of sequencing techniques (Kelly and Salinas, 2017). The mucus functions as a layer of protection between the external environment and the epithelial surface of the fish (Minniti et al., 2019) and is part of teleost innate immune system (Kelly and Salinas, 2017). It is mainly built up of mucins, along with lipids and different proteins. Some of these proteins include lysozymes, immunoglobins, and growth factors that are related to defense functions. Working as a semipermeable, yet robust, barrier makes it able to hinder unwanted chemicals and pathogens from breaking the mucosal layer and reaching the epithelial cells. The whole skin, gill, and gut of teleost fish is covered in a layer of mucus working in processes such as osmo- and ion regulation, gas exchange, as well as defense. These processes require a complex microbial community with both symbiotic and/or opportunistic bacteria in balance to ensure the health of the fish. A well-

functioning layer of mucus is especially important in farmed fish as they are stocked in higher densities than in the wild and therefore are more susceptible to pathogens (Minniti et al., 2019). The immune system of fish is divided into three based on its location. The mucosal-associated lymphoid tissue (MALT) further divided into gut-associated lymphoid tissue (GALT), skin-associated lymphoid tissue (SALT), and gill-associated lymphoid tissue (GIALT).

Keeping the mucosal microbiome in balance is a key to maintaining the health of the fish. The fish health is supported by defense mechanisms such as the innate immune system providing barriers to keep unwanted pathogens from entering the body of the fish, and the specific immune system producing antibodies mediated by T-lymphocytes. The difference between the two is the lack of memory from the innate immune system when encountering pathogens (Gómez and Balcázar, 2008). One factor that can cause changes in the innate immune system and hence the mucus composition is if the reared fish is experiencing stress (Llewellyn et al., 2014). Such stress factors can for reared fish be poor water quality, handling of the fish, or especially for Arctic charr, low biomass densities (Johnston, 2008). These factors may result in changes of mucus layer thickness and modulations in mucus composition, which can leave the fish more susceptible to pathogens (Llewellyn et al., 2014).

Not a lot of research has been conducted on the microbial community of Arctic charr mucus compared to for example Atlantic salmon. Seeing as they are both salmonids produced in aquaculture, further exploration of the microbiota in Arctic charr mucosal surfaces would allow for comparative studies with Atlantic salmon microbiota and generate new knowledge relevant for the production of both species in closed containment systems.

1.4.2 Skin

The skin, often referred to as the integumentary system, is the largest organ of the body consisting of many different tissues. The surrounding environment of the fish consists of both pathogenic and nonpathogenic organisms which give the skin importance while working as the first barrier against pathogenic invasion. Compared to terrestrial animals, the fish is in constant contact with microbes, including pathogens, in its aquatic environment (Ángeles Esteban and Cerezuela, 2015).

As well as functioning as a barrier against external damage, the complex tissues of its build-up gives it other functions such as maintenance of body shape, camouflage, communication, thermal regulation, and respiration (Ángeles Esteban, 2012). The skin of teleost organisms is divided into three layers: the outermost mucus, the epidermis, and then the dermis. The mucus is a complex composition of bacteria that forms the microbiota covering the living epithelial cells. It is a semipermeable membrane and functions by capturing the unwanted pathogens and hence removing them from the skin mucosa by the surrounding water. The epidermis is a layer of living cells such as the unicellular glands known as goblet- and club cells, secreting the mucus layer. These glands are present in a high number in teleost fish skin. The dermis, on the other hand, is a connective tissue containing collagen fibers (Ángeles Esteban and Cerezuela, 2015). If infected, the fish will experience changes in these three layers which can be crucial to the fish (Ángeles Esteban, 2012).

1.4.3 Gill

As opposed to fish skin, fish gills are fragile organs. It is the largest organ-specific surface interacting with the external milieu, estimated to a surface of 0.1-0.4 m^2/kg body weight

(Koppang et al., 2015). Teleost gills are complex structures consisting of four gill arches and five slits where the gill cover (operculum) covers it to protect the gills from mechanical damage. The operculum is a hard flap covering the gill directly in contact with the water (Koppang et al., 2015; Evans et al., 2005). The continuous flow of water makes the gill of a fish a difficult environment to inhabit for microbes. However, the microbial communities are known to be of the same order as for the skin (Merrifield and Rodiles, 2015). As well as with the skin, the gills are a point of entry for pathogens and a site for infection. The main function of the gills is in respiratory work, but they also function in hormone production, regulation of osmosis, and pH. They are, likewise to the skin, covered in a thin layer of mucus-forming a semipermeable barrier from the water and entry to the organism (Koppang et al., 2015).

1.4.4 Gut

The gastrointestinal tract of teleost organisms offers a variety of functions, including the gut's role as a physical barrier for entry to pathogens containing the GALT (Salinas and Parra, 2015). Same as for the skin and the gill, the fish's gut is also covered with a layer of mucus to protect the fish from its external environment and maintenance of tissue homeostasis (Castro and Tafalla, 2015). It is composed of mucins that are secreted by goblet cells. The thickness of the mucus layer can be altered by infection agents that can alter mucin gene expression and hence affect its defense mechanism (Salinas and Parra, 2015). Another function of gut mucus is the uptake of nutrients. The intestinal mucus is therefore permeable to macromolecules working in processes such as digestion while still working as a barrier to particles such as microorganisms. At the same time, the gut is colonized with a diverse microbiota which plays an important role for the hosts immune system development and nutrient absorption (Talwar et al., 2018). Since farmed fish is fed pellets with customized content, it has been demonstrated the fish farmer can influence the fish's health through its food (Salinas and Parra, 2015).

Of the three mucosal surfaces (skin, gill, and gut), it is thought that immune cells inhabit the gut earlier than the skin and gill (Castro and Tafalla, 2015). But, the biggest difference in microbial composition is seen between the gastrointestinal tract and external mucosal surfaces such as the skin and gill (Kelly and Salinas, 2017). The microbiota in the intestine of freshwater fish species, such as non-anadromous Arctic Charr, is proposed to be dominated by 5 genera representatives of the family *Enterobacteriaceae* (Pérez et al., 2010).

1.5 Microbiota Associated With Fish Skin, Gill, and Gut

The microbial communities present on skin, gill, and gut mucosal surface are, as already mentioned, an important contributor in defense mechanisms for the fish (Merrifield and Rodiles, 2015). A crucial factor of maintaining the overall health of the fish is maintenance of microbiome balance. This microbiome balance is, unique for aquatic animals, highly related to its immediate environment (Gómez and Balcázar, 2008). Fish hosts can live in different environments, but their skin microbiome is often composed of the same microorganisms. However, the determination of abundance of microbes present on the skin of fish has proven to be difficult of reasons such as contamination of the epidermal tissues during sampling (Merrifield and Rodiles, 2015). As previously mentioned, the gills are a difficult place to live for microbiomes because of the constant flow of water. It is reported that the microbiota of the gills is similar to those of the surrounding water. Same as for the skin, the gills of various environments harbor similar microorganisms (Merrifield and Rodiles, 2015). The gut microbiota is thought to be one of the most heavily populated

places for microbes in the fish, but it exhibits a low phylogenetic diversity dominated by a few bacterial groups (Pérez et al., 2010). A study done by Llewellyn et al. (2014) presents an overview of common bacterial phyla present in fish skin, gill, and gut of a variety of fish species found through several studies and is presented in Figure 1-3.

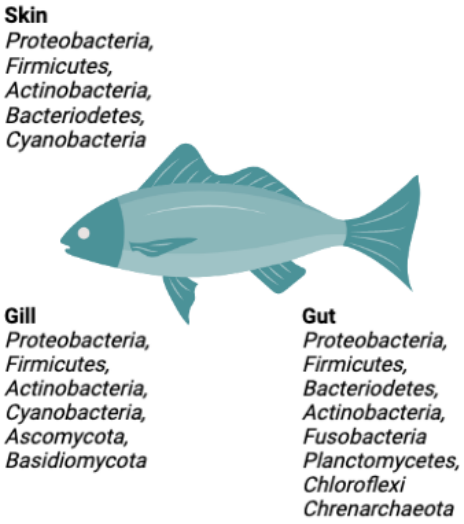

Figure 1-3: Major phyla present in fish microbiota on skin, gill, and gut. Only bacteria that correspond to those which made up > 80% of sequences characterized from a given species, and only studies that employed direct sequencing were included. Figure generated from Llewellyn et al. (2014).

Bacterial pathogens that can cause unwanted infection in teleost fish are found in genera such as *Vibrio, Streptococcus, Aeromonas, Flavobacterium, Photobacterium, Pasteurella, Tenacibacterium, Pseudomonas, Lactococcus, Edwarsiella, Yersinia, Renibacterium,* and *Mycobacterium* (Llewellyn et al., 2014). These are genera of almost all opportunistic pathogens. Studies based on commensal skin and intestinal microbiota have suggested that bacterial pathogens often appear as a minor component of teleost microbiome, but can cause harm under certain circumstances such as stress (Llewellyn et al., 2014).

1.6 Methods of Investigating Microbial Communities

The use of molecular methods to study microbial communities have been around since the mid-80s (Head et al., 1998) but over the past years, more and more studies are using next-generation sequencing (NGS) over the more traditional culture-dependent methods (Xue et al., 2017). The older methods have struggled with the differentiation of bacteria, and underestimation of the microbial diversity. This shift in methodology has improved the efficiency of post-sequencing bacterial community work (Xue et al., 2017) as well as broadening the understanding of the complex microbial communities that are present in various habitats (Ghanbari et al., 2015). Microbial community studies in fish typically focus on the skin, gill, and gastrointestinal tract because they are pathways of pathogen entry (Ángeles Esteban and Cerezuela, 2015; Koppang et al., 2015; Salinas and Parra, 2015).

1.6.1 16S rRNA gene

Investigation of the 16S ribosomal RNA (rRNA) gene has become the gold standard for analysis of microbial communities seeing as the gene is identical in all bacteria

(Chakravorty et al., 2007). The diversity in both water and biofilters of aquatic systems is investigated using 16S rRNA instead of culture-based techniques (Blancheton et al., 2013). The gene consists of 9 variable regions (V1-V9) positioned between conserved regions and can be used for species identification as the variable regions are divergent between bacterial species. The regions that are conserved makes for amplification by PCR using universal primers that target these regions (Chakravorty et al., 2007). In total, the gene is approximately 1 600 base pairs long divided into the variable- and conserved regions (Bukin et al., 2019). When investigating microbial communities, the 16S rRNA gene has been an important target. However, it is also encountering problems as 16S sequences from the same species often differ (Ghanbari et al., 2015) as well as lacking the sufficient discriminative information for taxonomic classification down to species level (Church et al., 2020).

1.6.2 Illumina sequencing of 16S rRNA

The complete human genome sequencing in 2001 emphasized the need for faster and more automated methods of sequencing (Rajesh and Jaya, 2017). Next-generation sequencing has improved the efficiency of sequencing compared to conventional methods, such as Sanger sequencing, by enabling the parallel/high-throughput sequencing of millions of DNA fragments instead of a single DNA fragment. By sequencing the DNA, one determines in what order the nucleotides are arranged in the genetic code of the desired organism. Further, the development of paired-end sequencing has also improved the efficiency by enabling sequencing of both ends of the DNA fragment at the same time (Illumina, 2017).

NGS refers to high throughput sequencing (HTS) methods that have made it possible to examine complex microbial communities including phylotypes of low abundance. The fish microbiota is in constant contact with its surrounding environment which is why many factors need to be taken into account when looking at the relationship between for example the fish gut microbiota and its environment. By the use of NGS, this can be done in a more quicker and accurately way than previously (Ghanbari et al., 2015). A dominating NGS-technology is the Illumina sequencing method which can sequence the 16S rRNA gene highly common for phylogeny and taxonomic studies (Illumina, 2017). But NGS techniques also has its limitations. They are based on short reads which can cause problems when mapping to a reference database and targeting only one gene, for example the 16S gene, is known to limit the taxonomic information such as underestimating the abundance of taxa with low copy numbers. These are important measures to take under consideration when measuring bacterial diversity (Ghanbari et al., 2015).

Illumina next-generation sequencing works in four main steps (Appendix A). The first is the library preparation phase where the DNA is fragmented and then ligated to 5’ and 3’ adaptors. They are further amplified by PCR and gel purified. Multiplexing the fragments by adding unique identifiers will help identify and sort the fragments before step four is performed. The second step is the cluster generation where the newly generated library is loaded onto flow cells and bound to oligonucleotides that are complementary to the adaptors. The third step is the sequencing which is conducted in a base-by-base manner. The last step is the data analysis. Here, the reads are aligned to a known genome for reference before multiple analysis methods are possible to conduct. If multiplexing has been performed in the library preparation phase, demultiplexing needs to be conducted before the final data analysis (Illumina, 2017).

1.7 Aims and Hypotheses

In this study, the aim was to characterize and describe microbial communities present in skin, gill, and gut mucus from Arctic charr as well as the microbial communities present in tank and source water, tank and biofilter biofilm collected at a facility operating with both FTS and RAS. Detailed and systematic monitoring of community composition and dynamics over time during different life stages of the fish and changing conditions in corresponding built environments is suggested to provide new knowledge on microbiota in Arctic charr aquaculture in land-based systems and how to improve fish welfare and production conditions. The rearing of Arctic charr is still in its infantry, and systematic investigation of its microbiota is for that reason of pioneering interest to the industry.

The objective of this study was therefore as followed:

- To systematically characterize and monitor the microbial communities in environments (intake and tank water, biofilm in tank and biofilter) as well as mucosal surfaces (skin, gill, and gut mucus) of Arctic charr in a commercial land-based aquaculture facility

More so, the sub-aims of this study were to answer the following hypotheses:

- Arctic charr skin, gill, and gut mucus harbors different microbial communities
- Built environment microbiota will influence the microbial communities in the skin and gill mucus of the fish
- Biofilter microbiota is stabilizing microbial water quality in RAS_1 and RAS_2
- Disinfection of the intake water will influence microbial communities in the tank water
- Microbial communities will differ in RAS_1 and RAS_2 versus the FTS
- Microbial communities will differ at different time points of the sampling

2 Methods

This master's thesis was conducted through BlueBio Cofund's financed project DIGIRAS (project #81), organized and managed by SINTEF Ocean. The overall aim of this trans-European multi-partner project is to close knowledge gaps on production of different fish species in RAS by the digitalization of parameters and processes ranging from systematic observations up to technological developments. The major objective of this study, however, is the characterization of microbial communities in intake and tank water, biofilm in tank and biofilter media as well as fish skin, gill, and gut mucus in Arctic charr. Samples were taken at a facility operating with both RAS and FTS and subjected to DNA extraction, quantification, quality control and 16S rRNA gene amplicon sequencing employing Illumina methodology. Bioinformatic processing of the sequenced data was performed using QIIME2 and statistical analyses executed in R.

2.1 Description of the Facility

The facility at Norwegian Fish Farms Tydal (NFFT) consisted of a total of 26 rearing tanks, divided into three departments (brood stock, fry and grow-out) in which three of the tanks were used for sampling in this master project. Rearing water is derived from groundwater wells with hygienic barriers in terms to ensure biosecurity before it enters the facility and supplies water to all tanks. Known water parameters in the facility are listed Appendix B. The first department was the brood stock department consisting of two tanks with a diameter of 3 meter each. This department was not part of sampling for this master project and will therefore not be further described. The second department was the fry department (Figure 2-1), operated as a RAS (RAS_1), where the water goes through a drum filter (Hydrotech 60 µm) before being pumped up to the trickling filter over a bioblock and down into a sump with degassing before being pumped back into the tanks.

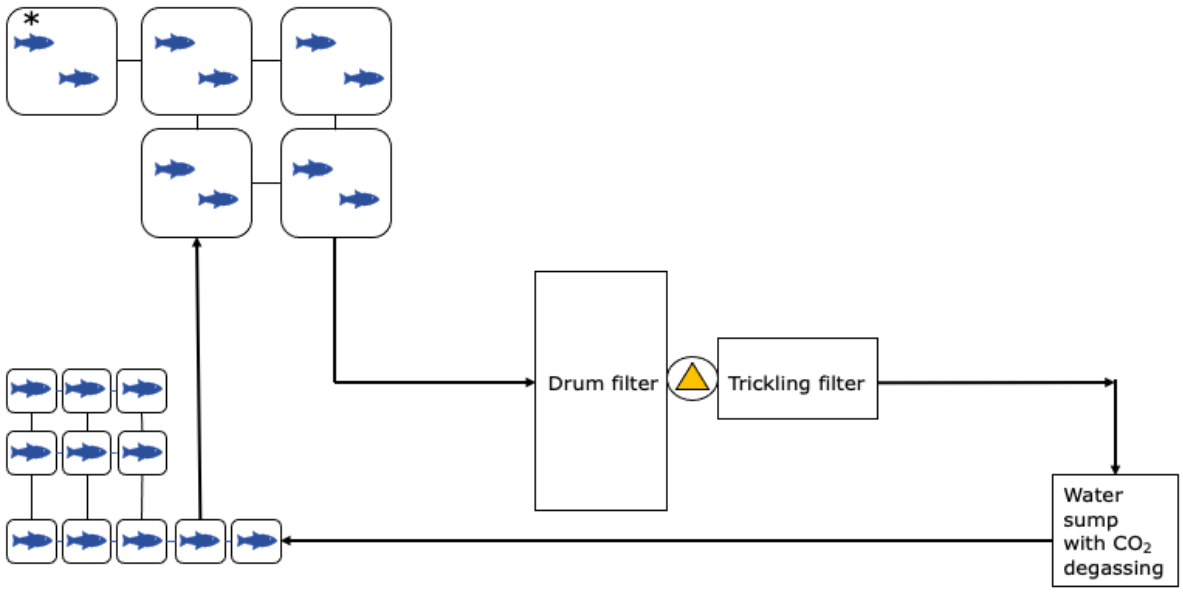

Figure 2-1: Schematics of the fry department, consisting of 11 tanks (diameter 1 meter) and 5 tanks (diameter 3 meters). Samples were taken from tank #16, marked with a star (*), as well as the trickling filter. The pump is illustrated by the yellow triangle.

The third compartment, the grow-out compartment, was based on a section of complete RAS (RAS_2) (Figure 2-2). The water is sent through a drum filter (Hydrotech 60 µm) before entering a moving bed biofilter (MBBF) and further into a sump with degassing. At the bottom of the sump, there is located a pump that pushes the water back into the tanks where it is being oxygenated in the pipes on its way back to the tanks. The bottom drain from the tanks goes into a particle sedimentation (collector) where the sludge is collected in a sludge collector. For the MBBF and degassing unit, no distributor could be found as it was set up by those starting the facility.

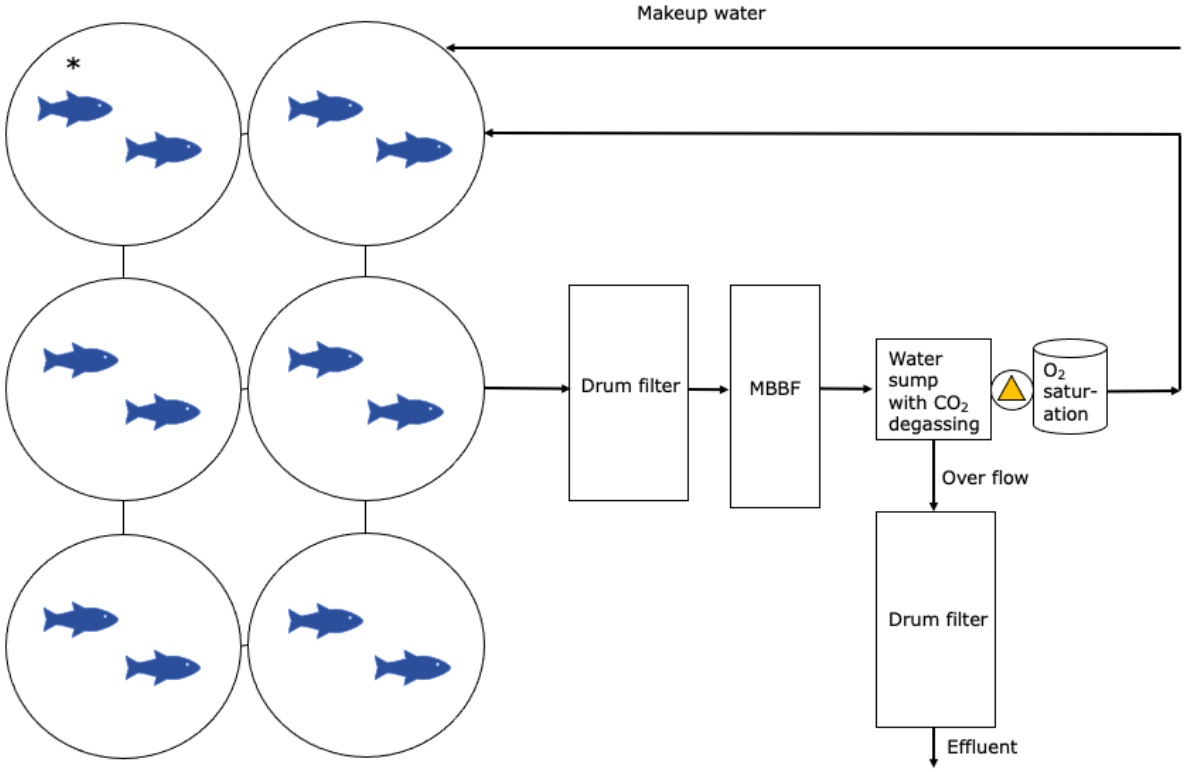

Figure 2-2: Schematics of the RAS-section of the growth department consisting of 6 tanks (diameter 8 meters). Samples were taken from tank #17, marked with a star (*), as well as the MBBF. The pump is illustrated by the yellow triangle.

The third compartment consisted of a section with two tanks based on FT-technology (FTS), containing the largest fish (Figure 2-3). In contrast to the previously described systems, this compartment is operated, more as a FT-system with partial water re-use, where the water is not recirculated to the tanks, but the majority is discharged after particle removal.

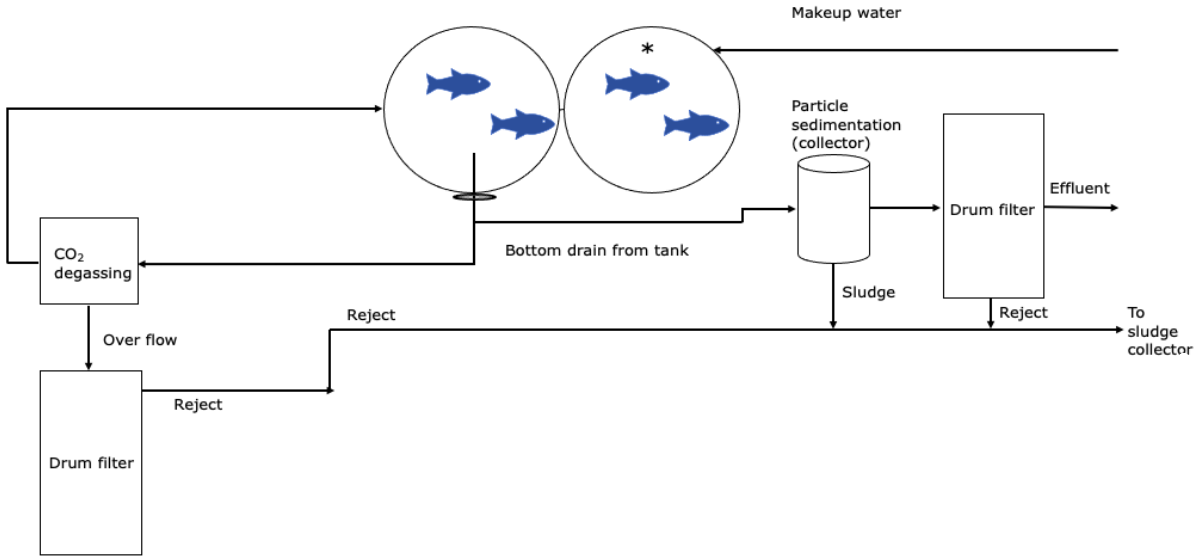

Figure 2-3: Schematics of the FT-section of the growth department consisting of two tanks (diameter 4 meters). Samples were taken from the tank, S1, marked with a star (*).

For all the compartments, all wastewater is filtered through a mechanical drum filter (Hydrotech 60 µm) before the water is discharged into the river. The particles that are collected are sedimented in a separate collection tank which is emptied manually and delivered as sludge.

The first sampling tank, #16, contained fish with an average starting weight of 51 g (cohort 1). The second sampling tank, #17, contained of fish with the average starting weight of 205 g (cohort 2). The third sampling tank, S1, contained of fish with the average starting weight of 458 g (cohort 3). Throughout the six months monitoring period, samples were taken from the same cohorts kept in the same individual tanks. Average weight of the fish in each tank for all sampling months was recorded and is presented in Table 2-1.

Table 2-1: The average weight in grams for the three sampled cohorts at the six sampling months, and biomass of the tanks in kg.

Sampling tank	**#16 (cohort 1)**		**#17 (cohort 2)**		**S1 (cohort 3)**	
Month 2021	Avg. Weight (g)	Biomass (kg)	Avg. Weight (g)	Biomass (kg)	Avg. Weight (g)	Biomass (kg)
April	51	1 094	205	9 472	458	1 284
May	58	1 242	225	10 392	520	1 458
June	62	1 327	232	10 716	547	1 534
July	70	1 498	241	11 129	592	1 660
August	74	1 582	248	11 449	653	1 831
September	Moved		260	12 000	Slaughtered	

2.1.1 Sampling

The sampling was conducted once a month over 6 months at NFFT. The sampling started on April 8th of 2021 and ended on September 13th of 2021. The samples were collected on approximately the same day of each of the six months, with assistance from the staff at NFFT. Samples collected from the fish were skin, gill, and gut mucus. Water samples were collected from the intake water before disinfection as well as tank water from three

sampling tanks (tank #16, #17, and S1). Biofilm from two biofilters in the facility was sampled, as well as tank biofilm from the three above-mentioned tanks. The water and biofilm samples were taken in triplicates, whereas mucus from five fish from each cohort was sampled at every sampling time point. This resulted in 72 samples each month and a total of 432 samples (Appendix C).

For the three cohorts of fish from the above-mentioned tanks, five fish each were moved with a dip net to a bucket before being euthanized with overdose of anesthesia (Benzoak vet., ACD Pharmaceuticals AS). The skin mucus samples were collected by swabbing both lateral sides of the fish to collect enough mucus material. The swabs (Copan diagnostic, California) were then placed in collection tubes prefilled with 1 ml DNA/RNA Shield – Bashing beads (Zymo Research R1104) before inverting the vial to bring the flocked surface in thorough contact with the liquid. This medium was used because it inactivates biological activity, facilitates chemical cell lysis and preserves nucleic acids. The collection tubes were labeled according to the sampling plan.

Gills of sampled fish specimens were swabbed on the inner gill arch with multiple strokes. The swabs were then placed in collection tubes prefilled with 1 ml DNA/RNA Shield – Bashing beads (Zymo Research R1104) before inverting the vial to bring the flocked surface in thorough contact with the liquid. The collection tubes were labeled according to the sampling plan.

For the gut samples, the sampling for the first month was conducted differently than the remaining months. Swabs were inserted approximately 5 cm into the distal gastrointestinal tract of the fish before placing the swabs in collection tubes prefilled with 1 ml DNA/RNA Shield – Bashing beads (Zymo Research R1104) before inverting the vial to bring the flocked surface in thorough contact with the liquid. The collection tubes were labeled according to the sampling plan. For the remaining sampling time points, the fish was cut open in lower area of the abdomen using a sterile scalpel, and approximately 150-200 mg of the posterior intestine was cut out and placed in 650 ml DNA/RNA Shield – Bashing beads (Zymo Research R1104) using sterile forceps before inverting the vial to bring the flocked surface in thorough contact with the liquid. The scalpel was disinfected using 70% ethanol between each fish to avoid cross-contamination.

Water samples (a total of 180 ml each) were collected by filtration through a sterile 0.22 µm Sterivex filter (Millipore) using a 60 ml Omnifix® syringe. 1 ml of DNA/RNA shield was then added using a disposable sterile Pasteur pipette, and the filter tilted gently a couple of times to ensure the DNA/RNA Shield had been in thorough contact with the whole filter before the filter was sealed, placed in a Falcon tube, and labeled accordingly to the sampling plan. The weight of the fish was registered starting from sampling month two and is shown in Table C-1 in Appendix C.

Biofilm samples were taken from the tank walls of each of the three tanks with corresponding cohorts of fish, at approximately the same location each. The swab was submerged into the water and scraped against the tank wall with an area of 5 cm x 10 cm. The swab was rotated to ensure that all areas were covered with biofilm. The swab was then placed into the lysis bead tube, containing 1 ml of DNA/RNA Shield, and labeled accordingly to the sampling plan.

Biofilter samples were taken for both the MBBF and the FBBF. For the MBBF, one biomedia carrier was taken out and biofilm swabbed from it before placing the swab into the lysis bead tube, containing 1 ml of DNA/RNA Shield. For the FBBF, the biofilter tank wall was

swabbed below the water line and placed into the lysis bead tube, containing 1 ml of DNA/RNA Shield. The samples were labeled accordingly to the sampling plan.

All the samples were transported back to SINTEF Ocean in styrofoam boxes where they were stored at -80ºC until further processing.

2.2 DNA Extraction

DNA extraction was performed for all 432 samples using the ZymoBIOMICS™ 96 MagBead DNA kit (Zymo Research, USA) at SINTEF Ocean. The content of the kit is presented in Appendix D. DNA extraction is necessary to separate the wanted DNA from other components present such as its membrane, proteins, and cellular components as they can be a disturbance to the downstream analysis. DNA extraction follows the common steps of chemical and mechanical cell lysis, separation of DNA from other molecules and isolating the DNA. The whole workflow is necessary to perform with caution to prevent contamination (Elkins, 2012).

Modifications were made to the manufacturers protocol for step 1 (Appendix D). DNA/RNA shield was used to replace the ZymoBIOMICS Lysis Solution, with 1 ml content for all samples except from gut samples containing 650 ml instead of 1 ml. After thawing, the swab samples were placed in the MP FastPrep (MP Biomedicals, USA) for step 2 with optimized bead beating conditions (24x2,6 m/s, 60-sec x 5). Step 3 a. was then conducted at 12,000 x g for 1 minute before sample purification was performed.

Sample purification was performed in line with the manufacturers protocol shown in Appendix D, except for the following modifications: 600 µl ZymoBIOMICS™ MagBinding Buffer was added in well A of the deep-well block along with 25 µl ZymoBIOMICS™ MagBinding Beads. 900 µl of ZymoBIOMICS™ MagWash 1 was added to deep well B, and 900 of ZymoBIOMICS™ MagWash 2 to both well C and D. 200 µl of the supernatant was at last transferred to well A and mixed well using the pipette. The DNA was then eluted employing the KingFisher Duo Prime (ThermoFisher Scientific, USA), and the supernatant (now containing the eluted DNA) was transferred to a clean microwell. The elution volume was 50 µl.

Following the extraction and purification, the purity and concentration of DNA extracts was measured using NanoDrop™ 1000 Spectrophotometer (ThermoFisher Scientific, USA) and Qubit® 3.0 Fluorometer (ThermoFisher Scientific, USA) before the total DNA was stored at -80°C.

2.2.1 NanoDrop

NanoDrop™ 1000 Spectrophotometer was used to measure the purity and concentration of the extracted DNA. 2 µl of HCl was placed on the lower pedestal of the instrument before lowering the sample arm to ensure that the instrument was cleaned. The HCl was then wiped off before pipetting 2 µl of Milli-Q water onto the pedestal. The sample arm was then lowered again before Milli-Q water was wiped off. To make sure that the instrument was fully cleaned, another round of 2 µl Milli-Q water was used to initialize the instrument. The ND-1000 program was opened and the default setting 'DNA-50' was used. A blank (ZymoBIOMICS DNase/RNase Free Water) was measured to ensure that the instrument was calibrated. Another blank was then measured as a regular sample indicating little to no DNA present when a relatively flat baseline was shown and a concentration of close to zero ng/µl. 2 µl of each DNA sample was then loaded onto the lower pedestal and the concentration of DNA was measured. The output was a graph showing the absorbance and

wavelength (nm), as well as the 260/280 and 260/230 ratios and total DNA concentration (ng/µl) of the sample. The purity is indicated by the 260/280 and 260/230 ratios of sample absorbance. A value of ~1.8 and ~1.8-2.2, for the absorbance ratios, respectively, is considered pure DNA. The ratio is therefore a good indication to whether the total DNA contains contamination. The data from the NanoDrop can be seen in Appendix E.

2.2.2 Qubit

For measuring the amount of dsDNA present, the Qubit™ 1X dsDNA HS (High Sensitivity) Assay Kit (Invitrogen, ThermoFisher Scientific) was used on a Qubit® 3.0 Fluorometer for specific DNA quantitation. The kit consists of two standards and the Qubit dsDNA working solution buffer (Appendix F). This was stored at 4ºC but was taken out of the refrigerator to reach room temperature before starting the measurements. The assay works with sample concentrations ranging from 10 ng/µl to 100 ng/µl. Present in the solution buffer is a fluorogenic dye that will bind to the dsDNA in the sample that is measured. A signal will then be emitted and measured by fluorometers present in the machine before it is used, combined with a calibration curve made from standards, to determine the concentration of the nucleic acids present.

Starting, assay tubes (Qubit Assay Tubes) were set up for all the samples and the two standards needed. For the standards, 190 µl of Qubit dsDNA working solution was added before adding 10 µl of the two standards in their respective tubes. The standards were then vortexed for 5 seconds and incubated at room temperature for no less than 2 minutes. 195-198 µl of the working solution was added to the assay tubes, along with 2-5 µl of sample DNA, leaving the total volume in the assay to be 200 µl. The sample DNA was diluted with ZymoBIOMICS DNase/RNase Free Water if the concentrations given from the NanoDrop displayed over 60 ng/µl. The Qubit Flex Fluorometer was then prepared, and the standards and samples were read according to the protocol shown in Appendix G. A minor moderation to the protocol was made by performing step 1.5 before steps 1.3 and 1.4. The data recorded from the Qubit can be seen in Appendix E.

2.3 Sequencing of DNA

The extracted DNA was sent to project partner Bielefeld University in Germany to generate 16S rRNA gene amplicon libraries according to the standard Illumina protocol '16S Metagenomic Sequencing Library Preparation' (Illumina Inc., USA). The sequencing of the amplicon libraries was conducted on an Illumina MiSeq platform applying the protocol for 2 x 300 bp paired-end sequences. The sequenced data was then provided for further bioinformatics analysis. Figure 2-4 shows the workflow for the 16S rRNA gene amplicon sequencing and bioinformatic processing.

Figure 2-4: Workflow for 16S rRNA gene amplicon sequencing and further bioinformatic processing. First step is collection of samples and further extraction of DNA. Subsequently 16S rRNA gene amplicon libraries are prepared before sequencing on Illumina MiSeq platform. Sequence data processing was conducted in the de-NBI cloud using QIIME2 and further taxonomic profiling. Illustration provided by Julia Hassa, Bielefeld University.

2.3.1 16S rRNA gene amplicon library preparation

The amplicon generation for the environment and fish samples were not sufficient by applying the standard Illumina protocol on page 6 to 15 and some alterations were therefore made. For amplification of the V3-V4 region, 16Spro primers (Takahashi et al., 2014) shown in Table 2-2 were used instead of the standard Illumina 16S primers (Klindworth et al., 2013) to cover the domains of Bacteria and Archaea. The first PCR round was run with 25 cycles as described in the protocol for the environment samples, whilst 30 PCR cycles were run for the fish samples. After the first PCR, the elution of the samples was done in 15 µl for ten minutes instead of 25 µl for 2 minutes to enhance the amplicon yield. 7.5 µl of the amplified amplicon product from the first PCR was used within the second index-PCR reaction instead of 2.5 µl and no additional water was added. After the second PCR, elution was done in 22 µl instead of 25 µl. These adaptions were to increase the amplicon yields for the environment and fish samples, resulting in a more stable amplicon library generation.

Table 2-2: PCR primers used at Bielefeld University for sequencing of the V3-V4 regions of the 16S rRNA gene (Takahashi et al., 2014).

Primer name	Oligonucleotide sequence (5'-3')
16S Pro341F	CCTACGGGNBGCASCAG
16S Pro805R	GACTACNVGGGTATCTAATCC

2.3.2 Quantification, dilution and pooling of the amplicon libraries

For quantification of the amplicon libraries, the Fragment Analyzer 5200 (Agilent, USA) was used, with applying the DNF-473 NGS Fragment Kit (1-6000 bp). The concentrations were used for dilution and pooling with the NGS STAR pipetting robot (Hamilton, USA). Final concentration measurements of the amplicon library pools before sequencing were done on the Bioanalyzer (Agilent, USA) applying the High Sensitivity DNA Kit.

2.3.3 MiSeq sequencing

For sequencing of the amplicon libraries, the Illumina MiSeq platform was used, applying the MiSeq Reagent Kit v3 (600-cycle) for 2x300 bp paired-end sequences. The indexed-based demultiplexing of the sequencing reads was then performed using an in-house pipeline.

2.4 QIIME2 for Processing of Sequencing Data

To centralize the bioinformatic analyses of the amplicon and metagenomic datasets and to standardize the bioinformatic procedures, a de-NBI (German Network for Bioinformatics Infrastructure and national Elixir node) cloud project was established. This enabled for consistent processing of all generated datasets as well as access for all project partners to the data and bioinformatic analyses. The microbial analysis was conducted using QIIME2™ (Quantitative Insight Into Microbial Ecology) (Bolyen et al., 2019) for the Illumina sequenced data. QIIME2™ is a bioinformatic study tool used for microbial community analysis. The software works by executing a series of commands where the output is displayed both graphical and textual (Kuczynski et al., 2011). By using the QIIME2 software, one can perform demultiplexing of sequences and out-filtration of hypervariable regions, whereas choosing OTUs (operational taxonomic units) or ASVs (amplicon

sequence variants) can be conducted before generation of phylogenic trees and assigning taxonomy. The commands executed for the wanted results from QIIME2 are listed in Appendix H.

The data in QIIME2 exists as QIIME artifacts, meaning that they contain metadata such as the type and origin of the data. The first step of the workflow was to import the raw sample sequences into artifacts and demultiplexing the sequences. The samples were further summarized and converted to a visualization file to view the output in QIIME2 View[1]. Further, quality checks and trimming were conducted using DADA2. DADA2 is a plugin that detects and corrects Illumina-sequenced amplicon errors before removal of chimeric sequences and allows classification of ASV. ASV allows for a higher resolution compared to classical OTU clustering at specific thresholds and can detect differences down to a single nucleotide in the sequenced region (Callahan et al., 2016). Quality control thresholds were therefore chosen, based on the outputs of line 2 (Appendix H).

A phylogenetic tree was generated before adding taxonomy. The sequence variants only give information about the diversity of the sample, not what types of organisms are present. Taxonomy was therefore added using the Silva classifier specifically pretrained for the 16S rRNA region amplified by the PCR primers (silva v.138). The ASV table with taxonomy of the QIIME output was then transferred as a BIOME-file to R for downstream analysis, along with the metadata and the phylogenetic tree.

2.5 Statistical Analyses Using R

Statistical analyses were conducted using the R packages "phyloseq" (McMurdie and Holmes, 2013), "vegan" (Oksanen et al., 2022), "microbiome" (Lahti and Shetty, 2017) and "rstatix" (Kassambara, 2021). Phyloseq (from "phylogenetic sequencing") is a tool for the analysis of complex sequence data sets that already has been clustered into OTUs, or ASVs in this case. Statistical analyses of sequence data were conducted to identify types and abundances of bacterial species, as well as calculation of alpha (α)- and beta (β)-diversity.

First, the table with added taxonomy, metadata file, DNA-sequences in FASTA-format and the phylogenetic tree was loaded into R. Then, chloroplast and mitochondria assigned sequences as well as "Unassigned" sequences at kingdom level were filtered out from the dataset, and ASVs with 5 or less sequence reads were omitted. The samples were then rarefied to even sampling depth (8 027), and further analyzed.

To test α-diversity for the different microbial communities present in all the samples, observed number of ASVs, estimated richness (Chao1) and Shannon's diversity index (H') was calculated using the "alpha" function of the "microbiome" package. Observed number of ASVs is a measure of species richness, meaning how many different species are observed in a specific niche. Nevertheless, it does not account for species that are neglected during sequencing and the non-parametric Chao1 index was therefore used to estimate richness as it measures the ASVs expected in the sample if all species were identified during sequencing. In other words, it estimates expected ASVs based on the observed ASVs. However, species richness does not consider the amount of each species present, which is why diversity is dependent on evenness along with richness. Evenness is a measure of the relative abundance of all the species in a community. A commonly used index for measure of species diversity in communities is the Shannon-Weaver index

[1] https://view.qiime2.org/

because it takes into account both the species richness and the evenness (Kim et al., 2017).

Assumptions for statistical analysis of α-diversity (outlier test, normality assumption and homogeneity) was tested, and it was chosen to go with the non-parametric statistical Kruskal-Wallis test (McKight and Najab, 2010) for testing of significant difference between the communities using the "rstatix" package. Here, a p-value lower than 0.05 is an indication that the communities significantly differ from each other and was therefore chosen as threshold for statistical significance.

β-diversity was then tested to compare microbial composition between samples, using the "vegan" package. Hence, a Bray-Curtis dissimilarity matrix was produced first for all samples before sub-setting for fish and environmental samples to exploit their differences. The matrix is given in values between 0 and 1, where 0 represents dissimilar communities whereas a value of 1 represents similar communities.

Principal Coordinate Analysis (PCoA) plots were further generated based on the Bray-Curtis dissimilarities to visualize the beta-diversity, using "ggplot2" (Wickham, 2016). Distance between data points in the plot indicates how similar or dissimilar the samples are. Data points closer to each other indicate similar microbial composition, whereas points further away from each other indicate different composition. Overlapping points indicate an identical composition of the microbiota. To check significance of difference between two or more groups of samples, a one-way permutational multivariate analysis of variance (PERMANOVA) was performed based on the Bray-Curtis dissimilarities (Anderson, 2001), using the "adonis" function of the "vegan" package. A p-value of 0.05 was chosen as threshold for statistical significance. Beta dispersion test was conducted to check homogeneity of dispersion, by employing "betadisper" function of the "vegan" package.

Microbial community composition was displayed by agglomerating the ASV table to order, family and genus level and further converted to relative abundance (%).

3 Results

The main objective of this study was to use an NGS-based microbiome profiling approach to analyze microbial community structures and dynamics of Arctic charr skin, gill, and gut mucus, as well as tank and source water, tank and biofilter biofilm. This was investigated by employing Illumina amplicon sequencing of the V3-V4 region of the 16S rRNA gene and subsequent bioinformatic and statistic data processing. This systematic and comprehensive spatiotemporal analysis of the microbiota in different built environments and corresponding host in a commercial Arctic charr aquaculture facility provides a profound data basis for generating new knowledge on microbial water quality and host microbiome dynamics covering the different life-stages of an entire production cycle. A total of 432 samples were collected at NFFT over a period of 6 months.

3.1 Purity of Total DNA Extracts

Purity and concentrations of total DNA from all samples (90 skin, 90 gill, 90 gut, 72 water and 90 biofilm) were measured for all 6 sampling months using NanoDrop 1000 and Qubit, as described in Chapter 2.

In general, DNA extracts from skin showed purity values close to ~1.8 for the 260/280 ratio (Figure 3-1 A) for all monitored rearing systems, indicating sufficient purity and quality of the extracted DNA for sequencing. Exceptions were seen at the start of the sampling period, where the values fell both below and above wanted ratio. For those falling below, it is an indication of other contaminants present, or proteins or phenols. The values falling above 1.8 indicates presence of RNA. For the 260/230 ratio, most of the skin samples from the three systems fell below the desired value of ~1.8-2.2 (Figure 3-1 B), indicating a low purity and presence of co-purified contaminants. However, some samples from the FTS and one from RAS_1 and RAS_2 displayed values within the wanted limits.

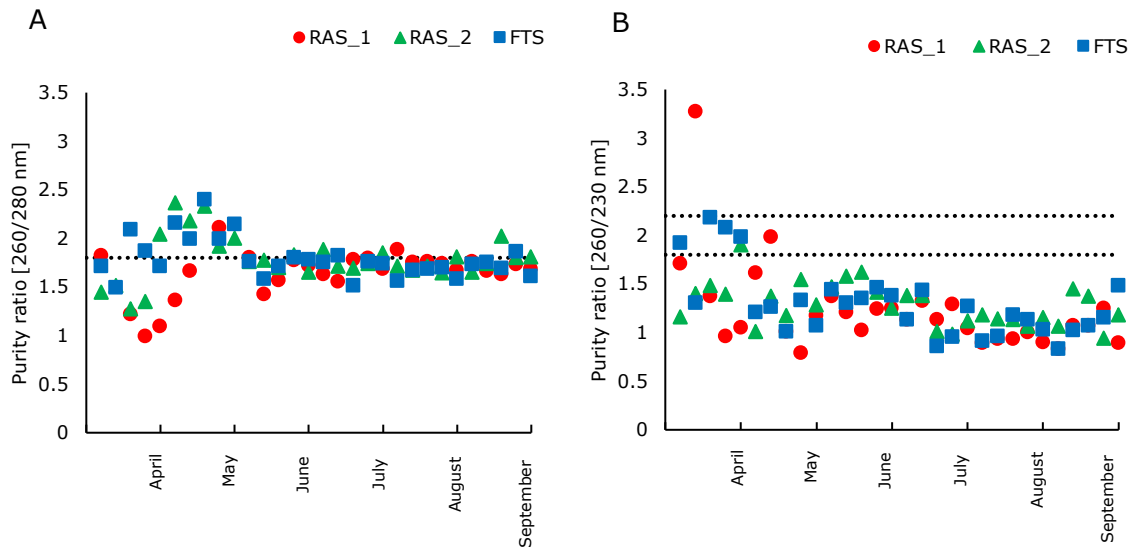

Figure 3-1: Scatter plots showing the 260/280 (A) and 260/230 (B) ratio values from skin samples in RAS_1, RAS_2, and FTS (n = 30 for each system). Dotted line(s) indicate optimal purity ratio of 1.8 (A) and 1.8-2.2 (B).

Generally, DNA extracts from gill showed values along the wanted purity ratio of ~1.8 for the 260/280 ratio for all systems (Figure 3-2 A). For the 260/230 ratio, DNA extracts from gill showed a variety of purities falling within and without the wanted purity ratio of ~1.8-2.2 (Figure 3-2 B), indicating lower purity. The greatest variation was seen at the end of the sampling period where the purity fell below the wanted purity limits for every system.

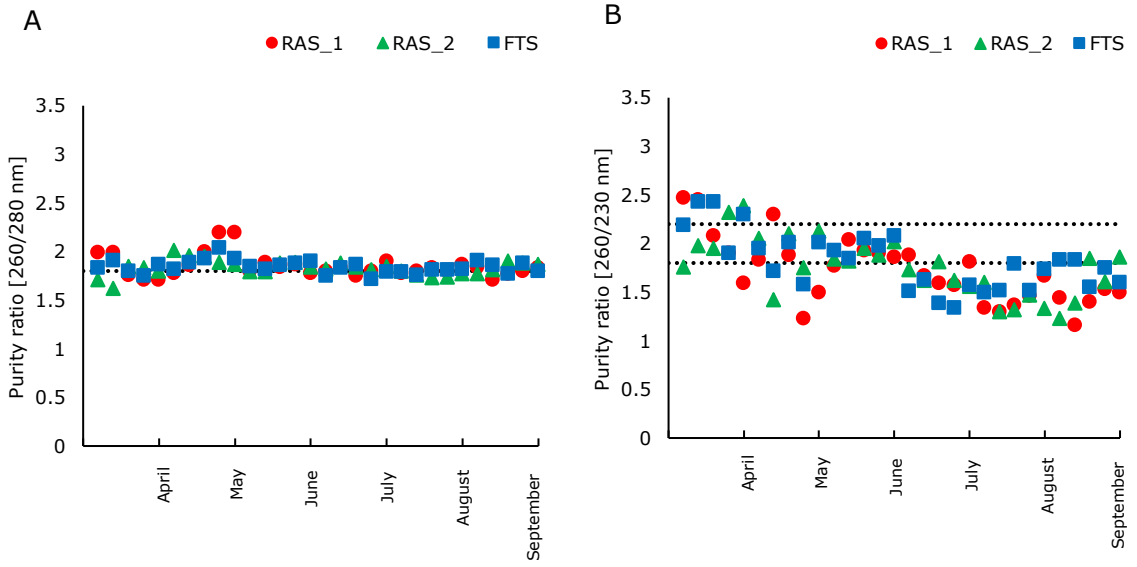

Figure 3-2: Scatter plots showing the 260/280 (A) and 260/230 (B) ratio values from gill samples in RAS_1, RAS_2, and FTS (n = 30 for each system). Dotted line(s) indicate optimal purity ratio of 1.8 (A) and 1.8-2.2 (B).

DNA extracts from gut samples showed values close to the optimal purity value of ~1.8 for ratio 260/280 (Figure 3-3 A) for all three systems, except from at the start of sampling of RAS_1 and RAS_2 which displayed a few values falling below. For the 260/230 ratio, DNA extracts from gut samples showed values falling mostly within the optimal purity value range of ~1.8-2.2 (Figure 3-3 B), except from some sampling points for RAS_1 and RAS_2. Overall, gut samples showed values closer to both purity ratios compared to skin and gill samples.

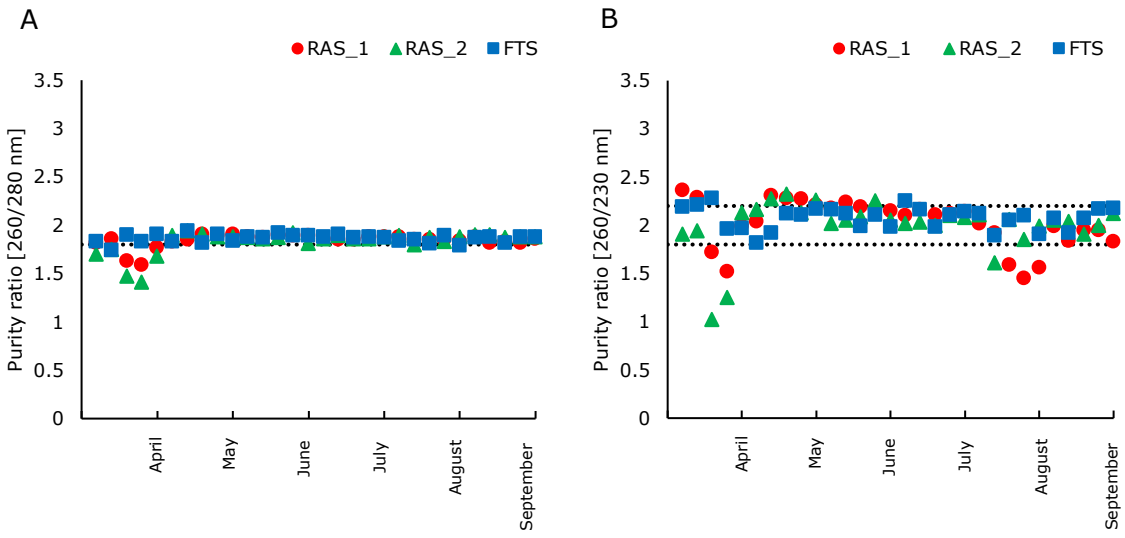

Figure 3-3: Scatter plots showing the 260/280 (A) and 260/230 (B) ratio values from gut samples in RAS_1, RAS_2, and FTS (n = 30 for each system). Dotted line(s) indicate optimal purity ratio of 1.8 (A) and 1.8-2.2 (B).

The water samples in the three systems showed in general values spreading below and above the wanted purity limit of ~1.8 for the 260/280 ratio (Figure 3-4 A). The same was observed for the source water (same for all three systems), which had especially low purity. All water samples showed values falling far below the optimal purity limits of ~1.8-2.2 for the 260/230 ratio (Figure 3-4 B), which indicates low purity in the samples and presence of contaminants.

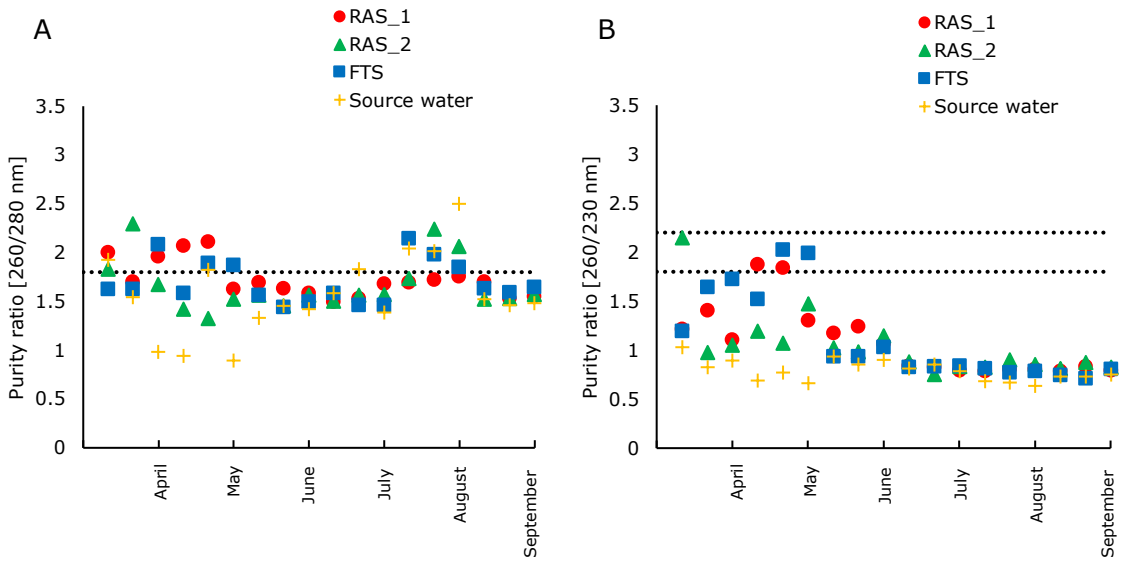

Figure 3-4: Scatter plots showing the 260/280 (A) and 260/230 (B) ratio values from water samples in RAS_1, RAS_2, FTS, and the source water (n = 18 for each). Dotted line(s) indicate optimal purity ratio of 1.8 (A) and 1.8-2.2 (B).

All three sampling tanks showed in general values falling on the optimal purity value of ~1.8 for the 260/280 ratio for biofilm samples (Figure 3-5 A). However, most values fell below the optimal purity value range of ~1.8-2.2 for the 260/230 ratio indicating lower purity (Figure 3-5 B). An exception was seen at the start of sampling, where the values fell closer to the purity range for all three tanks.

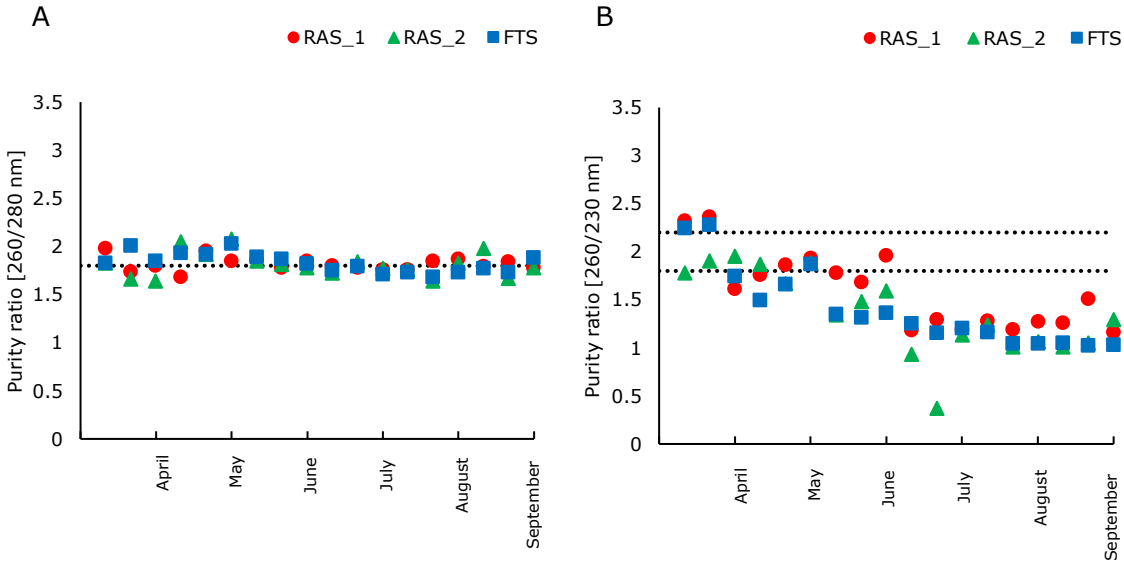

Figure 3-5: Scatter plots showing the 260/280 (A) and 260/230 (B) ratio values from tank biofilm in RAS_1, RAS_2, and FTS (n = 18 for each system). Dotted line(s) indicate optimal purity ratio of 1.8 (A) and 1.8-2.2 (B).

In general, both FBBF and MBBF showed values falling on the desired purity value of ~1.8 for the 260/280 for all samplings (Figure 3-6 A). Same as for the tank biofilm was seen for the biofilter biofilm for the 260/230 ratio (Figure 3-6 B). The samples displayed values within the range of ~1.8-2.2 before falling below the range mid-sampling.

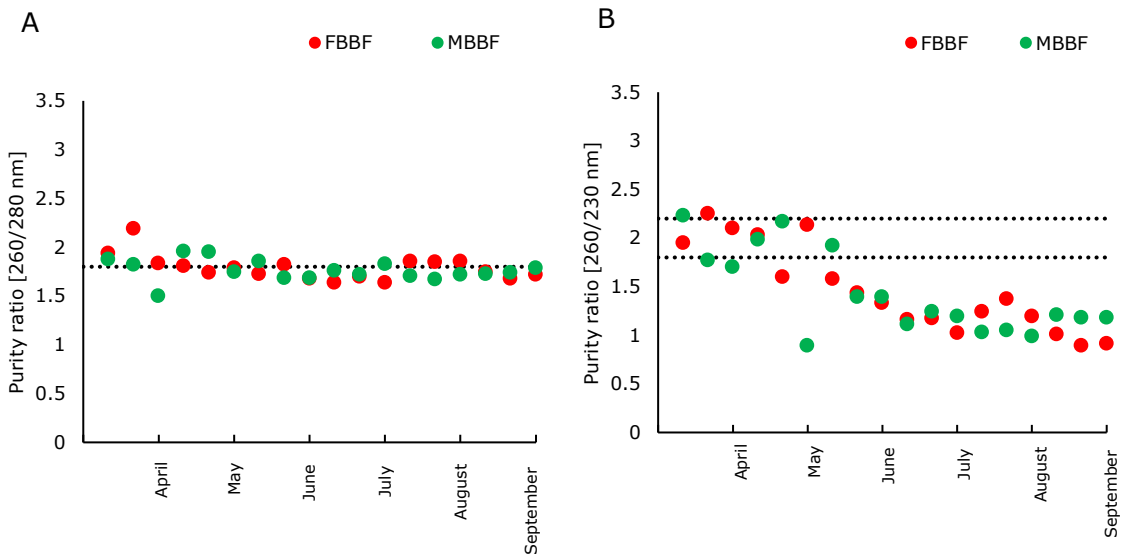

Figure 3-6: Scatter plots showing the 260/280 (A) and 260/230 (B) ratio values from biofilter biofilm samples from FBBF and MBBF. Dotted line(s) indicate optimal purity ratio of 1.8 (A) and 1.8-2.2 (B).

More precise measurements of the total DNA from skin, gill, and gut samples were conducted using Qubit for targeted quantification of dsDNA.

Overall, highest DNA concentration for skin samples (Figure 3-7 A) was measured in RAS_2 and FTS (median value of 12.2 ng/µ for both systems) compared to median value of 6.0 ng/µl for RAS_1. An outlier was observed for the FTS.

Gill samples (Figure 3-7 B) showed similar values of total DNA concentration for the three systems with median values of 39.6 ng/µl for both RAS_1 and RAS_2, and median value of 39.0 ng/µl for the FTS. An outlier each was observed for RAS_1 and RAS_2.

DsDNA analysis for gut (Figure 3-7 C) also showed the highest median total DNA concentration for RAS_1 and FTS (50.7 ng/µl) followed by RAS_2 (42.0 ng/µl).

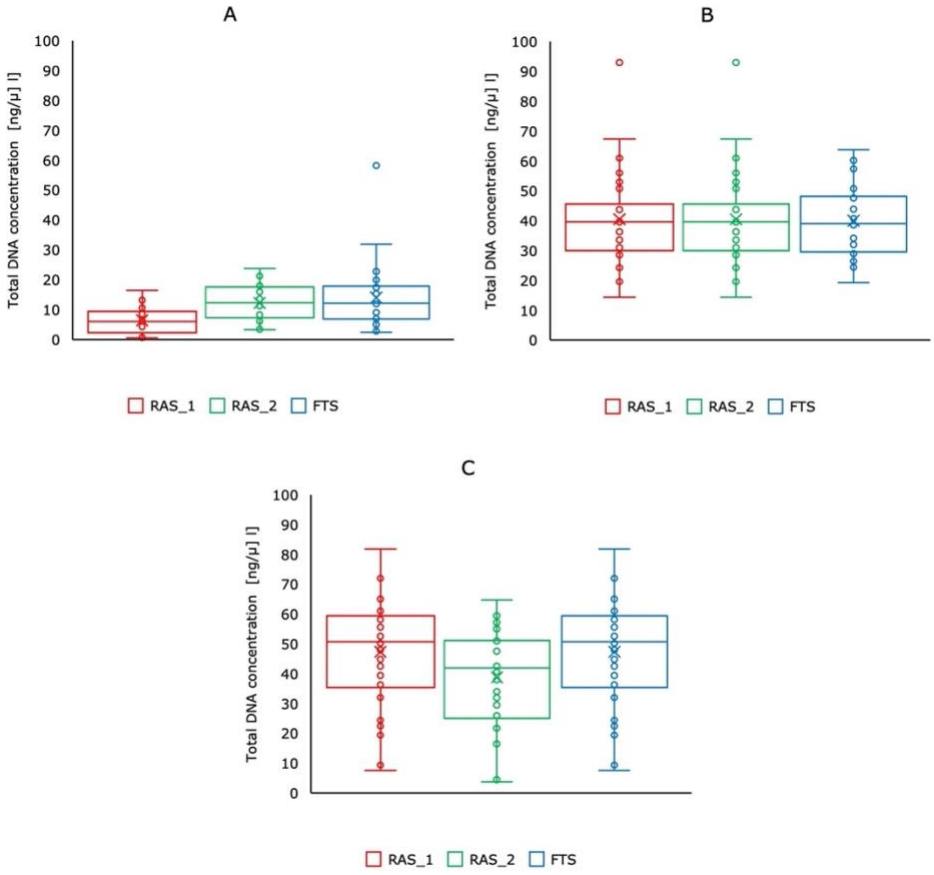

Figure 3-7: Box plot showing the total dsDNA concentration for the skin (A), gill (B), and gut (C) samples for each system obtained from sampling (n = 30 for each system). Each sample is represented by a dot, whereas the whiskers show the highest and lowest value of dsDNA.

Precise quantification of dsDNA was also conducted for environment samples. The tank water (Figure 3-8 A) for the three systems showed overall low, yet similar, median values of total DNA concentration (4.5 ng/µl, 4.5 ng/µl, and 2.1 ng/µl respectively), whereas the source water displayed a median value of 0.0037 ng/µl. Outliers were observed for RAS_2 and FTS.

The tank with the highest total DNA concentration for tank biofilm (Figure 3-8 B) was RAS_1 with a median value of 30.9 ng/µl, followed by RAS_2 and FTS (median value of 21.9 ng/µl and 21.1 ng/µl, respectively). The biofilter biofilm (Figure 3-8 C) samples displayed lower total DNA concentration than tank biofilm, where the MBBF showed a median value of 19.55 ng/µl whereas the FBBF showed a median value of 15.5 ng/µl.

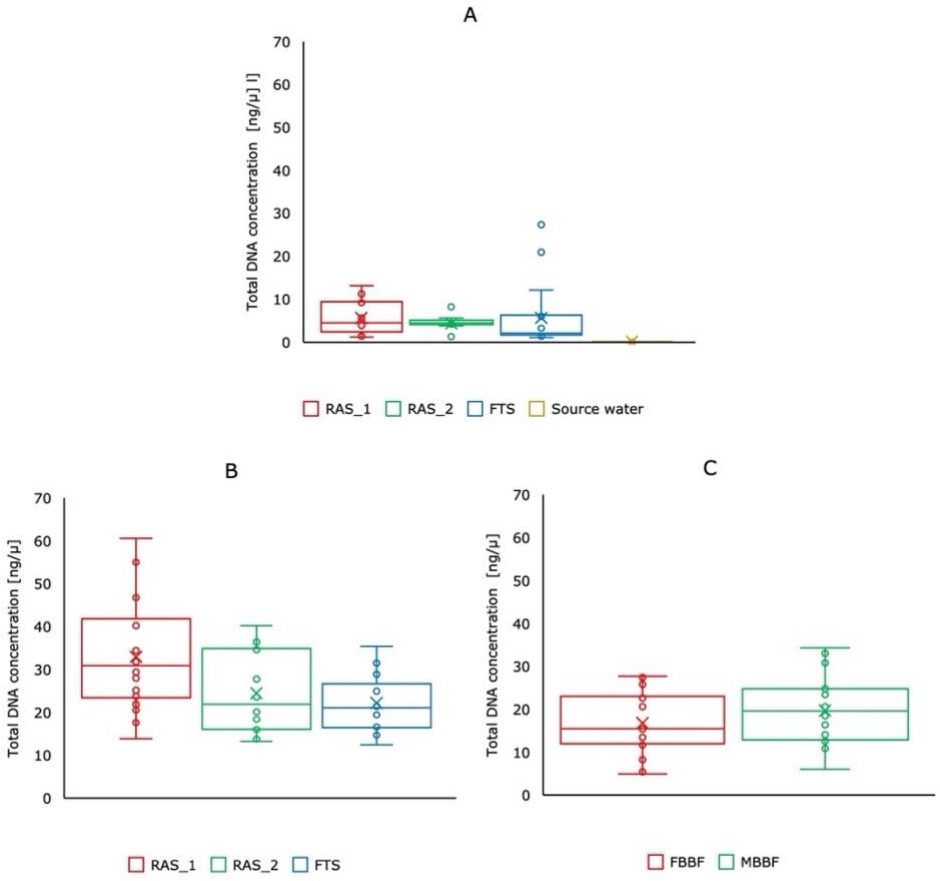

Figure 3-8: Box plot showing the total dsDNA concentration for the tank and source water (A), tank biofilm (B), and biofilter biofilm (C) samples for each system obtained from sampling (n = 18 for each system). Each sample is represented by a dot, whereas the whiskers show the highest and lowest value of dsDNA.

3.2 Microbial Community Analysis

In order to characterize the microbial composition of Arctic charr skin, gill, and gut samples from the three systems in the facility, Illumina 16S rRNA sequencing was conducted. The sequencing method was also conducted for the characterization of microbial composition in environmental samples such as the tank water, source water, tank biofilm, and biofilter biofilm. Systematic sampling over a 6 month period in different built environments harboring different life-stages of the host was conducted to reveal spatiotemporal microbial community structures and dynamics over an entire production cycle.

3.2.1 Downstream processing of sequence data

All samples (90 skin, gill, and gut, 72 water and 90 biofilm) were sent for DNA amplicon sequencing to CeBiTec (Centre of Biotechnology), Bielefeld University. After processing the sequenced data in QIIME2 by quality filtering and chimera removal as explained in Chapter 2, a total of 28 987 963 sequence reads were retrieved from the 432 samples. The numbers of average reads varied between the sample positions (Table 3-1), but in general, the highest average numbers of reads from fish samples were obtained from the gut mucus samples with an average of 60 027. The highest average numbers of reads from the

environment samples were obtained from the tank biofilm samples with an average of 104 042 reads.

Table 3-1: Average numbers of sequence reads (± standard deviation) retained after quality filtering and chimera removal for skin, gill, and gut mucus, source and tank water, tank and biofilter biofilm samples.

Sample position	Average number of reads (± SD)
Skin mucus	41 255 ± 13 556
Gill mucus	41 059 ± 12 310
Gut mucus	60 027 ± 23 530
Source water	90 136 ± 16 241
Tank water	101 886 ± 37 809
Tank biofilm	104 042 ± 53 195
Biofilter biofilm	95 411 ± 34 358

Filtering of chloroplast and mitochondria, as well as "Unassigned" sequences was performed as described in Chapter 2 and left 18 875 ASVs in total. The taxa were then pruned by removing ASVs consisting of less than five reads resulting in 15 502 ASVs. The samples were rarefied to 8 027 reads, resulting in 13 743 ASVs and 344 samples meaning that 88 samples were removed. The samples removed were 9 skin samples, 52 gill and 27 gut. 344 samples were then further analyzed.

3.2.2 Alpha diversity measures

Average observed and estimated ASV richness as well as Shannon's diversity index for fish samples (skin, gill, and gut mucus) for the three systems (RAS_1, RAS_2 and FTS) was calculated on ASV level (Figure 3-9). By comparison of estimated ASV richness (Chao1) and observed ASV richness, the average sequencing coverage was found to be 96.9% for skin samples, 97.4% for gill samples and 94.4% for gut samples.

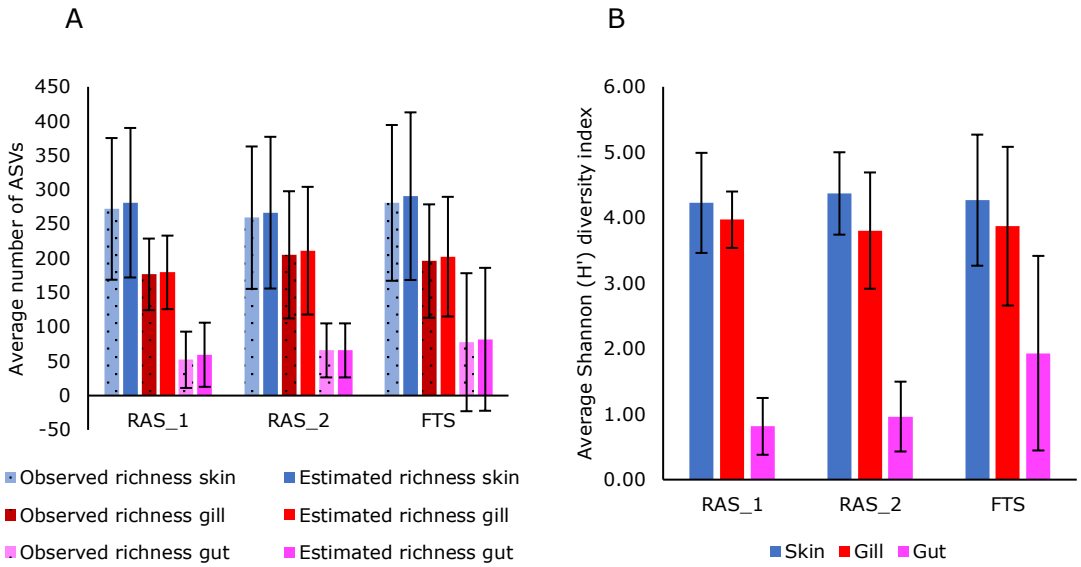

Figure 3-9: Alpha diversity indices for fish samples from the three systems (RAS_1, RAS_2, and FTS) in the facility. A: Average ASV richness, observed and estimated (Chao1) for skin, gill, and gut samples. B: Average Shannon's (H') diversity index for skin, gill, and gut samples in the three systems (RAS_1, RAS_2 and FTS). Error bars indicate standard deviation (± SD).

In general, observed richness values were in very good agreement with corresponding estimated richness values for fish samples (Figure 3-9 A). The skin samples displayed the highest Shannon's diversity index of the fish samples, suggesting that the skin samples have a higher diversity of species than the gill and the gut (Figure 3-9 B). However, a Kruskal-Wallis test did not reveal any significant differences in neither richness, nor Shannon diversity, between any of the three systems (for skin samples) indicating that the diversity throughout the systems is similar ($p > 0.05$).

The gill samples showed the second to largest richness and Shannon diversity of the fish samples (Figure 3-9). A Kruskal-Wallis test did not reveal any significant differences in richness, nor Shannon diversity, between any of the three systems for gill samples ($p > 0.05$).

The gut samples displayed the lowest richness and Shannon diversity in all systems (Figure 3-9). For Shannon diversity, the index was higher for the FTS than the two RAS. A Kruskal-Wallis test revealed significant difference for Shannon's diversity index between RAS_1 and FTS ($p < 0.05$), but not for measured richness ($p > 0.05$). There was not found significant differences between RAS_1 and RAS_2, nor RAS_2 and FTS, for any of the alpha diversity measures ($p > 0.05$).

Average ASV observed and estimated richness as well as Shannon's diversity index for built environment samples (tank water, tank biofilm and biofilter biofilm) for the three systems (RAS_1, RAS_2 and FTS), as well as the facility' native environment (source water) was calculated on ASV level (Figure 3-10). Biofilter biofilm is not included for the FTS as it did not have a biofilter in its system. By comparison of estimated ASV richness (Chao1) and observed ASV richness, the average sequencing coverage was found to be 88.7% for source water samples, 82.8% for tank water samples, 88.1% for tank biofilm samples, and 88.0% for biofilter biofilm samples.

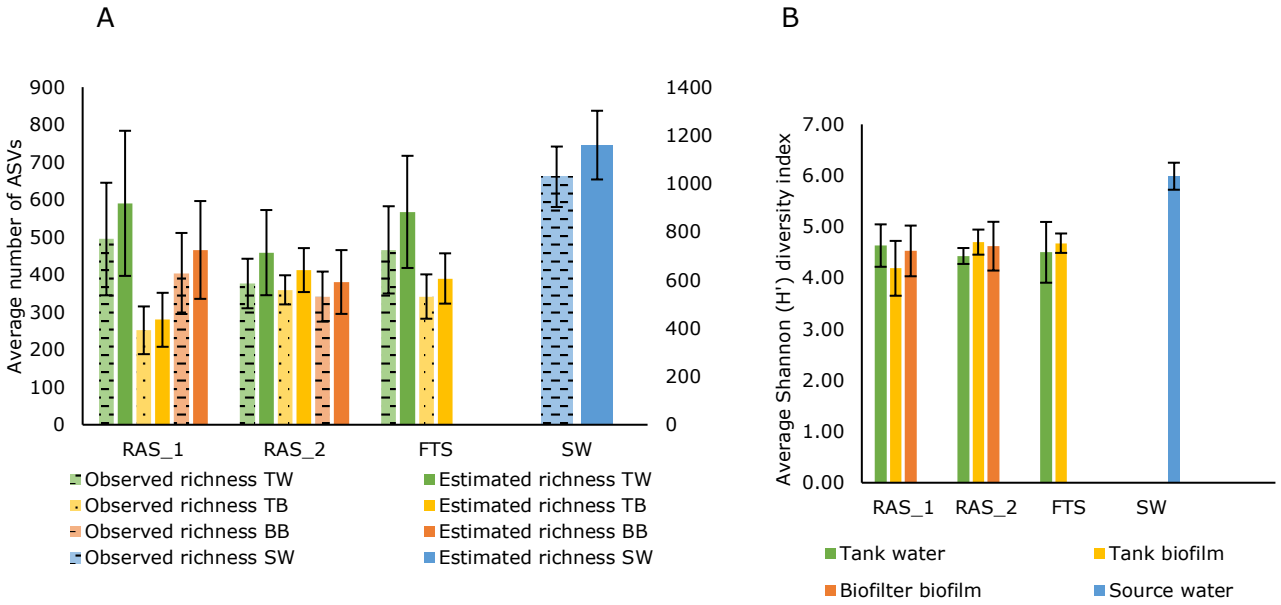

Figure 3-10: Alpha diversity indices for built environment samples (TW, TB, and BB) from the three systems (RAS_1, RAS_2, and FTS) in the facility as well as its native environmental sample (SW). A: Average ASV richness, observed and estimated (Chao1), for environment samples. TW = tank water, TB = tank biofilm, BB = biofilter biofilm, SW = source water. Values for SW are displayed on the secondary y-axis (right) due to high values. B: Average Shannon's (H') diversity index for environment samples (tank water, tank biofilm, biofilter biofilm), as well as the facility' source water. Error bars indicate standard deviation (± SD).

The tank water displayed highest observed and estimated richness in all three systems compared to the other built environment samples (Figure 3-10 A). Significant difference for observed richness between RAS_1 and RAS_2 was confirmed by a Kruskal-Wallis test ($p < 0.05$). In contrast, no significant differences were discovered between the tank water in the systems for neither estimated richness (Figure 3-10 A, $p > 0.05$) nor Shannon's diversity index (Figure 3-10 B, $p > 0.05$). For the native environment samples, the richness and Shannon's diversity index was much higher than the tank water and hence other built environmental samples (Figure 3-10). A Kruskal-Wallis test confirmed significant differences between native and built environmental samples between all systems for all alpha diversity measures ($p < 0.05$).

For tank biofilm samples, the richness was lowest in RAS_1 while RAS_2 and FTS showed similar richness (Figure 3-10 A). The same trend was seen for Shannon's diversity index where RAS_1 displayed the lowest index, whereas RAS_2 and FTS was quite consistent (Figure 3-10 B). A Kruskal-Wallis test revealed significant differences for all three measurements between RAS_1 and RAS_2, as well as RAS_1 and FTS ($p < 0.05$). No significant differences were discovered between RAS_2 and FTS ($p > 0.05$).

The FTS did not have a biofilter in connection to it. For the two RAS, RAS_1 connected to the FBBF displayed higher richness than the MBBF in connection to RAS_2 (Figure 3-10 A). For Shannon's diversity index, both biofilters showed approximately the same index of 4.5 and 4.6, respectively (Figure 3-10 B), suggesting that their species diversity is similar. When conducting a Kruskal-Wallis test, no significant differences were revealed between the two biofilters for any of the alpha diversity measures ($p > 0.05$).

The alpha diversity was also tested within the three production systems across all sampling positions. Minor differences regarding richness were observed (Figure 3-9 A and Figure 3-10 A), however statistically significant ($p < 0.05$), except from between biofilter biofilm

and tank biofilm and water for observed richness, and biofilter biofilm and tank biofilm for estimated richness within the three systems ($p > 0.05$). Also, calculated Shannon's diversity indices were quite consistent within the systems (Figure 3-9 B and Figure 3-10 B). However, a Kruskal-Wallis test revealed significant differences ($p < 0.05$) for Shannon diversity between all sample position except from between the built environment samples (TW, TW and BB, $p > 0.05$), and between the skin mucus and the built environment ($p > 0.05$). Nor was there found significant difference in Shannon diversity between the skin mucus and gill mucus ($p > 0.05$).

To check for temporal changes, the alpha diversity was tested for each sampling position in its respective system across the 6 sampling months. There were not found significant differences in richness or diversity for fish and environment samples in the systems ($p > 0.05$), and it is therefore not further presented.

To summarize, the environment samples displayed overall higher values for observed and estimated richness, and Shannon's diversity index than the fish samples. This was consistent observations for all three systems. Also, the three different production system does not affect richness as much, whereas treatment of the source water generally leads to lower diversity in all three systems.

3.2.3 Beta diversity measures

β-diversity is the diversity of species found between environments. A PCoA plot based on Bray-Curtis dissimilarities, where microbial profiles from all samples are visualized, provides a comprehensive overview of how similar or different the microbial communities in the individual samples are to each other and is shown in Figure 3-11. As expected, the plot shows that the environment samples cluster together, whereas the fish samples cluster together. However, some deviations are seen for the gut samples which cluster more independently of the other fish samples.

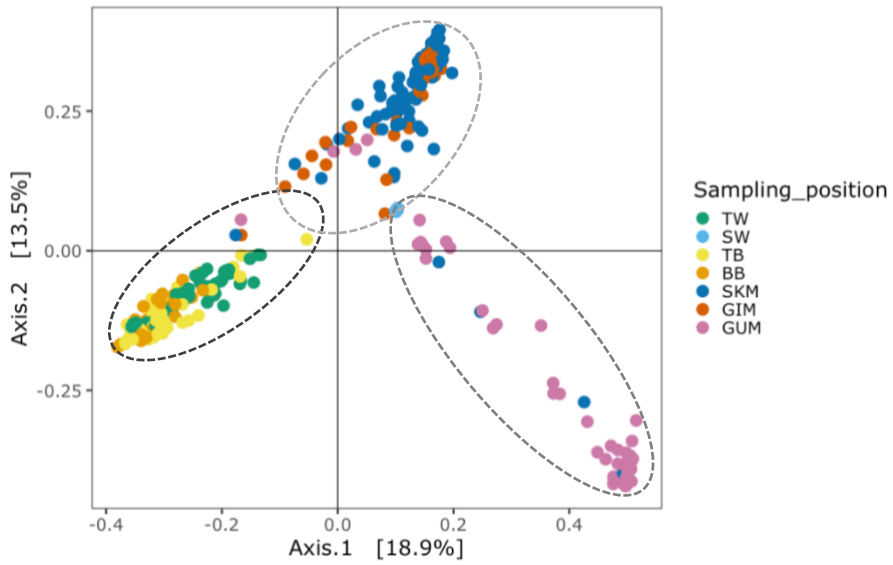

Figure 3-11: PCoA plot based on Bray-Curtis dissimilarities on ASV level for comparison of the microbial communities present in the samples collected at NFFT over a period of 6 months. The seven sample types are differentiated based on color. TW = tank water, SW = source water, TB = tank biofilm, BB = biofilter biofilm, SKM = skin mucus, GIM = gill mucus and GUM = gut mucus.

Beta diversity in host microbiomes

To investigate potential differences in community profiles between the three production systems, a PCoA plot based on Bray-Curtis dissimilarities visualizing bacterial profiles of all fish samples (skin, gill, and gut) in the three production systems (RAS_1, RAS_2, and FTS) on ASV level was prepared and is shown in Figure 3-12. When all sample results from the entire monitoring period are plotted without temporal resolution, no clear separation between skin and gill mucus microbiota in the three different production systems was obvious (Figure 3-12). Also, gut microbiome profiles were not clearly separated accordingly to the production system (Figure 3-12). However, while skin and gill mucus microbiomes separated horizontally along axis 2, and vertical to axis 1, gut microbiomes separated horizontally along axis 1. This suggests that gut microbiomes are more different from skin and gill microbiomes than the latter two to each other.

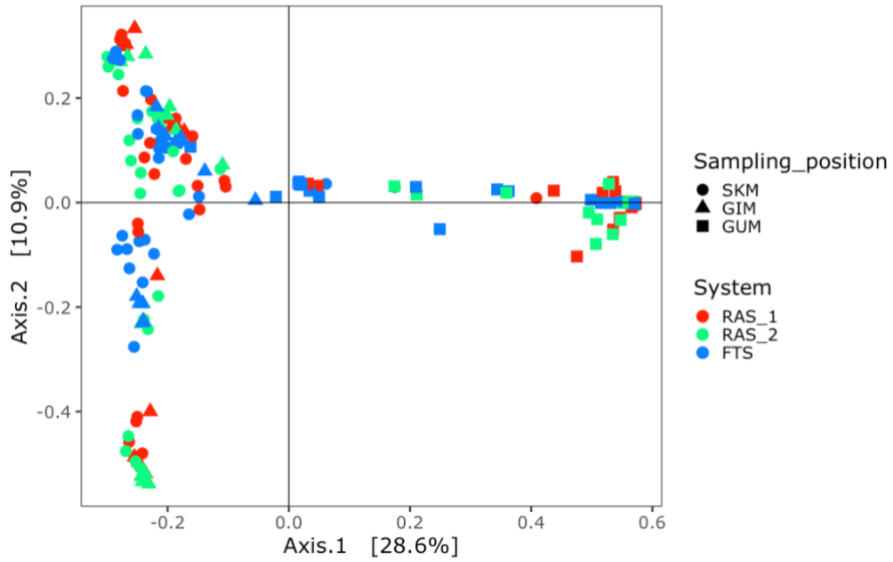

Figure 3-12: PCoA plot based on Bray-Curtis dissimilarities on ASV level for comparison of the microbial communities present in the fish mucus samples (SKM = skin, GIM = gill and GUM = gut) from the three different systems (RAS_1, RAS_2 and FTS) over a period of 6 months.

In order to verify the visual observations statistically, a one-way PERMANOVA test was conducted including all host samples from the three systems. The test revealed that microbiome profiles in skin, gill, and gut samples were significantly different ($p < 0.05$). In order to assess the microbiome variance and thus indicate reliability of beta-diversity data, a beta dispersion test was conducted on the same data. Results indicated that significant differences in microbiome profiles may be caused by the different dispersion of data.

To examine the potential differences further and increase resolution, PCoA plots based on Bray-Curtis dissimilarities were prepared on ASV level for the fish samples in each of the three production systems (Figure 3-13).

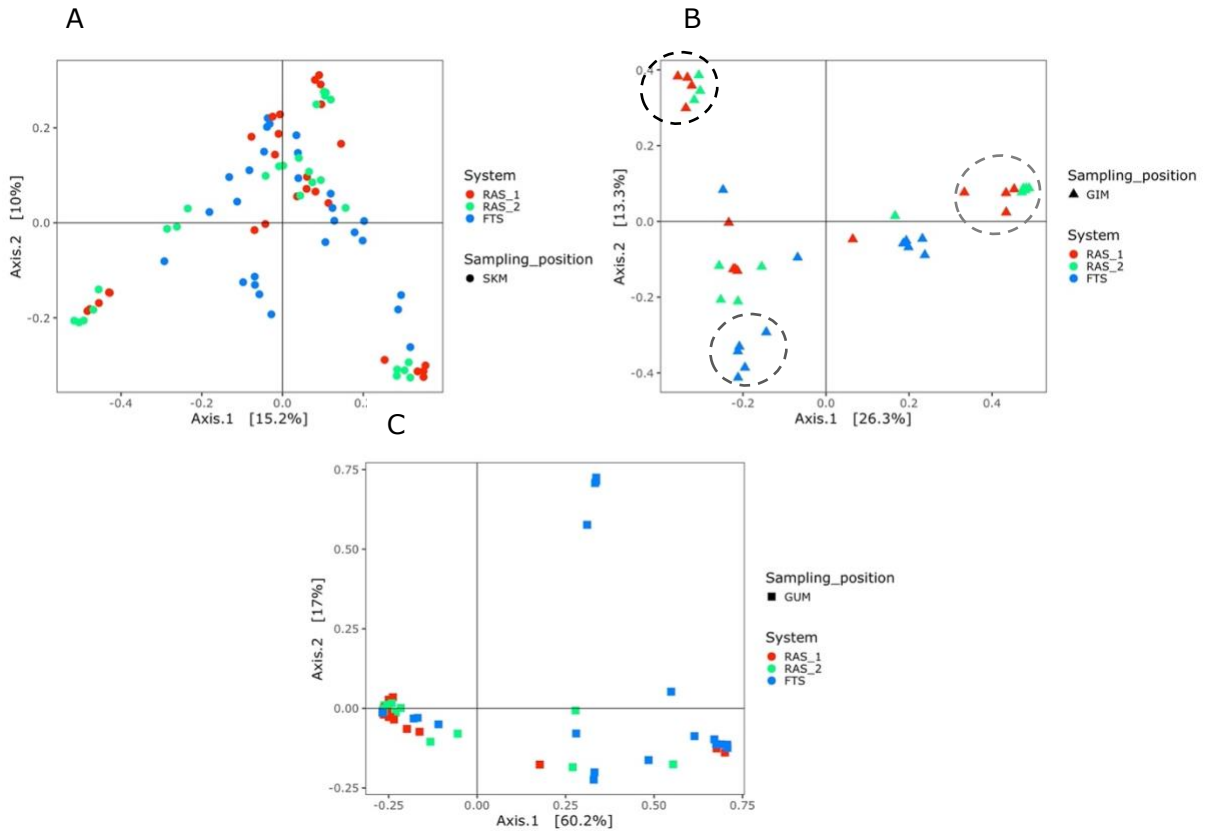

Figure 3-13: PCoA plots based on Bray-Curtis dissimilarities on ASV level for comparison of the microbial communities present in the skin samples (A), gill samples (B), and gut samples (C) from the three different systems (RAS_1, RAS_2 and FTS) over a period of 6 months.

Skin mucus samples: Bray-Curtis dissimilarities for skin mucus samples in the individual production systems on ASV level revealed no clear clustering according to the different systems, as seen in Figure 3-13 A. However, the plot shows that samples from RAS_1 and RAS_2 were tendentially closer located (more similar) and more distant (less similar) to samples from the FTS. The visual observations were tested statistically by a one-way PERMANOVA test confirming significant difference between skin samples from both RAS and the FTS ($p < 0.05$). Interestingly, no significant difference was revealed between RAS_1 and RAS_2 ($p > 0.05$). The beta dispersion test did not reveal significance ($p > 0.05$), meaning that one can be certain that the significance is the real significance and not due to the different dispersion of the data.

Gill mucus samples: As indicated by the circles in Figure 3-13 B, there are two clusters with gill samples from RAS_1 and RAS_2 that cluster further away from the remaining samples, indicating that their microbial community composition is more similar. However, there is also a cluster with FTS samples clustering further away from the two clusters from the RAS suggesting that the microbiota of the FTS is less similar to the RAS. Likewise, as for skin samples a one-way PERMANOVA test revealed significant difference between both RAS and the FTS ($p < 0.05$), but not between RAS_1 and RAS_2 ($p > 0.05$). Beta dispersion test confirmed that the significant differences in microbiome profiles may not be caused by the different dispersion of data ($p > 0.05$).

Gut mucus samples: As shown in Figure 3-13 C, gut samples are well dispersed independent of the production system and no obvious clusters was identified, indicating overall similar microbiota composition in the systems. A few samples from FTS are more

distant from the rest (less similar), but compared to the skin and gill samples, there was observed less clustering of the two RAS independent of the FTS. However, a one-way PERMANOVA test revealed significant difference between both RAS and the FTS ($p < 0.05$), but not between RAS_1 and RAS_2 ($p > 0.05$), as it also did for skin and gill mucus samples. However, a beta dispersion test revealed significance as well ($p < 0.05$), indicating that significant differences in microbiome profiles may be caused by the different dispersion of data.

In summary, the here-presented beta-diversity show that the microbial communities of fish samples from the two RAS are more similar to each other than the FTS. Since the three systems are operated with three different water treatments, these observations are thought to be caused by differences in water treatment in RAS_1, RAS_2 and FTS.

Beta diversity in built environment samples

As for the fish samples, a PCoA plot of only built environment samples was made to investigate potential differences in microbial composition between the three systems and different location in each system (Figure 3-14). The source water was not included in the plot, as it is not related to a specific system. Nevertheless, as the three systems are connected to the same source water, a PCoA plot of all environment samples can be found in Appendix I. It reveals (Figure I-1) that the built environment clusters far away from the native environment, suggesting that the native environment has different microbial composition than the built environment. This was tested statistically and significant difference between the native environment and all other samples were found (one-way PERMANOVA, $p < 0.05$).

As indicated by the ellipses in Figure 3-14, tank water samples scatter close for the three systems and apart from the biofilm samples. However, the tank biofilm samples from the FTS are clustering with the tank and biofilter biofilm samples from RAS_2. The plot indicates that the tank biofilm is relative similar for RAS_2 and FTS, whereas RAS_1 is clustered more by itself and more closely to the biofilter biofilm from the FBBF (connected to RAS_1). The MBBF biofilm (connected to RAS_2) is indicated to be similar to the tank biofilm of RAS_2 and the FTS.

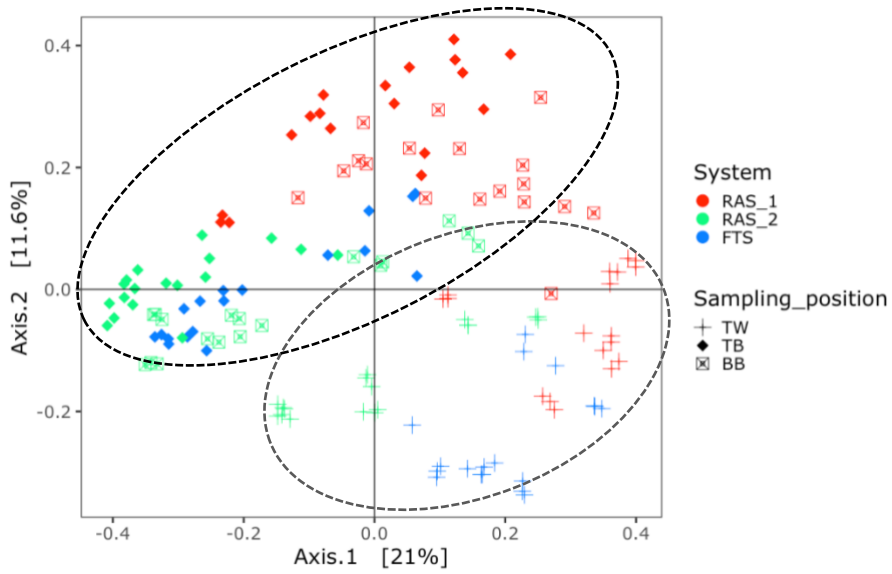

Figure 3-14: PCoA plot based on Bray-Curtis dissimilarities on ASV level for comparison of the microbial communities present in the built environment samples (TW = tank water, TB = tank biofilm and BB = biofilter biofilm) from the three different systems (RAS_1, RAS_2 and FTS) over a period of 6 months.

A one-way PERMANOVA test was conducted on built environment samples from the three systems to verify the visual observations statistically. It revealed significant difference in microbial composition between built environmental samples from all three systems ($p < 0.05$). However, a beta dispersion test was conducted to indicate reliability of beta-dispersion data, and it also revealed significant difference ($p < 0.05$) indicating that one cannot be certain that the significance in microbiome profiles is not caused by the different dispersion of the data.

To examine the potential differences further and increase resolution, PCoA plots based on Bray-Curtis dissimilarities were prepared on ASV level for the built environment samples in each of the three production systems (Figure 3-15).

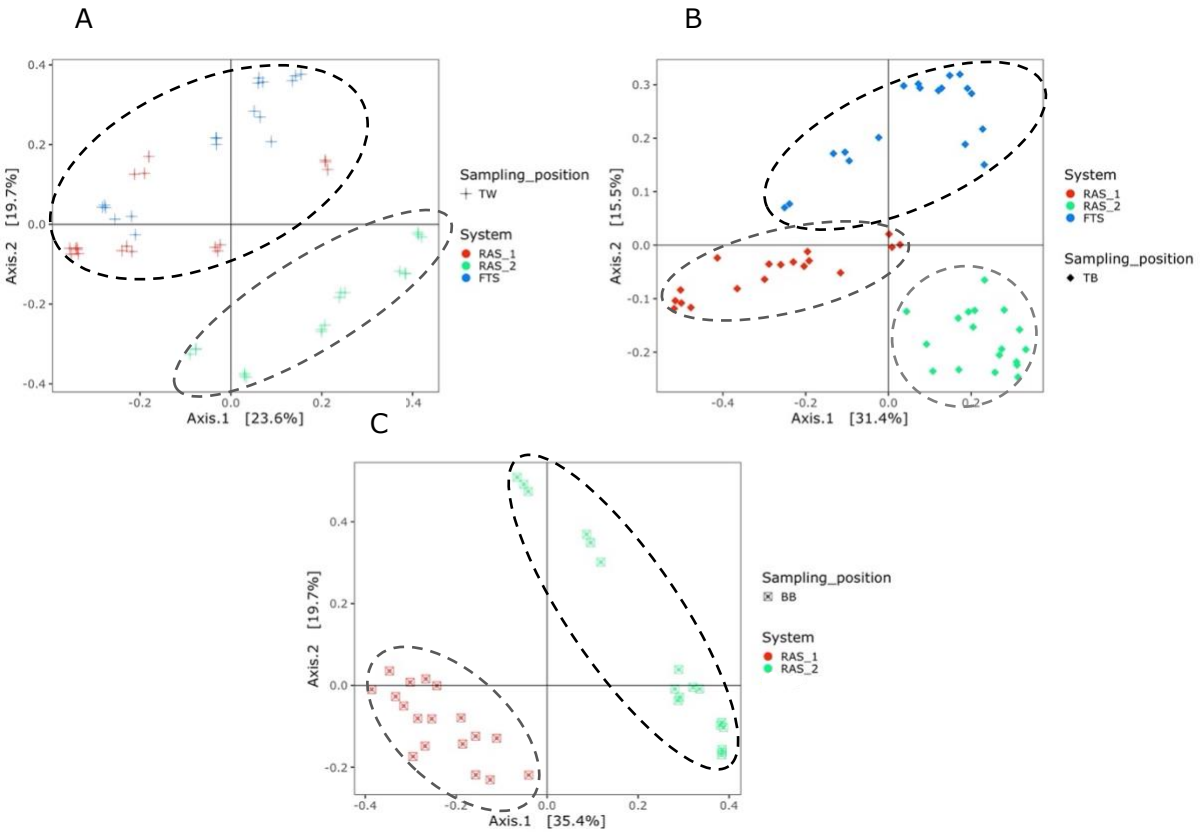

Figure 3-15: PCoA plots based on Bray-Curtis dissimilarities on ASV level for comparison of the microbial communities present in the tank water samples (A), tank biofilm samples (B), and biofilter biofilm samples (C) from the three different systems (RAS_1, RAS_2 and FTS) over a period of 6 months. The FTS did not have a biofilter connected to it and is therefore not present in C.

Tank water samples: As indicated by the ellipses in the PCoA plot displayed in Figure 3-15 A, samples from RAS_1 cluster closer to FTS than RAS_2 samples, suggesting a more similar microbial community profile in tank water in RAS_1 and FTS. RAS_2 samples cluster more distant from the rest. However, a one-way PERMANOVA test revealed significant difference between all three systems ($p < 0.05$). The corresponding beta dispersion test confirmed that the significant differences in microbiome profiles may not be caused by the different dispersion of data ($p > 0.05$).

Tank biofilm samples: The ellipses in the PCoA plot displayed in Figure 3-15 B indicates that tank biofilm from the three systems cluster independently of each other, suggesting that they have different microbial community composition which may be caused by different environmental conditions. A one-way PERMANOVA test confirmed the visual observations by revealing significant difference between all systems ($p < 0.05$). However, the corresponding beta dispersion test also revealed significance ($p < 0.05$) indicating that the significant difference found may be caused by the different dispersion of data.

Biofilter biofilm samples (only in RAS): The ellipses in the PCoA plot in Figure 3-15 C suggests that the biofilters in the two RAS units have different community composition since they cluster apart from each other. A one-way PERMANOVA test revealed significant difference between the two biofilters ($p < 0.05$), but the corresponding beta dispersion test also revealed significance ($p < 0.05$) meaning that one cannot be sure that the significance observed is the real significance and not due to the different dispersion of samples.

In summary, the here presented beta-diversity results showed that environment samples are significantly different in microbial composition between the systems.

As for alpha diversity, the beta diversity within each system was tested between all sampling positions. When considering the systems independent of each other, a one-way PERMANOVA test revealed significance ($p < 0.05$) between all sample positions within all three systems.

In total summary, the here presented beta diversity results for both fish and environment samples showed that the microbial composition is mainly caused by the sample type and its system (RAS versus FTS). The water and biofilm samples were significantly different across the systems, and also show in Figure 3-11 that they cluster closer to skin and gill samples, suggesting that the microbiomes of skin and gill samples were closer related to the built environment than gut samples.

3.2.4 Temporal changes in host microbiome

To investigate if the microbial composition of the different sampling position within each production system differed between the sampling months, PCoA plots based on Bray-Curtis dissimilarities were generated for the fish samples on ASV level (Figure 3-16, Figure 3-17, and Figure 3-18).

Skin mucus samples: As indicated by the circles in the PCoA plot of skin samples from RAS_1 (Figure 3-16 A), May and August cluster further from the rest, whereas no obvious clustering was seen for the remaining sampling months. PCoA plot from RAS_2 (Figure 3-16 B) suggest that July and September cluster closer together than the rest, whereas May and August scatter furthest away from the rest of the samples, indicated by the circles. This was seen in RAS_1 as well possibly explained by a dynamic microbiota over time. A one-way PERMANOVA revealed significant difference between all sampling months in both RAS ($p < 0.05$). This was also confirmed by a beta dispersion test ($p < 0.05$), meaning that the significance was not due to the different dispersion of the data. Indicated by the circles in Figure 3-16 C, some samples from April and July scatter away from the rest in the FTS, suggesting similar microbial community composition of the remaining months. A one-way PERMANOVA test revealed significant difference between all sampling months ($p < 0.05$), except from between April and May ($p > 0.05$).

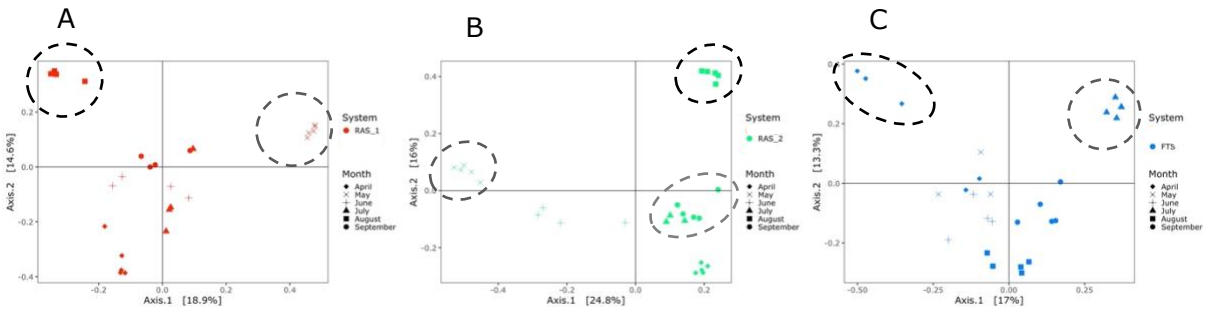

Figure 3-16: PCoA plots based on Bray Curtis dissimilarities for investigation of temporal differences in microbial composition in skin mucus samples from production system RAS_1 (A), RAS_2 (B) and FTS (C).

Gill mucus samples: Temporal changes in gill mucus samples differed from what observed in skin mucus samples. For RAS_1, the circles in Figure 3-17 A displays that April and August samples cluster by themselves whereas May and June cluster together. This suggests that May and June have similar microbial community composition. There were no

samples left after the rarefaction from July and September in RAS_1. The only significant difference revealed by one-way PERMANOVA was between samples from April and May, and April and August ($p < 0.05$). For RAS_2, no samples were present from July. The same trend was seen as in RAS_1, where May and June cluster together (Figure 3-17 B). August scatters away from the rest, in similarity with RAS_1, but here April and September are closer. Similar observations were made for skin samples, possibly explained by dynamics in the microbiota over time. A one-way PERMANOVA revealed significant difference between April and May, and May and August samples ($p < 0.05$). For the FTS, no samples were present from September. April and July samples cluster by themselves, whereas one sample from May, June, and August each scatter from the rest indicated by the circles in Figure 3-17 C. However, a one-way PERMANOVA only revealed significant difference between April and July samples ($p < 0.05$). Beta dispersion test confirmed significance found in RAS_2 and FTS.

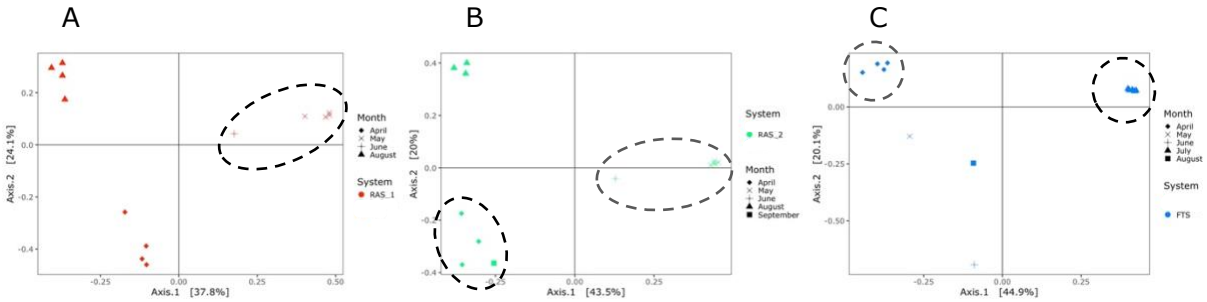

Figure 3-17: PCoA plots based on Bray Curtis dissimilarities for investigation of temporal differences in microbial composition in gill mucus samples from production system RAS_1 (A), RAS_2 (B) and FTS (C).

Gut mucus samples: The ellipse in the PCoA plot in Figure 3-18 A displayed that a couple of gut samples from RAS_1 sampled in July scatter away from the rest, as well as a couple of the samples from June. One sample from August and one from May scatter from the rest, whereas the rest cluster. A one-way PERMANOVA revealed significant difference ($p < 0.05$) in the microbial composition between April and June, April and July, May and June, and May and July in RAS_1. The observations were similar for RAS_2, where July scatter from the rest, as well as one sample from May and July, whereas the rest cluster as indicated by the circles in the PCoA plot in Figure 3-18 B. As for RAS_1, a one-way PERMANOVA revealed significant difference ($p < 0.05$) between April and July, and May and July. The PCoA plot from the FTS in Figure 3-18 C displayed similar observations as for both RAS, with a less prominent clustering. There was found significant difference ($p < 0.05$) between April and May, June, July, and August. There was also found significant difference between May and June, July, and September. These observations suggest dynamics also in the gut samples over time.

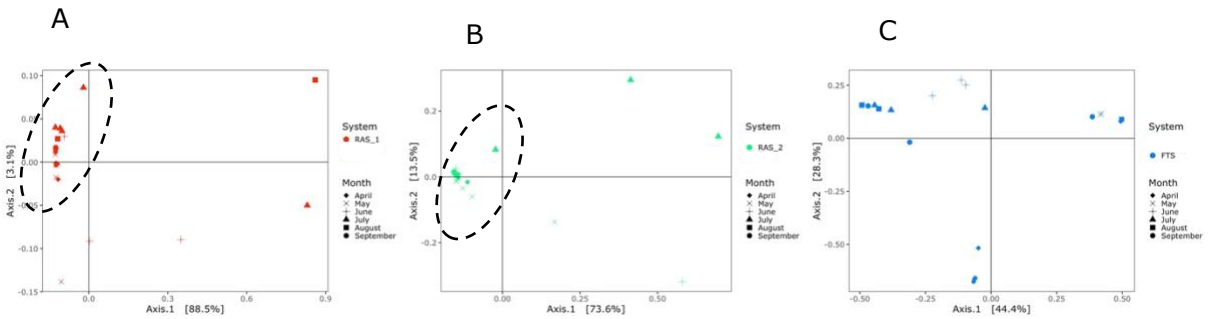

Figure 3-18: PCoA plots based on Bray Curtis dissimilarities for investigation of temporal differences in microbial composition in gut mucus samples from production system RAS_1 (A), RAS_2 (B) and FTS (C).

Temporal changes were also investigated in the environment samples within the three systems. There were not found significant differences (one-way PERMANOVA, $p > 0.05$) between any of the sampling months in the systems for tank water, tank biofilm, nor biofilter biofilm samples and the PCoA plots are therefore presented in Appendix J. There were also not found significant differences (one-way PERMANOVA, $p > 0.05$) between sampling months for the source water, and the PCoA plot is therefore also presented in Appendix J. These findings suggest little dynamic in environment samples across the sampling period, whereas the fish samples likely display a higher dynamic caused by factors other than its surrounding environment.

3.3 Microbial Community Composition and Dynamics

16S rRNA amplicon sequencing on an Illumina MiSeq platform has been used for mapping the microbial community structures in all samples. This method is well established and provides an excellent cost-value ratio. However, due to the sequencing of short amplicons, taxonomic resolution is limited and does typically not allow for classification down to species level. The reliability of classification using 16S rRNA amplicon data is declining by descending in the taxonomic hierarchy. Accordingly, amplicon sequencing data were annotated to the taxonomic levels of order, family, and genus, but not species in Figure 3-19-Figure 3-25.

Microbial community composition of host samples

Skin mucus samples: Microbial community composition of skin mucus samples is presented in Figure 3-19. The most abundant bacterial genus in all skin samples combined from the three systems was *Pseudomonas* with an average abundance of 15.6% (± 16.5%). This was also the highest abundant genus in RAS_1 and RAS_2 (16.4% ± 18.4% and 18.3% ± 18.3%, respectively), and the second most abundant in FTS (12.0% ± 12.2%). However, *Pseudomonas* was not present in high average abundance in April for any of the systems. RAS_1 and RAS_2 had the same genera as top five in abundance, whereas FTS showed *Mycoplasma* instead of *Acinetobacter* in its top five (Table 3-2). However, *Mycoplasma* was of high abundance in one skin sample in the FTS collected from April, causing its high average abundance. *Mycoplasma* was also present in a few samples from the systems in July. *Chryseobacterium*, present in top five abundance in all systems, was more equally distributed between the samples and sampling months in all systems.

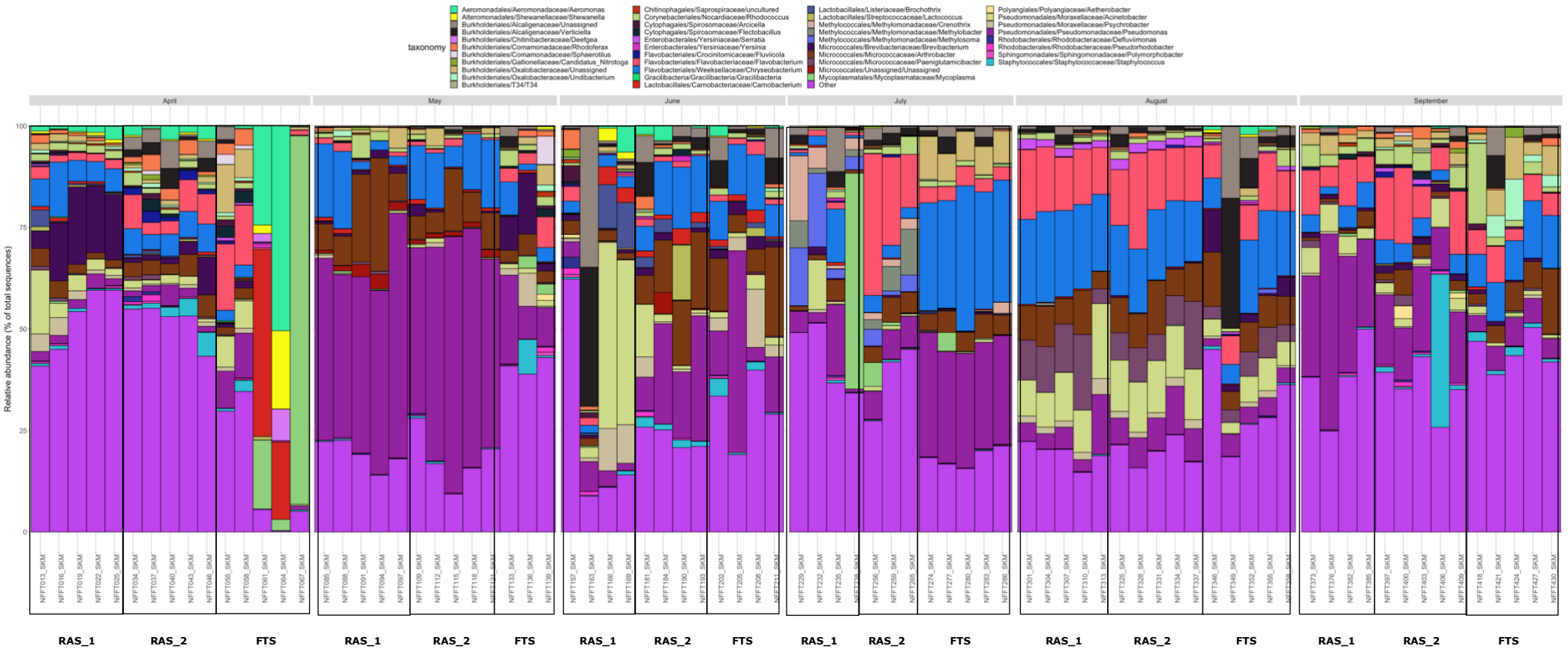

Figure 3-19: Microbial community composition displayed at order, family, and genus level for skin mucus samples from the three systems (RAS_1, RAS_2 and FTS) over all 6 sampling months. Genera with relative abundance less than 10% are displayed as 'Other'.

Gill mucus samples: Microbial community composition of gill mucus samples is presented in Figure 3-20. As for skin mucus samples, the predominant bacterial genus in all gill samples combined from the three systems was *Pseudomonas* with an average abundance of 25.5% (± 24.2%). This was also the most abundant bacterial genus across all three systems (18.5% ± 21.6%, 28.5% ± 30.3% and 23.4% ± 20.2%, respectively). In line with skin samples, *Pseudomonas* was not present in high abundance in April in any of the systems. RAS_1, RAS_2 and FTS displayed four out of five similar genera in its top five average abundance (Table 3-2). They differed by RAS_1 having abundance of *Acinetobacter* whereas RAS_2 showed high abundance of *Paeniglutamicibacter*, and FTS of *Oxalobacteraceae* (8.8% ± 5.2%). In fact, these four genera predominant in gill samples across the systems were also found in skin samples (Table 3-2). The bacterial composition was fairly similar throughout the systems, except from the FTS differing from the two RAS at the sampling point in June. However, there was only one sample from each system to compare from this month. For July, there was no samples to compare from the RAS, as well as only one sample from RAS_2 in September. For the FTS, there was less samples than the RAS to compare in May and August. This was caused by the normalization of the data explained in chapter 2, which removed samples for further analysis. Overall, the bacterial composition was quite consistent with the skin samples.

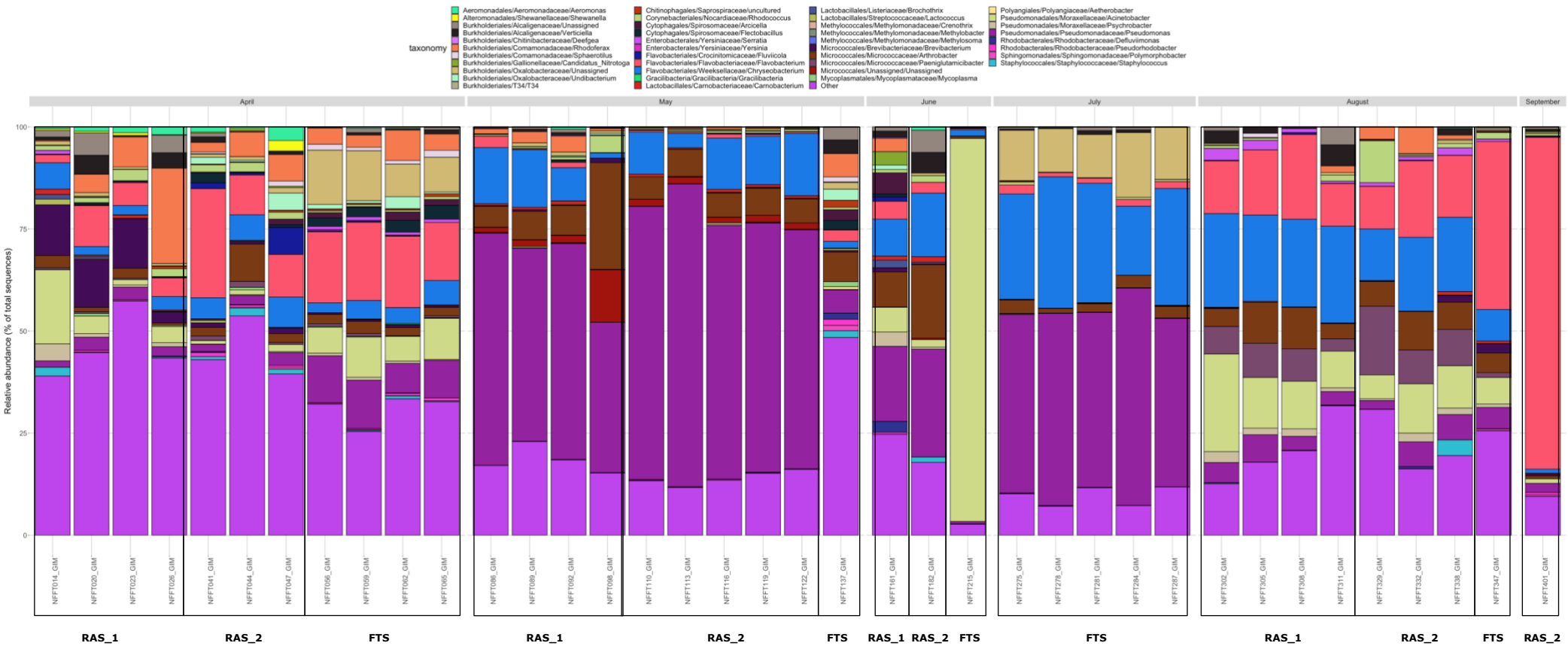

Figure 3-20: Microbial community composition displayed at order, family, and genus level for gill mucus samples from the three systems (RAS_1, RAS_2 and FTS) over all 6 sampling months. Genera with relative abundance less than 10% are displayed as 'Other'.

Gut mucus samples: Microbial community composition of gut mucus samples is presented in Figure 3-21. The predominant bacterial genus in all gut samples combined from the three systems was *Mycoplasma* with an average abundance of 64.6% (± 39.6%). This was also the most abundant bacterial genus across all three systems (83.4% ± 28.7%, 78.5% ± 27.8% and 35.9% ± 40.7%, respectively). However, the FTS did not show high abundance of *Mycoplasma* in April, July, and August. RAS_1 and RAS_2 displayed identical genera in top five average abundance, whereas *Shewanella* in the FTS was represent in the top five deviating from RAS_1 and RAS_2 presence of *Deefgea* (Table 3-2). Overall, the FTS deviated more in bacterial composition from the two RAS with its high abundance of *Aeronomas* in the later sampling months. Whereas the skin and gill had similar microbial community composition, the gut was clearly different, in agreement with the beta-diversity results presented in chapter 3.2.3.

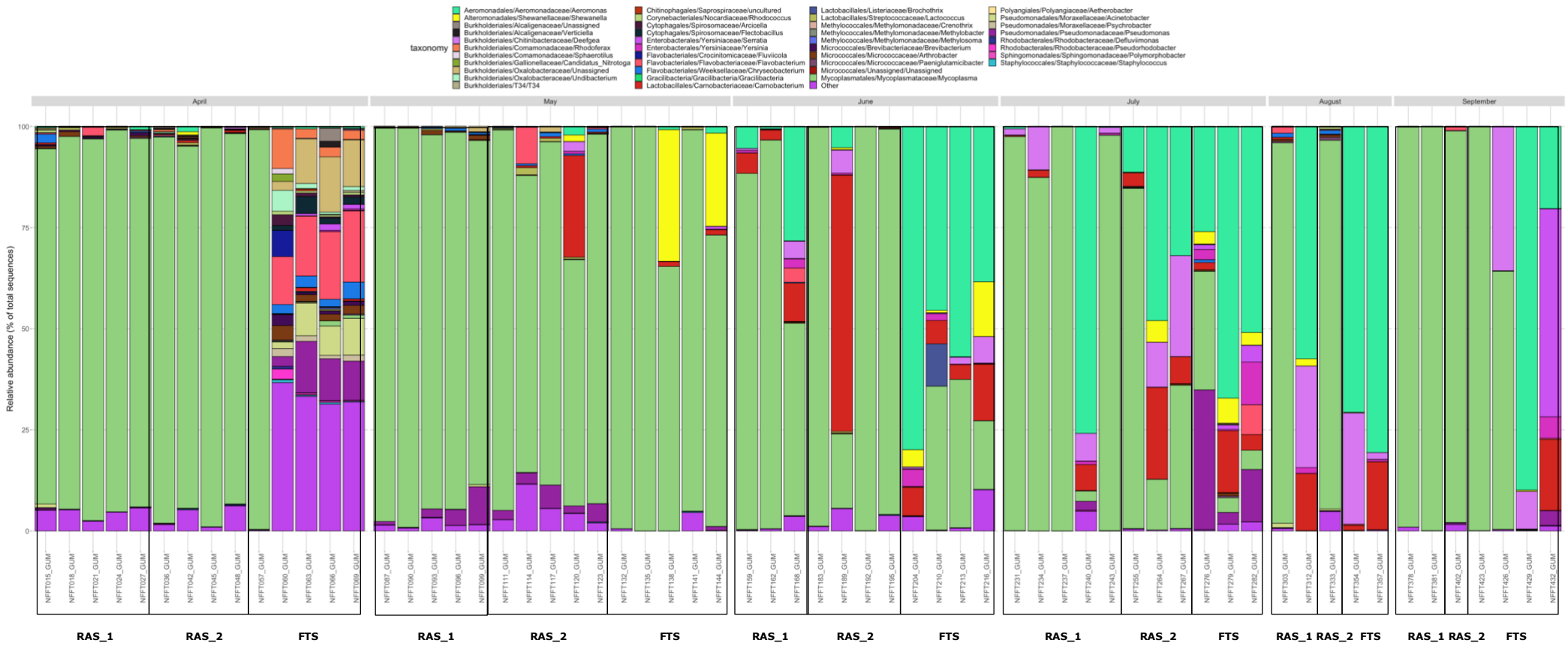

Figure 3-21: Microbial community composition displayed at order, family, and genus level for gut mucus samples from the three systems (RAS_1, RAS_2 and FTS) over all 6 sampling months. Genera with relative abundance less than 10% are displayed as 'Other'.

Top five bacterial genera based on average abundance of fish mucus samples are shown in Table 3-2.

Table 3-2: The top five bacterial genera based on average abundance (%) of skin, gill, and gut samples from the three systems where all sampling months were included. Genera with less than 10% were categorized as 'Other', but not included as part of top five. f.: family

	Average relative abundance in system (%)		
Sampling position	**RAS_1**	**RAS_2**	**FTS**
Skin mucus	*Pseudomonas* (16.4 ± 18.4)	*Pseudomonas* (18.3 ± 18.3)	*Chryseobacterium* (12.2 ± 10.1)
	Chryseobacterium (8.6 ± 7.9)	*Flavobacterium* (9.4 ± 9.0)	*Pseudomonas* (12.0 ± 12.2)
	Acinetobacter (7.7 ± 11.6)	*Chryseobacterium* (9.4 ± 5.4)	*Arthrobacter* (6.0 ± 5.2)
	Arthrobacter (5.5 ± 6.4)	*Arthrobacter* (7.2 ± 4.7)	*Flavobacterium* (5.7 ± 4.5)
	Flavobacterium (4.9 ± 5.5)	*Acinetobacter* (4.0 ± 4.9)	*Mycoplasma* (4.5 ± 17.5)
	(Other 32.3 ± 16.9)	(Other 30.9 ± 13.7)	(Other 29.1 ± 13.7)
Gill mucus	*Pseudomonas* (18.5 ± 21.6)	*Pseudomonas* (28.5 ± 30.3)	*Pseudomonas* (23.4 ± 20.2)
	Chryseobacterium (11.4 ± 8.4)	*Flavobacterium* (13.6 ± 22.1)	*Chryseobacterium* (13.5 ± 12.4)
	Flavobacterium (7.0 ± 6.7)	*Chryseobacterium* (10.6 ± 5.6)	*Acinetobacter* (11.1 ± 26.5)
	Acinetobacter (7.0 ± 7.7)	*Arthrobacter* (6.7 ± 4.3)	*Flavobacterium* (10.1 ± 12.4)
	Arthrobacter (7.0 ± 6.5)	*Paeniglutamicibacter* (2.9 ± 5.4)	*f: Oxalobacteraceae* (8.6 ± 5.2)
	(Other 28.1 ± 13.8)	(Other 22.9 ± 13.9)	(Other 20.6 ± 14.2)
Gut mucus	*Mycoplasma* (83.4 ± 28.7)	*Mycoplasma* (78.5 ± 27.8)	*Mycoplasma* (35.9 ± 40.7)
	Aeromonas (7.8 ± 20.4)	*Carnobacterium* (6.9 ± 16.0)	*Aeromonas* (27.4 ± 32.8)
	Deefgea (2.2 ± 5.6)	*Aeromonas* (5.6 ± 13.1)	*Carnobacterium* (4.0 ± 6.0)
	Carnobacterium (1.8 ± 3.7)	*Deefgea* (2.5 ± 6.2)	*Pseudomonas* (4.0 ± 8.0)
	Pseudomonas (0.84 ± 2.1)	*Pseudomonas* (1.0 ± 1.7)	*Shewanella* (3.8 ± 8.2)
	(Other 2.0 ± 2.1)	(Other 3.3 ± 3.0)	(Other 6.9 ± 12.6)

Microbial community composition of environment samples

Source water samples: The bacterial composition of the source water was overall consistent throughout the sampling showing little dynamic (Figure 3-22), yet large differences from the built environment likely caused by the disinfection of the source water. The most abundant genus of the source water when combining all samples over the entire sampling period was *Crenothrix* (7.8% ± 3.4%) followed by *Methylosoma* (4.7% ± 1.6%), *Methylobacter* (3.0% ± 2.8%), *Gracilibacteria* (0.75% ± 0.30%) and *Rhodoferax* (0.45% ± 0.16%). Genera with average relative abundance less than 10% were grouped into 'Other' and was 82.5% ± 4.8%.

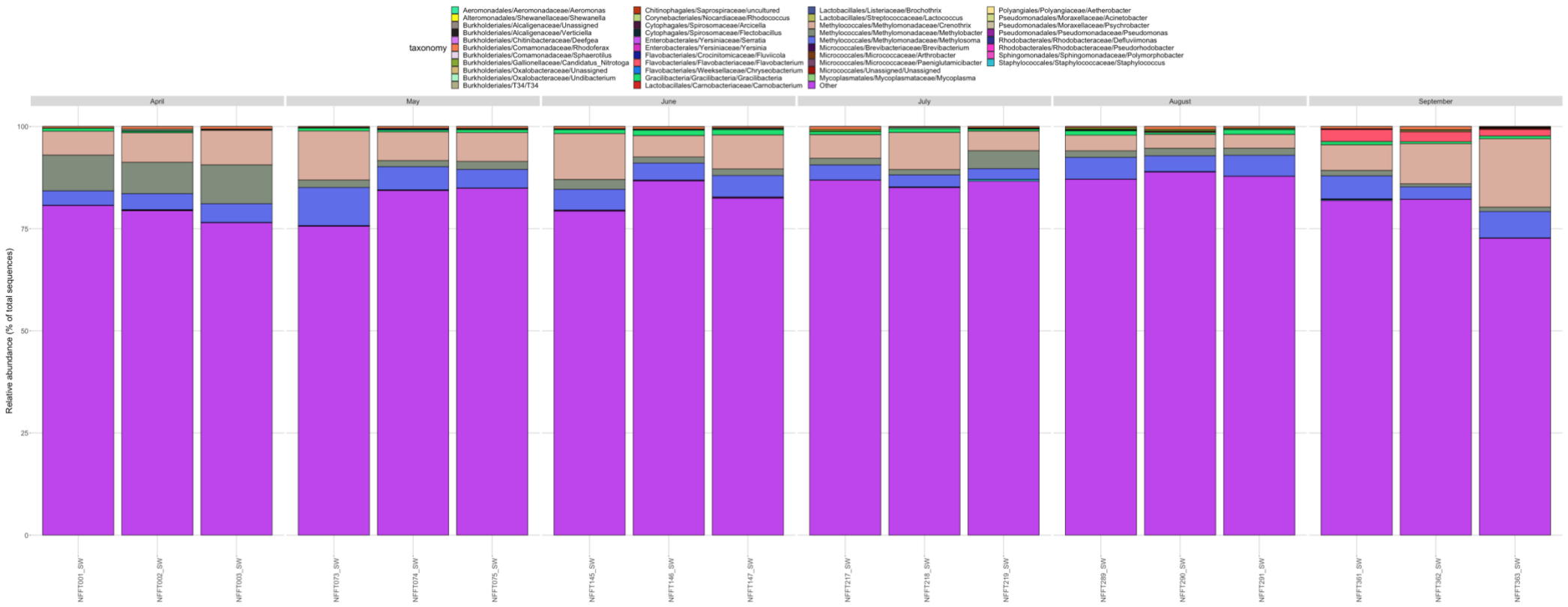

Figure 3-22: Microbial community composition displayed at order, family, and genus level for source water samples of the system over all 6 sampling months. Genera with relative abundance less than 10% are displayed as 'Other'.

Tank water samples: Microbial community composition of tank water samples is presented in Figure 3-23. The predominant bacterial genus in all tank water samples combined from the three systems was *Flavobacterium* with an average abundance of 18.5% (± 10.1%). This was also the most abundant genus in all three systems (20.4% ± 6.6%, 11.8% ± 4.4% and 24.0% ± 12.7%, respectively). RAS_1 and RAS_2 only differed in the top five abundant genera where RAS_1 exhibiting presence of *Pseudorhodobacter* while RAS_2 showed presence of the genus *Saprospiraceae*. FTS shared three top genera with the two RAS units but showed presence of *Sphaerotilus* and *Pseudomonas* which the RAS units did not (in top five) (Table 3-3). The bacterial communities seemed overall quite consistent within the systems.

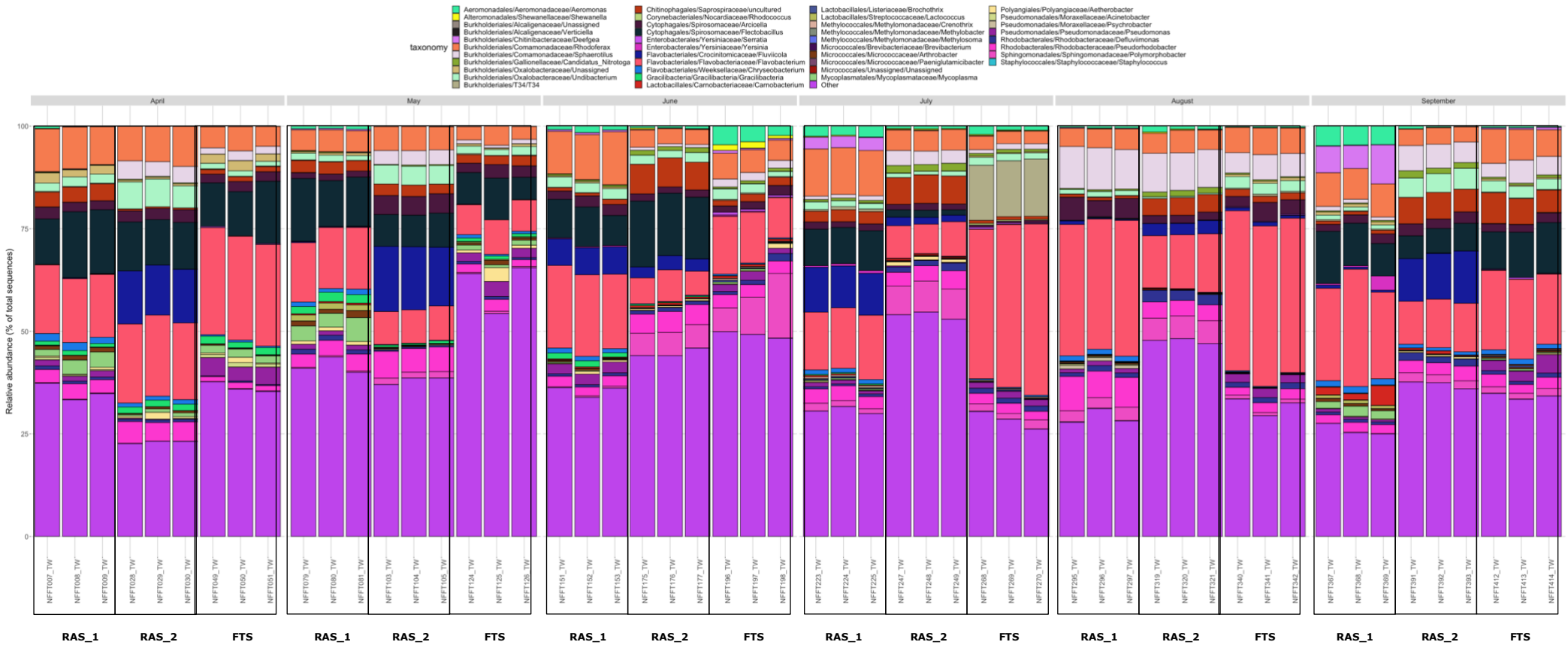

Figure 3-23: Microbial community composition displayed at order, family, and genus level for tank water samples from the three systems (RAS_1, RAS_2 and FTS) over all 6 sampling months. Genera with relative abundance less than 10% are displayed as 'Other'.

Tank biofilm samples: Microbial community composition of tank biofilm samples is presented in Figure 3-24. The predominant bacterial genus in all tank biofilm samples combined from the three systems was *Arcicella* with an average abundance of 7.5% (± 4.3%). This was also the predominant genus in RAS_1 (11.1% ± 5.0%), whereas it was member of top five abundant genera in RAS_2 and FTS. RAS_2 showed highest abundance of *Nitrotoga* (8.9% ± 4.2%) and FTS of *Saprospiraceae* (7.7% ± 3.2%). RAS_2 showed more similar top five abundant genera with FTS than RAS_1 (Table 3-3). Overall, the bacterial communities were consistent within, and between, the systems (Figure 3-24).

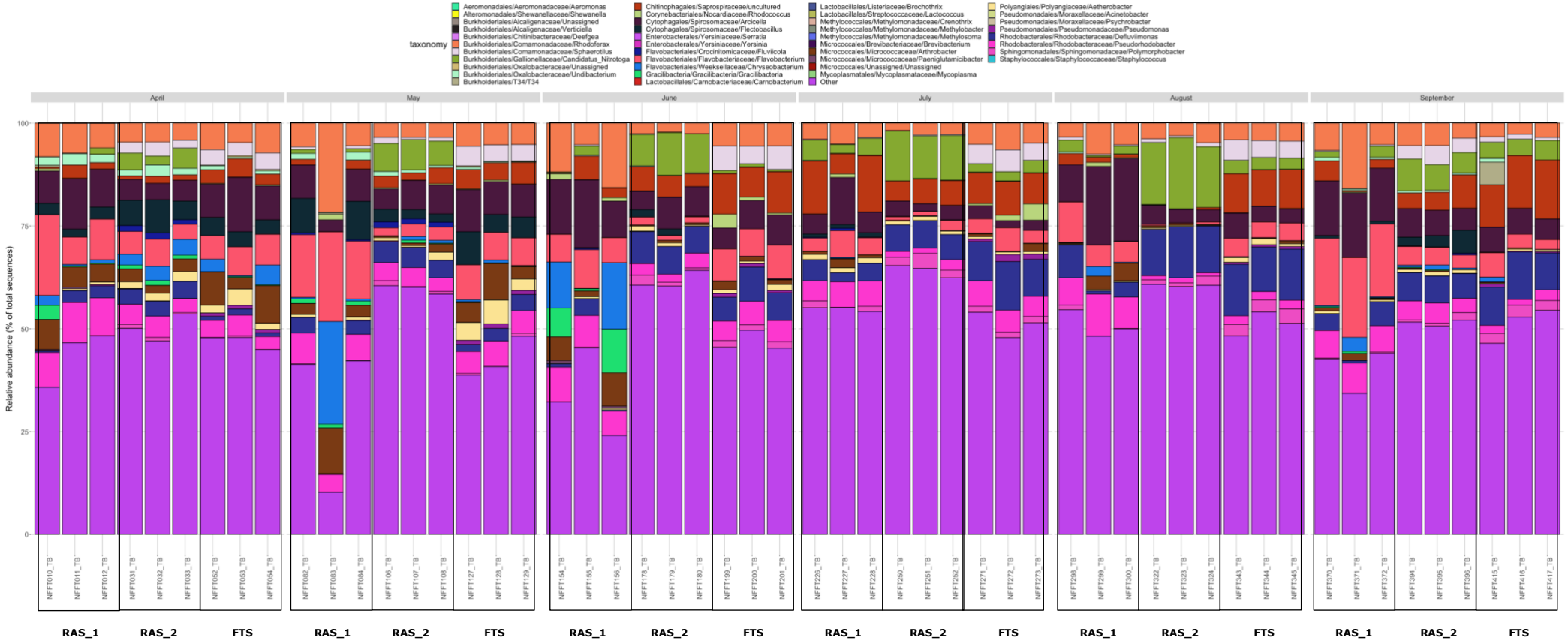

Figure 3-24: Microbial community composition displayed at order, family, and genus level for tank biofilm samples from the three systems (RAS_1, RAS_2 and FTS) over all 6 sampling months. Genera with relative abundance less than 10% are displayed as 'Other'.

Biofilter biofilm samples: Microbial community composition of biofilter biofilm samples is presented in Figure 3-25. The predominant bacterial genus in all biofilter biofilm samples combined from the FBBF and MBBF was *Flavobacterium* with an average abundance of 13.0% (± 9.6%). This was also the highest abundant genus in both FBBF (in connection to RAS_1) and MBBF (in connection to RAS_2), 18.9% ± 7.8% and 7.1% ± 7.5% respectively. The only other genus shared in top five abundance between the two biofilters was *Rhodoferax* (6.9% ± 1.8% and 4.0% ± 3.0%, respectively) (Table 3-3). Overall, the bacterial composition was quite consistent within the two biofilters (Figure 3-25). Observed similarities are likely since both RAS are operated with the same source water, and other parameters such as feed-type, host species, physico-chemical water parameters are the same.

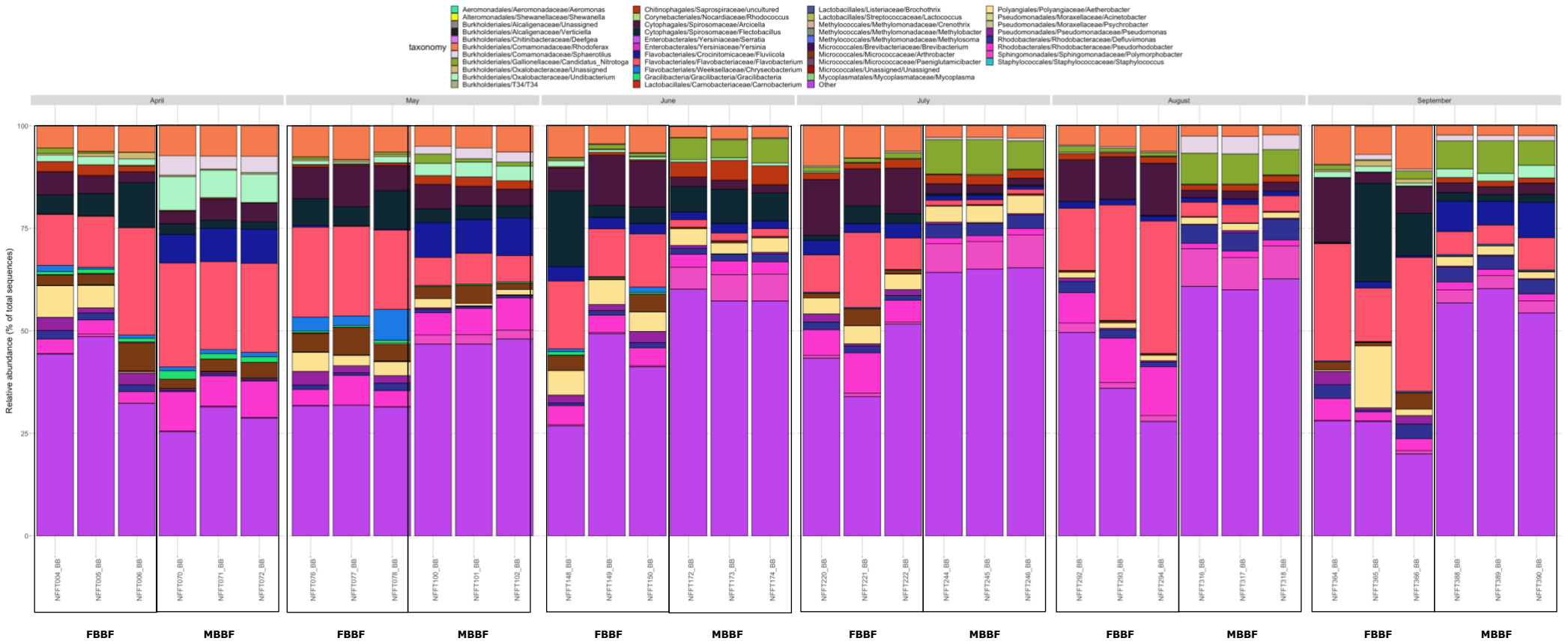

Figure 3-25: Microbial community composition displayed at order, family, and genus level for biofilter biofilm samples from the two biofilters (FBBF and MBBF) over all 6 sampling months. Genera with relative abundance less than 10% are displayed as 'Other'.

Top five bacterial genera based on average abundance of built environment samples are shown in Table 3-3.

Table 3-3: The top five bacterial genera based on average abundance (%) of tank water, tank biofilm and biofilter biofilm samples from the three systems where all sampling months were included. Genera with less than 10% were categorized as 'Other', but not included as part of top five. No biofilter was in connection to the FTS hence why no bacterial genera are shown. f.: family

	Average relative abundance in system (%)		
Sampling position	**RAS_1**	**RAS_2**	**FTS**
Tank water	*Flavobacterium* (20.4 ± 6.6)	*Flavobacterium* (11.8 ± 4.4)	*Flavobacterium* (24.0 ± 12.7)
	Flectobacillus (9.4 ± 4.8)	*Fluviicola* (7.8 ± 5.6)	*Flectobacillus* (5.1 ± 5.6)
	Rhodoferax (8.3 ± 4.8)	*Flectobacillus* (6.9 ± 5.4)	*Rhodoferax* (5.0 ± 1.6)
	Pseudorhodobacter (3.8 ± 1.8)	*Rhodoferax* (5.4 ± 1.6)	*Sphaerotilus* (2.6 ± 1.8)
	Fluviicola (2.9 ± 4.1)	*f: Saprospiraceae* (4.5 ± 2.5)	*Pseudomonas* (2.6 ± 1.1)
	(Other 33.0 ± 5.1)	(Other 40.8 ± 9.9)	(Other 40.1 ± 12.4)
Tank biofilm	*Aricella* (11.1 ± 5.0)	*Candidatus_Nitrotoga* (8.9 ± 4.2)	*f: Saprospiraceae* (7.7 ± 3.2)
	Flavobacterium (10.7 ± 6.1)	*Defluviimonas* (6.8 ± 2.5)	*Defluviimonas* (7.2 ± 4.2)
	Rhodoferax (8.0 ± 5.3)	*Arcicella* (5.1 ± 1.6)	*Arcicella* (6.4 ± 3.1)
	Pseudorhodobacter (7.4 ± 1.8)	*Rhodoferax* (3.6 ± 1.6)	*Flavobacterium* (5.5 ± 1.9)
	Chryseobacterium (3.4 ± 6.7)	*f: Saprospiraceae* (3.4 ± 2.5)	*Rhodoferax* (5.1 ± 1.3)
	(Other 42.7 ± 11.8)	(Other 57.7 ± 5.7)	(Other 48.4 ± 4.3)
Biofilter biofilm	*Flavobacterium* (18.9 ± 7.8)	*Flavobacterium* (7.1 ± 7.5)	-
	Aricella (8.8 ± 3.6)	*Fluviicola* (4.7 ± 3.5)	-
	Rhodoferax (6.9 ± 1.8)	*Candidatus_Nitrotoga* (4.7 ± 3.4)	-
	Flectobacillus (6.1 ± 6.4)	*Polymorphobacter* (4.5 ± 3.0)	-
	Pseudorhodobacter (5.6 ± 2.9)	*Rhodoferax* (4.0 ± 3.0)	-
	(Other 36.3 ± 9.5)	(Other 52.8 ± 12.5)	-

In summary, the here presented results of microbial community composition show that when assessing the five most common genera sorted based on average abundance in the systems, the microbial composition across the sample types were in general similar across the systems. The skin and gill were more similar to each other than the gut, whereas built environment samples were similar. The source water showed little dynamic and high difference to the built environment samples.

4 Discussion

This master's thesis has systematically characterized and monitored the microbial communities in environment (intake and tank water, biofilm in tank and biofilter) as well as mucosal surfaces (skin, gill, and gut mucus) of Arctic charr in a commercial land-based aquaculture facility with different production systems. This was conducted and examined through Illumina 16S rRNA gene amplicon sequencing of total DNA extracted from environmental and host samples, before subsequent bioinformatic and statistic data processing.

4.1 DNA Purity

The purity of the extracted samples was measured using Nanodrop. Results showed that in general, for all the three systems in the facility, the gut displayed the most precise purity values followed by gill and skin in fish samples for both 260/280 and 260/230 ratio (Figure 3-1, Figure 3-2, and Figure 3-3). This is an indication that the gut samples had less presence of RNA than the skin and the gill, and that they also had the least amount of co-purified contaminants stemming from the extraction process. Purity of DNA present on mucosal surfaces on fish can be problematic due to mucus containing proteins that will absorb at or near the ratios of 280 and 230 nm. A study done by Minniti et al. (2017) proved it difficult to extract DNA from fish mucus. Here, 16S rRNA gene sequencing was used to examine the bacterial composition of skin mucus, but 15 of the 45 samples did not generate PCR product. Fish mucus will contain both bacterial and host DNA, which is an explanation for the lower purity found in skin samples. Similar observations were made by Persson et al. (2022, manuscript submitted) and Sandberg (2021) where bacterial communities were studied in skin and gill mucus of Atlantic salmon smolt in different commercial RAS.

For the environment samples, one could generally see satisfactory purity for the 260/280 ratio, whilst it dropped for the 260/230 ratio (Figure 3-4, Figure 3-5, and Figure 3-6). This was general for all systems. The water samples, including the source water, had comparably low measured DNA concentrations (Table E-1), which could be an issue causing the low 260/280 ratios (Matlock, 2015). Some water samples displayed values over the optimal 1.8 purity value, but this does not necessarily imply an issue (Matlock, 2015). However, the source water had especially low DNA concentration, and this was reflected in its low purity (Figure 3-4). The low DNA concentration leads to contaminants showing up much more here than in samples with higher DNA concentration, such as the biofilm samples, and could therefore be a cause of the lower purity observed in the water sample.

4.2 Total DNA Concentration

The highest DNA concentration in **skin samples** was measured in the FTS (Figure 3-7 A), which was the system consisting of fish in its grow-out phase and highest weight (Table C-1), followed by RAS_2 and RAS_1. This is an indication of increasing mucus production in the skin during growth. However, the same trend was not observed for the gill samples. The **gill samples** showed overall higher concentration of DNA compared to skin samples, with minor differences in the three systems (Figure 3-7 B). This could indicate that the mucus production in the gills is not as affected by fish growth as skin mucus. Another

explanation for the higher dsDNA concentration could also be that mucus can be trapped in the gills arches, where it is more protected by the operculum as stated in the introduction. The gills are the largest organ-specific surface, mentioned in the introduction, where goblet cells that secrete the mucus are present in high number (Dash et al., 2018). Fish skin is constantly exposed to its aqueous environment, causing mucus to be washed away, and hence explaining why the skin samples measured the lowest dsDNA concentrations compared to the other fish samples (Figure 3-7). It has also been proposed that skin mucus contains low bacterial biomass (Minniti et al., 2017; Sandberg, 2021; Persson et al., 2022, manuscript submitted). However, the **gut samples** displayed the highest dsDNA concentration of the fish samples (Figure 3-7 C), which was in line with the results of measured purity in the fish samples. The overall highest concentrations were found in RAS_1 and FTS, indicating that the mucus composition is not as affected by the fish weight in the gut. Infections can alter the thickness of the mucus layer (Dash et al., 2018), and the high dsDNA concentration found in the gut could therefore be an indication of a healthy fish since the mucus would be sloughed off if infected by pathogens.

The water samples showed overall lower total DNA concentration than the fish samples (Figure 3-8 A and Figure 3-7, respectively). This is in agreement with purity measurements of the 260/230 ratio for the environment samples which were generally lower than for fish samples, indicating presence of other contaminants. As mentioned above, low DNA concentrations lead to contaminants showing up more here compared to for example fish samples which measured higher DNA concentrations. There was observed outliers in the box plot of tank water for the FTS (Figure 3-8 A), which could be another indication of co-purified contaminants. The skin of the fish is in constant contact with its surrounding water, and an explanation for the higher total DNA concentration found in skin samples compared to water samples could be the presence of host DNA in skin samples, and not only bacterial DNA.

4.3 Microbial Community Analyses

4.3.1 Downstream processing of sequence data

Based on the total DNA concentration (Figure 3-7 and Figure 3-8), one expected the highest number of reads in the gill and gut samples. However, as seen in Table 3-1, this was not the case. These results strongly indicate that the gill and gut samples contained high amount of fish DNA. This is in line with the previously mentioned study by Sandberg (2021), where it was found little bacterial DNA in skin and gill mucus. When comparing the number of reads found in Arctic charr to what was found in Atlantic salmon, we observe an indication that farmed Arctic charr has more bacterial DNA in the mucus than Atlantic salmon reared in RAS. Nevertheless, this cannot be verified in terms of the results from this study as quantification of bacterial numbers was not conducted. However, in this study, a large amount of gill and gut samples were removed after rarefaction, which is also in line with what was found in Atlantic salmon (Sandberg, 2021). That study did not include gut samples and it is therefore not directly comparable, however one can draw the same conclusion based on data from skin and gill mucus samples. The largest number of samples retained from the gut samples after rarefaction came from the FTS, which was the system with fish in its grow-out phase. The largest number of samples lost were from the gill samples, but the samples remaining were equally distributed between the three production systems.

4.3.2 Microbial richness measures and diversity

Alpha diversity in fish samples

A study done by Wang et al. (2021) characterized the microbiota of gut Atlantic salmon samples by 16S rRNA sequencing, and the study stated that gut mucus from Atlantic salmon displayed an increase in richness when moved from the freshwater phase to the seawater phase. Since NFFT is operated in all land-based and freshwater systems, the result from the study is in line with the low richness found in our gut samples (Figure 3-9 A). One could hypothesize that the richness would increase if adapting to a seawater phase during the production cycle, or if the source water would not be disinfected as is the case in sea cages. This is supported by a study done by Uren Webster et al. (2018), characterizing the skin and gut microbiomes of wild and hatchery-reared Atlantic salmon, where they found that the microbial diversity of wild populations of salmon was significantly higher than hatchery populations for skin and gut mucus. However, this is not relevant for non-anadromous Arctic charr at NFFT. A likely explanation for this could therefore be that disinfection of the intake water leads to lower diversity in RAS and hence fish mucus. The gill samples displayed higher richness and Shannon diversity than gut samples, but lower richness and lower Shannon diversity than skin samples (Figure 3-9). Observation of lower diversity in gill than skin is in line with a study done by Minich et al. (2020) which showed that gill samples had less richness and lower phylogenetic diversity than skin samples of Atlantic salmon. Since this study was conducted on Atlantic salmon, our results suggests that the mucus microbiota diversity of Arctic charr is similar to Atlantic salmon.

When comparing fish mucus samples between the systems, the only significant difference found was in Shannon diversity for gut samples between RAS_1 and FTS whereas no significant difference in diversity was found between the systems for skin and gill samples (Figure 3-9 B). This could possibly be explained by the size of the fish. RAS_1 contained the smallest fish, whereas FTS the largest fish in its grow-out phase (Table 2-1). One possible reason could therefore be that the microbiota in the gut has matured in line with fish growth, and the diversity therefore is significantly different in the smallest and the biggest fish, which also has been suggested in a review paper by Butt and Volkoff (2019).

However, when comparing the three mucus sample types within each system, there was not found significant difference in richness between fish samples from the three different production systems (Figure 3-9 A). This emphasizes that the richness of the fish samples is similar for mucosal surfaces within the same rearing conditions. When in addition to richness, evenness is assessed, skin and gill samples were significantly different to gut mucus samples within the systems suggesting that the different water treatments in the systems influences diversity of the skin and gill more than it modulates diversity of the gut. Nonetheless, the low Shannon diversity in gut samples (Figure 3-9 B) is likely caused by a few dominating ASVs present whereas the skin and gill most likely have a more equal distribution of ASVs.

Alpha diversity in environment samples

Analyzing microbiota at different locations in the different production systems revealed in general higher alpha diversity measures than the fish mucus samples (Figure 3-9 and Figure 3-10, respectively). This is in agreement with the mentioned study by Minich et al. (2020), investigating microbial communities of farmed Atlantic salmon in two RAS and one FTS, which showed that the richness and diversity was higher in water samples compared to skin, gill, and digesta. Persson et al. (2022, manuscript submitted) also found higher diversity in the rearing environment than on gill mucus, supporting our findings. This thesis

reports, to the best of my knowledge, for the first time the systematic spatiotemporal mapping of microbial communities in Arctic charr reared in closed containment systems. Based on the results presented in this thesis, we observed similar conditions and trends in host and built environment microbiota between Arctic charr and Atlantic salmon aquacultured in RAS. These similarities are beneficial for further exploitation to improve the production of both species until market size in large-scale RAS.

Focusing on built environment locations, tank water displayed highest richness and Shannon diversity across all three systems (Figure 3-10). However, the source water displayed much higher richness, as well as higher Shannon diversity, than the tank water samples and fish mucus samples. Source water samples were taken before disinfection of the water, and one reason for the resulting significant difference in alpha diversity between the built and native environment across the three systems could be that hygienic barriers inactivates/kills many bacterial species. Hence lowering not only the load, but also eventually the diversity. Disinfection of the water is required by biosafety regulations. This is to prevent pathogens from entering the systems, however it also lowers the number of heterotrophic bacteria competing for organic matter as substrate (Hess-Erga et al., 2008). Our results imply that treatment of the water leads to lower diversity in all three systems, suggesting that disinfection lowered the number of bacteria present in competition for available substrate. This could also be a disadvantage since less bacteria could contribute to proliferation of opportunistic or pathogenic heterotrophs, due to sudden increase in carrying capacity of the system (Vadstein et al., 2018). Since the richness and evenness was consistent between the systems for built environment samples, disinfection of intake water could also result in a stable environment for built environment samples. However, quantification of bacterial numbers would be necessary to substantiate this postulation.

Interestingly, the tank biofilm richness and Shannon diversity differed significantly between the two RAS, as well as between RAS_2 and FTS. The reasons for these differences are not evident, but a possible explanation could be the different selection pressure for bacteria in the different system's tanks operating with different rearing conditions, which led to variations in species richness and diversity. The lack of significant difference in alpha diversity measures between the two biofilters, which exhibited similar richness and Shannon diversity, indicates that even though the build-up of the biofilters is different, their selection pressure within the biofilm is similar.

When comparing sampling locations within each system, the results were the same throughout the three different production systems. Significant differences were found between all sampling positions, except between biofilter biofilm samples and tank biofilm samples for the two RAS (Figure 3-9 and Figure 3-10). This suggests that the selection pressure in the biofilms is similar. There was also no significant difference in observed richness for biofilter biofilm and tank water (Figure 3-10 A). For Shannon diversity (Figure 3-9 B), the skin mucus samples only showed significant difference to the gut mucus indicating that the diversity of the skin mucus is affected by, and therefore, similar to its surrounding environment. As there was not found significant difference in Shannon diversity between skin and gill either, it emphasizes that also gill mucus is affected by the rearing environment. This was as expected, as the fish is in constant contact with the tank water associated microbiota, which substantiates that the diversity in fish skin and gill is influenced by its environment. A similar suggestion was presented in the study by Minich et al. (2020), where they suggested that tank biofilm has a higher impact on the fish mucus richness than the tank water. However, there is lacking studies evaluating in detail how the built environment influences fish microbiota on mucus surfaces (Minich et al., 2020).

The tank water in our study did not show significant differences in Shannon diversity between the biofilter biofilm and tank biofilm within the systems (Figure 3-10 B), suggesting that the evenness in the biofilm is influenced by the tank water (or vice versa).

4.3.3 Microbial communities in host and environment samples

Beta diversity in host microbiomes

The mucus is, as described in the introduction, an important protective barrier for the fish and determinant of fish health, and it was therefore of interest to see if the microbial composition in mucosal surfaces differed in the host and between the production systems. This was especially of interest since, to my knowledge, no scientific literature investigating the microbial community composition in Arctic charr reared in land-based aquaculture systems is available.

The PCoA plot in Figure 3-12 showed no clear separation between skin and gill mucus microbiota, whereas gut samples were separated from skin and gill samples horizontally along axis 1. The observations were confirmed statistically and there were significant differences between the three mucus type microbiomes. These findings are also in good agreement with the study done by Minich et al. (2020) which revealed that the microbiome of Atlantic salmon skin, gill, and digesta was unique. The different microbial composition in skin and gill versus gut mucus was therefore confirmed as hypothesized. This is also supported by the taxonomic chart for skin (Figure 3-19), gill (Figure 3-20), and gut (Figure 3-21) samples where especially gut samples show a clearly different pattern from the skin and gill taxonomic charts. However, there is some uncertainty as to why there is a significant difference in microbial composition between skin and gill samples, even though both tissues are in permanent contact with the surrounding water microbiota (Minich et al., 2020). We hypothesize that the filamentous structure of gill tissue provides a different microenvironment than the comparably smooth skin surface and thereby stimulating colonization of differently specialized taxa.

Even though the alpha diversity did not reveal significant differences between the three systems for skin and gill samples (Figure 3-9), significant variations in microbial composition were observed between the two RAS and the FTS for gill samples (Figure 3-13 B) and confirmed statistically. The skin showed no obvious clusters, yet the two RAS tendentially cluster together (Figure 3-13 A), but the differences were nevertheless significant between the two RAS and the FTS. Most significant differences in microbial composition were revealed between the two RAS and the FTS for gut samples (Figure 3-13 C). This is also supported by the taxonomic chart of gut samples (Figure 3-21) which show that the two RAS are more similar to each other than the FTS. These results are confirming our hypothesis that microbial communities would differ in RAS versus FTS, for all mucosal surfaces. The water treatment for the three systems is different (biofilter versus no biofilter) and this suggests that different water treatments modulates fish mucus microbiota and leads to different colonized microbiota on mucosal surfaces in RAS versus FTS. Minich et al. (2020) found significant differences in microbial community composition for skin, gill, and digesta in RAS versus FTS, with RAS being more similar. This was in line with our results. Even though the mentioned study was done on Atlantic salmon, this is an indication that similar production systems (RAS and FTS) will select for similar mucus composition characteristic in farmed Artic charr and other salmonids reared in the same production systems.

Beta diversity in environment samples

The built environment microbiota of land-based systems has not been explored to a large extent (Minich et al., 2020) and was therefore of interest in this study. Based on the Bray-Curtis dissimilarities on ASV level, there were found significant differences between all environment samples across the systems (Figure 3-15). There were also found significant differences between all environment samples within their respective system. This emphasizes a rather unique microbiota for tank water and biofilm, and biofilter biofilm in their respective systems, even though the intake water was the same for all systems. The source water showed little dynamic (Figure 3-22) compared to the built environment (Figure 3-23, Figure 3-24, and Figure 3-25), emphasizing that the dynamics in the built environment samples is caused by factors other than the source water. These results support the hypothesis that microbial communities would differ in the RAS versus FTS, but it also emphasized significant differences between the two RAS as well (since they also were different). This is contradicting to what Minich et al. (2020) found in their study, where tank biofilm was more similar in the two RAS versus the FTS. The reason for this contradicting finding is probably because the two RAS used in their study did not have structural differences, whereas our RAS differed in structural composition of the biofilter. However, in a study on microbial community dynamics in Atlantic salmon post-smolt RAS at different salinities, conducted by Bakke et al. (2017), one of the major findings was that biofilm microbiota was significantly different from the water microbiota within each individual RAS, which supports our findings.

Microbial community structures in the source water and built environments were also significantly different. As mentioned in the section above, a probable explanation for this is that the source water samples were taken before disinfection of the water, and hence harbored different microbial community compositions than water behind the hygienic barrier in the rearing tanks. There is also a selection pressure in the systems where the source water is entering an environment with high organic load, influenced by the biofilter (for RAS) and the disinfection, likely causing differences in microbial communities between the native and built environment. As seen for the alpha diversity, disinfection of the source water lowers the diversity of the built environment samples (Figure 3-10). This could also be the cause for the seemingly consistent profiles of tank water samples across the systems, as seen in the taxonomic chart (Figure 3-23). The biofilter and tank biofilm were significantly different to each other, and an explanation for this could be the selection pressure in the biofilms caused by different micro-environments at the two locations. Obvious differences at both locations are e.g., host-biomass, suspended particle concentration, differences in dissolved O_2, CO_2, TAN, etc. Interestingly, the microbial community composition in the biofilters of the two RAS were also quite consistent (Figure 3-25), despite the fact that both are based on different principles and designs, namely fast-bed vs moving-bed biofilter, as well as seemingly similar to the tank biofilm composition (Figure 3-24), as seen in its taxonomic chart. The reason for this remains unclear.

As microbial communities are important determinants of water quality in rearing systems, and hence fish health, it was of interest to see how the microbiomes in the different built environments influenced the fish mucus microbiota in both RAS and FTS. We hypothesized that built environment microbiota will influence the microbial communities in the skin and gill mucus of the fish, meaning that we expected the skin and gill microbiota to be of similar structural composition to the corresponding tank water and biofilm microbiota.

However, the results visualized in Figure 3-11 showed significant differences in microbial composition between fish mucus samples and the corresponding tank water and tank biofilm samples, which deviated from the afore mentioned hypothesis. This suggests that the fish harbors a unique microbiota deviating, at least partially, from its surrounding environment. Several studies (Minniti et al., 2017; Bakke et al., 2013) have shown that host microbiota and water microbiota are significantly different from each other, which substantiates our results. Since the fish microbiota in the RAS was significantly different from the fish microbiota in the FTS, the different water treatments are thought to be an explanation causing the differences between the rearing systems. Minich et al. (2020) found that skin and gill microbial communities in aquacultured Atlantic salmon are more similar to tank biofilm and water than digesta. Similar results were observed in our studies with farmed Arctic charr, as shown in the PCoA plot of all samples (Figure 3-11). The plot clearly shows that the water and biofilm samples, independent of system, cluster closer to skin and gill samples than the gut samples. This emphasizes that the gut microbiota is not only different, but also follows its own and unique trajectory, eventually heavily influenced by the feed and different internal environmental conditions in the fish's gut compared to the external rearing environment. This could also be used to identify certain bioindicators species for fish welfare in the gut, rather than in the skin and gill mucus, that have the potential to be used as early warning indicators.

Abundant bacterial taxa in fish mucus

Mucosal surfaces in fish are integral parts of the host immune system and harbors mutualistic and commensal microbes associated with the protection against infections. Detailed mucus microbiota composition analysis is therefore mandatory to identify key players and correlations between environment and host.

Pseudomonas is a known bacterial genus containing pathogenic species present on both the host and outside the host in its aquatic environment (Llewellyn et al., 2014). Members of *Pseudomonas* were predominant in skin and gill samples, whereas *Chryseobacterium* was the highest abundant genus in skin samples derived from FTS (Table 3-2). Also, FTS derived samples displayed the highest abundance of *Pseudomonas* in gill samples. *Pseudomonas* belongs to the phylum Proteobacteria, which is one the major phyla found in skin and gill mucus in a study by Llewellyn et al. (2014) conducted across different fish species. However, *Chryseobacterium* is member of the phylum Bacteroidetes, which also was one of the major phyla found in the study (Llewellyn et al., 2014). This emphasizes that the microbiota is not as affected by type of rearing system, but rather by the sampling position (host or environment). It also underlines that Arctic charr displays similar bacterial composition patterns as other fish species, and this adds new knowledge to the understanding of producing this species in land-based aquaculture systems.

Pseudomonas and *Acinetobacter* were present among the top average abundance genera in skin samples in both RAS. Both genera have been found on stressed individuals in an experimental study on brook charr, a close relative to Arctic charr, cultivated in RAS (Boutin et al., 2013). However, pathogenicity is usually species specific, and we did not classify further down the taxonomic hierarchy than genus level as 16S rRNA does not provide sufficient discriminative information for taxonomic classification down to species level (Church et al., 2020). Suboptimal rearing conditions can cause stressed individuals but will most likely also result in increased fish mortality. In case of Arctic charr, suboptimal rearing conditions could for example be low density in the fish tanks. During the monitoring period used for this thesis, no increased mortality was reported, and it is therefore suggested that

the afore described opportunistic pathogenic bacteria containing genera were present, but no infection outbreaks occurred since the pathogenic species of *Pseudomonas* and *Acinetobacter* were not present. However, this cannot be verified in terms of the result from this study. Nevertheless, no increased mortality or outbreak suggests a good welfare and fit fish populations during the monitoring period.

Detailed analysis of gut samples revealed significant differences in microbiota compared to skin and gill mucus, as hypothesized. The low abundance of 'Other' (< 6.9%) compared to skin (< 32.3%) and gill (< 28.1%) samples (Table 3-2) indicated low diversity, found by the alpha diversity analyses (Figure 3-9). Three out of five of the highest average abundant genera in gut microbiomes across the three systems belonged to the phylum Proteobacteria, a commonly known phylum in gut microbiomes of different fish species (Llewellyn et al., 2014). *Mycoplasma* was the genera of highest average abundance in all three systems (Table 3-2). *Mycoplasma* was also previously found in a study on Atlantic salmon gut (Wang et al., 2021) which characterized the microbiota of gut in farmed Atlantic salmon samples by 16S rRNA sequencing before and after transferring the fish from freshwater to seawater. Today's knowledge of gut microbiota in fish is limited, especially of fish from Artic areas (Wang et al., 2018), such as Arctic charr. However, *Mycoplasma* is a known human pathogen and a natural occurring in distal intestine of wild salmon (Holben et al., 2002). That genus was found to increase in abundance from the start to the end of the sampling in the study by Wang et al. (2021), which is not in line with our observations. In our study, *Mycoplasma* was of highest average relative abundance in RAS_1, the system with the smallest fish, and of least average relative abundance in the FTS, the system with the biggest fish in its grow-out phase. However, Wang et al. (2021) transferred the fish from fresh water to sea water, which was not similar to our study, and which can be a possible explanation for the observed differences. In a study performed in a land-based facility of rearing Atlantic salmon, the presence of *Mycoplasma* was found in correlation with healthy salmon gut microbiota (Bozzi et al., 2021). This suggests that the presence of *Mycoplasma* may have a positive effect on gut microbiota, also in Arctic charr. *Aeromonas* was also present in top five average abundance in all systems, a known genus containing pathogenic bacteria for freshwater fish species (Butt and Volkoff, 2019). It was of highest abundance in the FTS, indicating that the rearing conditions influences gut microbiota. This is also in line with findings made by Butt and Volkoff (2019).

Abundant bacterial taxa in environment samples

As the fish lives in constant contact with its surrounding tank water microbiota, detailed mapping of microbiota composition of its environment is crucial to identify important bacteria that interacts with the host.

All built environment samples in the systems were dominated by the phylum Bacteroidetes and Proteobacteria in highest average abundance (Table 3-3). The microbial community composition of the tank water was, as shown in Figure 3-15 A and Figure 3-23, rather consistent throughout the sampling months in its respective system. The finding that also the biofilter in both RAS were very stable, and that only minor dynamics were observed, supports our hypothesis that the biofilter stabilizes the microbial communities in the tank water of RAS. In addition, the very stable microbiota in tank water of the FTS and significant reduction in diversity compared to the source water (Figure 3-10) indicates an effective hygienic barrier that also contributes to a built environment microbiota in all three systems. In general, aquatic microbial communities are known to be highly dynamic (Bakke et al., 2017). This supports the hypothesis that disinfection of the intake water will

influence microbial communities in tank water by significantly reducing diversity, which is not necessarily positive. Whereas disinfection is destabilizing the system and decreasing diversity, the selection pressure inside the built environments is high and will promote diversity, especially in connection to the biofilter, which stabilizes the system (Blancheton et al., 2013). The high abundance of Flavobacteria may represent a biosafety risk, supporting that a more diverse microbiota in the native environment does not allow the predominance of one or a few taxa. The native environment is nutrient poor compared to the built environment with high organic load, which provides permissive growth conditions for certain fast-growing microbes.

Nitrifying bacteria are present in the biofilm in the biofilter where they convert toxic ammonia to nitrate. The genus *Candidatus_Nitrotoga* is a nitrite-oxidizing bacteria working in the second step of the nitrification process. This genus was present in the FBBF in very low abundance (0.86%), suggesting that the MBBF (presence 8.9%) has a higher nitrification efficiency. This could also be explained by RAS_1 containing the smallest fish. It is therefore expected to find lower levels of NH_3, as smaller fish will excrete less NH_3 than bigger fish, and consequently lower concentration of nitrifying bacteria in its biofilter (FBBF). Since the biofilter is a critical component in a RAS, with a large surface area for possible growth of bacteria, one wants to keep the opportunistic pathogens at a minimum to obtain well-functioning nitrification. However, the biofilters had a high percentage of 'Other' (> 36%) indicating a high diversity, also reflected in its alpha diversity (Figure 3-10). For a more detailed assessment of the nitrification efficiencies/capacities in the two biofilter types, analyzing ammonia and nitrate/nitrite levels would have been necessary, which has not been involved in this thesis.

Comparison of fish and environment microbiota

Mucosal surfaces, such as the skin and gill, are continuously exposed to their rearing environment. Yet, few studies have investigated how the surrounding environment impacts the mucosal microbiomes (Minich et al., 2020). The microbiota of the sampled mucosal surfaces in this study was therefore seen in line with the microbiota of its corresponding built environment.

Proteobacteria and Bacteroidetes were dominating phyla throughout skin, gill, and water samples in the three rearing tanks (Table 3-2 and Table 3-3). This is in line with a previous study investigating microbial communities in mucus and rearing water of Atlantic salmon before and after transferring the fish from freshwater RAS to seawater cages, using 16S rRNA gene sequencing (Lorgen-Ritchie et al., 2022). These two phyla were also found in skin and gill samples in a study on different teleost fish species (Llewellyn et al., 2014). Whereas Proteobacteria and Bacteroidetes were dominating in skin and gill, Proteobacteria was of high average abundance in gut mucus samples but dominated by *Mycoplasma* (phylum Mycoplasmatota). Tank water samples in all rearing tanks were also dominated by Proteobacteria and Bacteroidetes, in line with results found from the above-mentioned study by Lorgen-Ritchie et al. (2022) investigating the rearing freshwater and seawater open cage production of Atlantic salmon.

Significant differences between fish and environment samples were found in our work, and the only common genus of highest average relative abundance in RAS_1 skin and gill mucus similar to its respective tank water and biofilm was *Flavobacterium*. RAS_2 shared the observed similarity of *Flavobacterium* in skin, gill, and tank water microbiota. *Flavobacterium* is a genus known to harbor pathogenic species, and has been found in freshwater aquaculture where it potentially can cause high mortality under the right

conditions (Wahli and Madsen, 2018). It is well known that *Flavobacterium* can survive in the aquatic environment outside of its host (Llewellyn et al., 2014). Consequently, this explains our findings of this taxa colonizing both host as well as its environment. Even though this genus was highly abundant in environment samples, but also fish mucus samples, no infliction was observed regarding the health of the fish during the sampling period. This suggests that pathogenic species of the genus were not present. However, it cannot be verified from the results of this study that the found *Flavobacterium* is neither pathogenic nor non-pathogenic. Since the gut did not share genera in highest average abundance with the tank water and tank biofilm in both RAS, it again emphasizes that the gut colonizes its own microbiota less affected by external environment than skin and gill mucus. The main shaping factor of gut microbiota is proposed to be dominated by the diet (Uren Webster et al., 2018). These findings supports that the microbiota of skin and gill is more similar to tank water, compared to gut mucus, also proposed by Minich et al. (2020). The results from the present study indicates that the mucosal surfaces of reared Arctic charr has specialized microbial communities that are different, yet influenced by, the microbial communities in its rearing environment. This was also proposed by Uren Webster et al. (2018) in a study characterizing skin and gut microbiome of juvenile Atlantic salmon inhabiting hatchery-reared and wild environments.

Similar observations were made for the FTS, where *Flavobacterium* was found in skin and gill mucus, tank water and tank biofilm. Tank biofilms are known to be challenging to monitor, but positively correlated with fish mucus (Minich et al., 2020). Cai et al. (2013) suggested that *Flavobacterium* colonizes in the biofilm, which is in line with our results displaying the genus in high average abundance in both tank- and biofilter biofilm. *Pseudomonas* was also found in skin, gill, and tank water in the FTS. Since *Pseudomonas* also was found of high abundance in fish mucus samples, in line with Minich et al. (2020), it suggests that it is colonized on fish mucus throughout the system.

4.3.4 Temporal changes in microbial communities

Since the microbial communities present in a RAS are affected by a variety of factors such as the feed- and feeding regimes, the make-up water, management routines, selection pressure in the system as well as the fish itself, it can also change over time (Attramadal et al., 2012; Blancheton et al., 2013; Vadstein et al., 2018). The microbial communities were hypothesized to be different at different time points of the sampling.

RAS are closed and controlled systems, but variation in for example compounds such as CO_2, TAN and O_2 can occur and lead to dynamic changes in the microbiota. When investigating temporal changes in microbial composition, we found significant differences in fish mucosal microbiota composition. For skin mucus samples, the microbiota was significantly dynamic in both RAS between all sampling months. The biggest shift was, however, observed in RAS_1 and RAS_2 from April to May, where *Pseudomonas* increased from 2.3% and 2.2% to 46.8% and 52.4%, respectively. This increase is therefore suggested to have occurred by the treatment of the water causing favorable growth conditions for *Pseudomonas*. *Pseudomonas* was not present in high abundance in the tank water during the two months, indicating that *Pseudomonas* colonizing the skin followed its own internal environmental condition.

For gill samples, a possible trend was seen with significant difference in microbial composition between the early and the late sampling months, suggesting that the microbial composition develops as the fish grows. Similar trends were seen within the same RAS, whereas the dynamics of the microbiota in the FTS differ. Likewise, as for the skin samples,

the gill samples from the two RAS experienced an increase in *Pseudomonas* from April to May (from 2.5% and 2.4% to 48.5% and 64.5%, respectively). This shift is likely the cause of difference in microbial community composition found in both RAS for skin and gill samples. The afore mentioned study by Lorgen-Ritchie et al. (2022), investigating microbial communities in mucus and rearing water of Atlantic salmon before and after transferring the fish from freshwater to seawater, found significant temporal difference in mucus microbiota. This is in line with our results. Proteobacteria was found to be temporally dynamic in their gill samples (Lorgen-Ritchie et al., 2022), also supporting our result by the varying abundance of *Pseudomonas* especially in the gills from the two RAS.

Similarity in microbial community composition in skin and gill is again found in the study by Minich et al. (2020), and as expected in our study. As *Pseudomonas* is a genus containing opportunistic pathogenic species, it is tempting to draw the conclusion that the fish experienced a shift in stress level from April to May, causing reduced mucus and hence favorable growth conditions for *Pseudomonas*. However, the increase could also be caused by an increase of available substrate for heterotrophic bacteria that will interfere with the gill health. It cannot be confirmed nor denied that *Pseudomonas* found in this study was pathogenic.

For gut mucus samples, both RAS showed significant differences between April and July, and May and July. This difference can probably be explained by the high presence of *Aeromonas* mid- to end sampling. *Aeromonas* is known to contain species pathogenic for salmonids (Ringø et al., 2004). The fact that this taxon was found in high abundance in the gut compared to skin and gill emphasizes the gut as a major route for pathogen entry in fish. However, as earlier mentioned, there was not noticeable concerns regarding fish health during the entire sampling period. Since there were minor similarities in microbiota of the gut and its corresponding tank water throughout the sampling months, this suggests that the gut colonizes its unique microbiota affected by factors other than the water. For the FTS, the gut microbiota in April was significantly different to all other months. The reason for this remains unclear.

Interestingly, we did not observe any significant difference in microbial composition for the environment samples over time. This low microbial dynamic indicates that the microbial composition in the production environments is more stable over time than in the fish. This could possibly be explained by hygienic barriers ensure biosecurity and creates a stable environment, since the source water also showed little dynamic. When comparing the taxonomic profiles of the tank water (Figure 3-23) of the two RAS versus the FTS, one can see indication of the RAS being more stable than the FTS. This could be explained by the biofilter working as a stabilizing agent for the RAS, and hence supports our hypothesis. The reason for little dynamic in the source water remains unclear. Hence, this emphasizes that the fish colonizes its unique microbiota driven by internal factors as well as external.

4.4 Future Work and Perspectives

This thesis has provided pioneering insight in bacterial communities in farming of Arctic charr. This was done by characterizing the microbial communities present in the host mucosal surfaces (skin, gill, and gut mucus) as well as corresponding built environments (intake and tank water, biofilm in tank and biofilter) in a commercial land-based aquaculture facility operating with both RAS and FTS. This is important since the research on microbial communities of Arctic charr is scarce as of today, in a time where the species has become an interesting candidate for land-based seafood production. Most studies on microbiota in aquaculture focus on Atlantic salmon and rainbow trout, but expanding the focus to include other industrially relevant species of salmonids is an advantage to the industry. There is also a knowledge gap in term of how host microbiota is influenced by its environment, and vice versa. This thesis has contributed to novel insights by systematic spatiotemporal comparison of the microbiota found in fish mucus to the microbiota found in the corresponding surrounding environment and generated a solid basis for future work.

Since the samples from this master project were obtained over a time span of 6 months, a longer sampling timespan would be of advantage for further work in order to eventually reveal temporal dynamics, especially in the source water. The samples lost to rarefaction in this project mostly came from gill and gut mucus, and further work could therefore advantageously include a larger number of evenly distributed samples. An advantage for this thesis would have been to quantify the number of bacteria to gain knowledge about how much bacterial DNA is present on Arctic charr mucus. It would also be interesting to quantify bacteria in environment, especially to assess hygienic barrier efficiency, because the higher diversity found in the source water does not necessarily imply that the total bacteria number is higher than tank water. Further studies on microbial communities present in reared Arctic charr should be conducted to increase knowledge in this area. Analysis and integration of other water quality parameters such as DO, CO_2, TAN would be interesting to explain dynamics and differences in microbiota composition, especially for biofilter systems.

Since the microbial communities present on fish mucosal surfaces and its environment is known to affect the overall health of the fish, it would be interesting to further explore these relationships to increase fish health in land-based aquaculture systems. Since gut microbiota was found to be different to skin and gill, while also following its own and unique trajectory influenced by the feed and different internal environmental conditions, compared to the external rearing environment, this could also be used to identify certain bioindicator species for fish welfare in the gut rather than in the skin and gill mucus. This has the potential to be used as early warning indicators.

5 Conclusion

To our knowledge, this is the first study investigating microbial communities present on mucosal surfaces (skin, gill, and gut) of Arctic charr in a commercial-based system operating with both RAS and FTS. The microbial communities present on mucosal surfaces were seen in line with its respective surrounding environment, such as tank water and biofilm, the intake water, and biofilter biofilm connected to the systems. The results of this thesis can further be implemented to increase knowledge of Arctic charr reared in land-based aquaculture systems.

The major findings in this thesis were:

- Skin mucus samples were more diverse than gill and gut mucus samples for both RAS and FTS
- Built environment samples (tank water, tank biofilm, biofilter biofilm) were more diverse than fish samples (skin, gill, and gut mucus) in all three systems
- The native environment was significantly more diverse than the built environment and fish samples
- Significant differences in microbial composition between fish mucus samples were found, and between environmental samples
- Significant differences in microbial composition for skin, gill, and gut mucus samples were found between the two RAS and FTS
- Significant differences in microbial composition between built environment samples were found between each system indicating unique microbiota in both RAS and FTS
- Significant differences over time were found in fish samples, but not in environment samples
- Skin and gill mucus samples were in general dominated by *Pseudomonas*, whereas gut samples were dominated by *Mycoplasma*. *Flavobacterium* dominated in tank water and biofilm biofilter, whereas *Arcicella* dominated in tank biofilm. *Crenothrix* dominated in the source water

References

ANDERSON, M. J. 2001. A new method for non-parametric multivariate analysis of variance. *Austral ecology,* 26**,** 32-46. https://doi.org/10.1111/j.1442-9993.2001.01070.pp.x

ÁNGELES ESTEBAN, M. 2012. An Overview of the Immunological Defenses in Fish Skin. *ISRN immunology,* 2012**,** 1-29. https://doi.org/10.5402/2012/853470

ÁNGELES ESTEBAN, M. & CEREZUELA, R. 2015. 4 - Fish mucosal immunity: skin. *In:* BECK, B. H. & PEATMAN, E. (eds.) *Mucosal Health in Aquaculture.* San Diego: Academic Press.

ASHLEY, P. J. 2007. Fish welfare: Current issues in aquaculture. *Applied Animal Behaviour Science,* 104**,** 199-235. https://doi.org/10.1016/j.applanim.2006.09.001

ATTRAMADAL, K. J. K., SALVESEN, I., XUE, R., ØIE, G., STØRSETH, T. R., VADSTEIN, O. & OLSEN, Y. 2012. Recirculation as a possible microbial control strategy in the production of marine larvae. *Aquacultural Engineering,* 46**,** 27-39. https://doi.org/10.1016/j.aquaeng.2011.10.003

AZARIA, S. & VAN RIJN, J. 2018. Off-flavor compounds in recirculating aquaculture systems (RAS): Production and removal processes. *Aquacultural Engineering,* 83**,** 57-64. https://doi.org/10.1016/j.aquaeng.2018.09.004

BAKKE, I., SKJERMO, J., VO, T. A. & VADSTEIN, O. 2013. Live feed is not a major determinant of the microbiota associated with cod larvae (G adus morhua). *Environmental Microbiology Reports,* 5**,** 537-548. https://doi.org/10.1111/1758-2229.12042

BAKKE, I., ÅM, A. L., KOLAREVIC, J., YTRESTØYL, T., VADSTEIN, O., ATTRAMADAL, K. J. K. & TERJESEN, B. F. 2017. Microbial community dynamics in semi-commercial RAS for production of Atlantic salmon post-smolts at different salinities. *Aquacultural Engineering,* 78**,** 42-49. https://doi.org/10.1016/j.aquaeng.2016.10.002

BLANCHETON, J. P., ATTRAMADAL, K. J. K., MICHAUD, L., D'ORBCASTEL, E. R. & VADSTEIN, O. 2013. Insight into bacterial population in aquaculture systems and its implication. *Aquacultural Engineering,* 53**,** 30-39. https://doi.org/10.1016/j.aquaeng.2012.11.009

BOLYEN, E., RIDEOUT, J. R., DILLON, M. R., BOKULICH, N. A., ABNET, C. C., AL-GHALITH, G. A., ALEXANDER, H., ALM, E. J., ARUMUGAM, M., ASNICAR, F., BAI, Y., BISANZ, J. E., BITTINGER, K., BREJNROD, A., BRISLAWN, C. J., BROWN, C. T., CALLAHAN, B. J., CARABALLO-RODRÍGUEZ, A. M., CHASE, J., COPE, E. K., DA SILVA, R., DIENER, C., DORRESTEIN, P. C., DOUGLAS, G. M., DURALL, D. M., DUVALLET, C., EDWARDSON, C. F., ERNST, M., ESTAKI, M., FOUQUIER, J., GAUGLITZ, J. M., GIBBONS, S. M., GIBSON, D. L., GONZALEZ, A., GORLICK, K., GUO, J., HILLMANN, B., HOLMES, S., HOLSTE, H., HUTTENHOWER, C., HUTTLEY, G. A., JANSSEN, S., JARMUSCH, A. K., JIANG, L., KAEHLER, B. D., KANG, K. B., KEEFE, C. R., KEIM, P., KELLEY, S. T., KNIGHTS, D., KOESTER, I., KOSCIOLEK, T., KREPS, J., LANGILLE, M. G. I., LEE, J., LEY, R., LIU, Y.-X., LOFTFIELD, E., LOZUPONE, C., MAHER, M., MAROTZ, C., MARTIN, B. D., MCDONALD, D., MCIVER, L. J., MELNIK, A. V., METCALF, J. L., MORGAN, S. C., MORTON, J. T., NAIMEY, A. T., NAVAS-MOLINA, J. A., NOTHIAS, L. F., ORCHANIAN, S. B., PEARSON, T., PEOPLES, S. L., PETRAS, D., PREUSS, M. L., PRUESSE, E., RASMUSSEN, L. B., RIVERS, A., ROBESON, M. S., ROSENTHAL, P., SEGATA, N., SHAFFER, M., SHIFFER, A., SINHA, R., SONG, S. J., SPEAR, J. R., SWAFFORD, A. D., THOMPSON, L. R., TORRES, P. J., TRINH, P., TRIPATHI, A., TURNBAUGH, P. J., UL-HASAN, S., VAN DER HOOFT, J. J. J., VARGAS, F., VÁZQUEZ-BAEZA, Y., VOGTMANN, E., VON HIPPEL, M., WALTERS, W., et al. 2019. Reproducible, interactive, scalable and extensible microbiome data science

using QIIME 2. *Nature Biotechnology,* 37**,** 852-857. https://doi.org/10.1038/s41587-019-0209-9
BORGSTRØM, R., EBNE, I. & SVENNING, M.-A. 2010. High lacustrine gillnet catchability of anadromous Arctic charr. *Hydrobiologia,* 650**,** 203-212. https://doi.org/10.1007/s10750-010-0119-9
BOUTIN, S., BERNATCHEZ, L., AUDET, C. & DERÔME, N. 2013. Network analysis highlights complex interactions between pathogen, host and commensal microbiota. *PloS one,* 8**,** e84772. https://doi.org/10.1371/journal.pone.0084772
BOZZI, D., RASMUSSEN, J. A., CARØE, C., SVEIER, H., NORDØY, K., GILBERT, M. T. P. & LIMBORG, M. T. 2021. Salmon gut microbiota correlates with disease infection status: potential for monitoring health in farmed animals. *Animal microbiome,* 3**,** 1-17. https://doi.org/10.1186/s42523-021-00096-2
BREGNBALLE, J. 2015. A Guide to Recirculation Aquaculture An introduction to the new environmentally friendly and highly productive closed fish farming systems.
BUKIN, Y. S., GALACHYANTS, Y. P., MOROZOV, I. V., BUKIN, S. V., ZAKHARENKO, A. S. & ZEMSKAYA, T. I. 2019. The effect of 16S rRNA region choice on bacterial community metabarcoding results. *Scientific Data,* 6**,** 190007. https://doi.org/10.1038/sdata.2019.7
BUTT, R. L. & VOLKOFF, H. 2019. Gut microbiota and energy homeostasis in fish. *Frontiers in endocrinology,* 10**,** 9. https://doi.org/10.3389/fendo.2019.00009
CAI, W., DE LA FUENTE, L. & ARIAS, C. R. 2013. Biofilm formation by the fish pathogen Flavobacterium columnare: development and parameters affecting surface attachment. *Applied and environmental microbiology,* 79**,** 5633-5642. https://doi.org/10.1128/AEM.01192-13
CALLAHAN, B. J., MCMURDIE, P. J., ROSEN, M. J., HAN, A. W., JOHNSON, A. J. A. & HOLMES, S. P. 2016. DADA2: High-resolution sample inference from Illumina amplicon data. *Nature Methods,* 13**,** 581-583. https://doi.org/10.1038/nmeth.3869
CASTRO, R. & TAFALLA, C. 2015. 2 - Overview of fish immunity. *In:* BECK, B. H. & PEATMAN, E. (eds.) *Mucosal Health in Aquaculture.* San Diego: Academic Press.
CHAKRAVORTY, S., HELB, D., BURDAY, M., CONNELL, N. & ALLAND, D. 2007. A detailed analysis of 16S ribosomal RNA gene segments for the diagnosis of pathogenic bacteria. *Journal of microbiological methods,* 69**,** 330-339. https://doi.org/10.1016/j.mimet.2007.02.005
CHURCH, D. L., CERUTTI, L., GÜRTLER, A., GRIENER, T., ZELAZNY, A. & EMLER, S. 2020. Performance and Application of 16S rRNA Gene Cycle Sequencing for Routine Identification of Bacteria in the Clinical Microbiology Laboratory. *Clinical Microbiology Reviews,* 33**,** e00053-19. https://doi.org/10.1128/CMR.00053-19
DASH, S., DAS, S., SAMAL, J. & THATOI, H. 2018. Epidermal mucus, a major determinant in fish health: a review. *Iranian journal of veterinary research,* 19**,** 72. https://dx.doi.org/10.22099/ijvr.2018.4849
DEROME, N. 2019. *Microbial Communities in Aquaculture Ecosystems*, Springer Cham.
ELKINS, K. M. 2012. Forensic DNA biology : a laboratory manual. Oxford: Elsevier.
EVANS, D. H., PIERMARINI, P. M. & CHOE, K. P. 2005. The Multifunctional Fish Gill: Dominant Site of Gas Exchange, Osmoregulation, Acid-Base Regulation, and Excretion of Nitrogenous Waste. *Physiol Rev,* 85**,** 97-177. https://doi.org/10.1152/physrev.00050.2003
FAO. 2020. The State of World Fisheries and Aquaculture 2020. In Brief. Sustainability in action.
FJELLHEIM, A. J., HESS-ERGA, O.-K., ATTRAMADAL, K. & VADSTEIN, O. 2016. Recycling of water in hatchery production.
GHANBARI, M., KNEIFEL, W. & DOMIG, K. J. 2015. A new view of the fish gut microbiome: Advances from next-generation sequencing. *Aquaculture,* 448**,** 464-475. https://doi.org/10.1016/j.aquaculture.2015.06.033
GÓMEZ, G. D. & BALCÁZAR, J. L. 2008. A review on the interactions between gut microbiota and innate immunity of fish. *FEMS Immunology & Medical Microbiology,* 52**,** 145-154. https://doi.org/10.1111/j.1574-695x.2007.00343.x

HEAD, I. M., SAUNDERS, J. R. & PICKUP, R. W. 1998. Microbial Evolution, Diversity, and Ecology: A Decade of Ribosomal RNA Analysis of Uncultivated Microorganisms. *Microbial Ecology,* 35**,** 1-21. https://doi.org/10.1007/s002489900056

HESS-ERGA, O.-K., ATTRAMADAL, K. J. K. & VADSTEIN, O. 2008. Biotic and abiotic particles protect marine heterotrophic bacteria during UV and ozone disinfection. *Aquatic Biology,* 4**,** 147-154. https://doi.org/10.3354/ab00105

HOLBEN, W. E., WILLIAMS, P., SAARINEN, M., SÄRKILAHTI, L. & APAJALAHTI, J. H. 2002. Phylogenetic analysis of intestinal microflora indicates a novel Mycoplasma phylotype in farmed and wild salmon. *Microbial ecology,* 44**,** 175-185. https://doi.org/10.1007/s00248-002-1011-6

ILLUMINA. 2017. *An introduction to Next-Generation Sequencing Technology* [Online]. Illumina Inc. Available: https://www.illumina.com/Documents/products/Illumina_Sequencing_Introduction.pdf [Accessed 02.02.2022].

IMSLAND, A. K. & GUNNARSSON, S. 2011. Growth and maturation in Arctic charr (Salvelinus alpinus) in response to different feed rations. *Aquaculture,* 318**,** 407-411. https://doi.org/10.1016/j.aquaculture.2011.05.049

JENSEN, A. J., FINSTAD, B., FISKE, P., DISERUD, O. H. & THORSTAD, E. B. 2020. Repeatable individual variation in migration timing in two anadromous salmonids and ecological consequences. *Ecology and evolution,* 10**,** 11727-11738. http://dx.doi.org/10.1002/ece3.6808

JOHNSTON, G. 2008. *Arctic charr aquaculture*, John Wiley & Sons.

JØRGENSEN, E. H., CHRISTIANSEN, J. S. & JOBLING, M. 1993. Effects of stocking density on food intake, growth performance and oxygen consumption in Arctic charr (Salvelinus alpinus). *Aquaculture,* 110**,** 191-204. https://doi.org/10.1016/0044-8486(93)90272-Z

KASSAMBARA, A. 2021. rstatix: Pipe-Friendly Framework for Basic Statistical Tests.

KELLY, C. & SALINAS, I. 2017. Under Pressure: Interactions between Commensal Microbiota and the Teleost Immune System. *Frontiers in Immunology,* 8. https://doi.org/10.3389/fimmu.2017.00559

KIM, B.-R., SHIN, J., GUEVARRA, R. B., LEE, J. H., KIM, D. W., SEOL, K.-H., LEE, J.-H., KIM, H. B. & ISAACSON, R. E. 2017. Deciphering diversity indices for a better understanding of microbial communities. *Journal of Microbiology and Biotechnology,* 27**,** 2089-2093.

KLINDWORTH, A., PRUESSE, E., SCHWEER, T., PEPLIES, J., QUAST, C., HORN, M. & GLÖCKNER, F. O. 2013. Evaluation of general 16S ribosomal RNA gene PCR primers for classical and next-generation sequencing-based diversity studies. *Nucleic Acids Res,* 41**,** e1-e1. https://doi.org/10.1093/nar/gks808

KOBAYASHI, M., MSANGI, S., BATKA, M., VANNUCCINI, S., DEY, M. M. & ANDERSON, J. L. 2015. Fish to 2030: The Role and Opportunity for Aquaculture. *Aquaculture Economics & Management,* 19**,** 282-300. https://doi.org/10.1080/13657305.2015.994240

KOPPANG, E. O., KVELLESTAD, A. & FISCHER, U. 2015. 5 - Fish mucosal immunity: gill. *In:* BECK, B. H. & PEATMAN, E. (eds.) *Mucosal Health in Aquaculture.* San Diego: Academic Press.

KUCZYNSKI, J., STOMBAUGH, J., WALTERS, W. A., GONZÁLEZ, A., CAPORASO, J. G. & KNIGHT, R. 2011. Using QIIME to analyze 16S rRNA gene sequences from microbial communities. *Current protocols in bioinformatics,* Chapter 10**,** Unit10.7-10.7. https://doi.org/10.1002/0471250953.bi1007s36

LAHTI, L. & SHETTY, S. 2017. microbiome R package.

LEKANG, O.-I. 2020. *Aquaculture Engineering,* Oxford, Wiley Blackwell.

LLEWELLYN, M. S., BOUTIN, S., HOSEINIFAR, S. H. & DEROME, N. 2014. Teleost microbiomes: the state of the art in their characterization, manipulation and importance in aquaculture and fisheries. *Frontiers in Microbiology,* 5. https://doi.org/10.3389/fmicb.2014.00207

LORGEN-RITCHIE, M., CLARKSON, M., CHALMERS, L., TAYLOR, J. F., MIGAUD, H. & MARTIN, S. A. M. 2022. Temporal changes in skin and gill microbiomes of Atlantic

salmon in a recirculating aquaculture system – Why do they matter? *Aquaculture,* 558**,** 738352. https://doi.org/10.1016/j.aquaculture.2022.738352
MATLOCK, B. 2015. *Assesment of Nucleic Acid Purity* [Online]. Available: https://assets.thermofisher.com/TFS-Assets/CAD/Product-Bulletins/TN52646-E-0215M-NucleicAcid.pdf [Accessed 20.05 2022].
MCKIGHT, P. E. & NAJAB, J. 2010. Kruskal-wallis test. *The corsini encyclopedia of psychology***,** 1-1.
MCMURDIE, P. J. & HOLMES, S. 2013. phyloseq: An R package for reproducible interactive analysis and graphics of microbiome census data.
MERRIFIELD, D. L. & RODILES, A. 2015. 10 - The fish microbiome and its interactions with mucosal tissues. *In:* BECK, B. H. & PEATMAN, E. (eds.) *Mucosal Health in Aquaculture.* San Diego: Academic Press.
MINICH, J. J., POORE GREG, D., JANTAWONGSRI, K., JOHNSTON, C., BOWIE, K., BOWMAN, J., KNIGHT, R., NOWAK, B., ALLEN ERIC, E. & LIU, S.-J. 2020. Microbial Ecology of Atlantic Salmon (Salmo salar) Hatcheries: Impacts of the Built Environment on Fish Mucosal Microbiota. *Applied and Environmental Microbiology,* 86**,** e00411-20. https://doi.org/10.1128/AEM.00411-20
MINNITI, G., HAGEN, L. H., PORCELLATO, D., JØRGENSEN, S. M., POPE, P. B. & VAAJE-KOLSTAD, G. 2017. The skin-mucus microbial community of farmed Atlantic salmon (Salmo salar). *Frontiers in microbiology,* 8**,** 2043. https://doi.org/10.3389/fmicb.2017.02043
MINNITI, G., SIMEN RØD, S., JÁNOS TAMÁS, P., LIVE HELDAL, H., LINDÉN, S., POPE, P. B., ARNTZEN, M. Ø. & VAAJE-KOLSTAD, G. 2019. The Farmed Atlantic Salmon (*Salmo salar*) Skin–Mucus Proteome and Its Nutrient Potential for the Resident Bacterial Community. *Genes,* 10**,** 515. https://doi.org/10.3390/genes10070515
OKSANEN, J., SIMPSON, G. L., BLANCHET, F. G., KINDT, R., LEGENDRE, P., MINCHIN, P. R., O'HARA, R. B., SOLYMOS, P., STEVENS, M. H. H., SZOECS, E., WAGNER, H., BARBOUR, M., BEDWARD, M., BOLKER, B., BORCARD, D., CARVALHO, G., CHIRICO, M., CACERES}, M. D., DURAND, S., EVANGELISTA, H. B. A., FITZJOHN, R., FRIENDLY, M., FURNEAUX, B., HANNIGAN, G., HILL, M. O., LAHTI, L., MCGLINN, D., OUELLETTE, M.-H., CUNHA}, E. R., SMITH, T., STIER, A., BRAAK}, C. J. F. T. & WEEDON, J. 2022. vegan: Community Ecology Package.
PÉREZ, T., BALCÁZAR, J. L., RUIZ-ZARZUELA, I., HALAIHEL, N., VENDRELL, D., DE BLAS, I. & MÚZQUIZ, J. L. 2010. Host–microbiota interactions within the fish intestinal ecosystem. *Mucosal Immunology,* 3**,** 355-360. https://doi.org/10.1038/mi.2010.12
PERSSON, D., IAKHNO, S., DAHLE, S. W., NETZER, R., SANDBERG, R., SØRUM, H. & RIBICIC, D. 2022, manuscript submitted. Bacterial community composition in gill mucus and corresponding environment in four commercial Atlantic salmon smolt RAS. *In:* NMBU (ed.).
RAJESH, T. & JAYA, M. 2017. 7 - Next-Generation Sequencing Methods. *In:* GUNASEKARAN, P., NORONHA, S. & PANDEY, A. (eds.) *Current Developments in Biotechnology and Bioengineering.* Elsevier.
RINGØ, E., JUTFELT, F., KANAPATHIPPILLAI, P., BAKKEN, Y., SUNDELL, K., GLETTE, J., MAYHEW, T. M., MYKLEBUST, R. & OLSEN, R. E. 2004. Damaging effect of the fish pathogen Aeromonas salmonicida ssp. salmonicida on intestinal enterocytes of Atlantic salmon (Salmo salar L.). *Cell and tissue research,* 318**,** 305-311. https://doi.org/10.1007/s00441-004-0934-2
ROJAS-TIRADO, P., AALTO, S. L., ÅTLAND, Å. & LETELIER-GORDO, C. 2021. Biofilters are potential hotspots for H2S production in brackish and marine water RAS. *Aquaculture,* 536**,** 736490. https://doi.org/10.1016/j.aquaculture.2021.736490
ROSTEN, T. W., HENRIKSEN, K., HOGNES, E. S., VINCI, B. & SUMMERFELT, S. Land-based RAS and open pen salmon aquaculture: Comparative economic and environmental assessment. Aquaculture Innovations Workshop, 2013.
RURANGWA, E. & VERDEGEM, M. C. J. 2015. Microorganisms in recirculating aquaculture systems and their management. *Rev Aquacult,* 7**,** 117-130. https://doi.org/10.1111/raq.12057

SALINAS, I. & PARRA, D. 2015. 6 - Fish mucosal immunity: intestine. *In:* BECK, B. H. & PEATMAN, E. (eds.) *Mucosal Health in Aquaculture.* San Diego: Academic Press.

SANDBERG, R. 2021. *Mapping bacterial community structures in skin and gill mucus of Atlantic salmon (Salmo salar) smolt from four commercial RAS facilities.* NTNU.

TAKAHASHI, S., TOMITA, J., NISHIOKA, K., HISADA, T. & NISHIJIMA, M. 2014. Development of a prokaryotic universal primer for simultaneous analysis of Bacteria and Archaea using next-generation sequencing. *PLoS One,* 9**,** e105592-e105592. https://doi.org/10.1371/journal.pone.0105592

TALWAR, C., NAGAR, S., LAL, R. & NEGI, R. K. 2018. Fish gut microbiome: current approaches and future perspectives. *Indian journal of microbiology,* 58**,** 397-414. https://doi.org/10.1007/s12088-018-0760-y

TLUSTY, M. 2002. The benefits and risks of aquacultural production for the aquarium trade. *Aquaculture,* 205**,** 203-219. https://doi.org/10.1016/S0044-8486(01)00683-4

UREN WEBSTER, T. M., CONSUEGRA, S., HITCHINGS, M. & GARCIA DE LEANIZ, C. 2018. Interpopulation variation in the Atlantic salmon microbiome reflects environmental and genetic diversity. *Applied and Environmental Microbiology,* 84**,** e00691-18. https://doi.org/10.1128/AEM.00691-18

VADSTEIN, O., ATTRAMADAL, K. J. K., BAKKE, I. & OLSEN, Y. 2018. K-Selection as Microbial Community Management Strategy: A Method for Improved Viability of Larvae in Aquaculture. *Frontiers in Microbiology,* 9. https://doi.org/10.3389/fmicb.2018.02730

WAHLI, T. & MADSEN, L. 2018. Flavobacteria, a never ending threat for fish: a review. *Current Clinical Microbiology Reports,* 5**,** 26-37. https://doi.org/10.1007/s40588-018-0086-x

WANG, A. R., RAN, C., RINGØ, E. & ZHOU, Z. G. 2018. Progress in fish gastrointestinal microbiota research. *Reviews in Aquaculture,* 10**,** 626-640. https://doi.org/10.1111/raq.12191

WANG, J., JARAMILLO-TORRES, A., LI, Y., KORTNER, T. M., GAJARDO, K., BREVIK, Ø. J., JAKOBSEN, J. V. & KROGDAHL, Å. 2021. Microbiota in intestinal digesta of Atlantic salmon (Salmo salar), observed from late freshwater stage until one year in seawater, and effects of functional ingredients: a case study from a commercial sized research site in the Arctic region. *Animal Microbiome,* 3**,** 14. https://doi.org/10.1186/s42523-021-00075-7

WICKHAM, H. 2016. ggplot2: Elegant Graphics for Data Analysis.

XUE, S., XU, W., WEI, J. & SUN, J. 2017. Impact of environmental bacterial communities on fish health in marine recirculating aquaculture systems. *Veterinary Microbiology,* 203**,** 34-39. https://doi.org/10.1016/j.vetmic.2017.01.034

Appendix A: Illumina Workflow

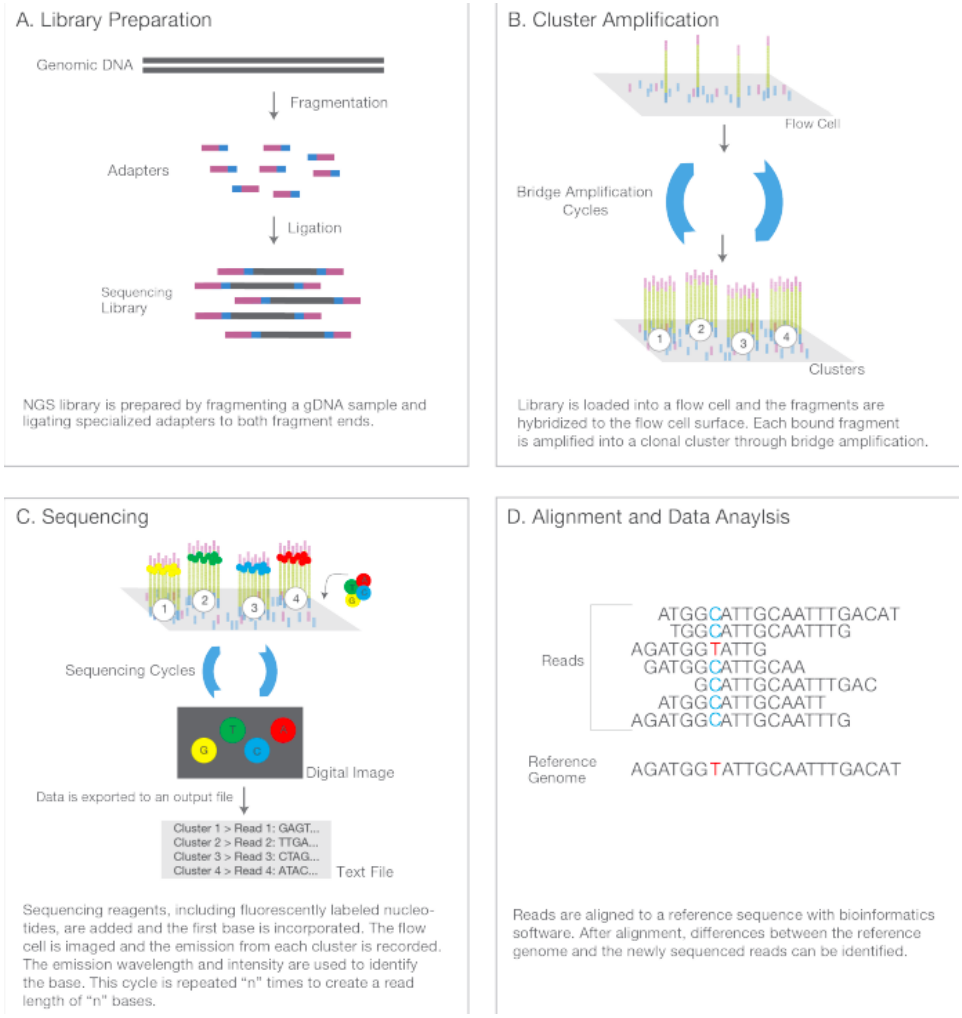

Appendix B: Water Parameters

Parameters for the sampled water treatment (CO_2 and pH). The facility has a stable temperature year around at 6°C and an automated O_2 system with a target of 100% saturation at the outlet.

Table B-1: Water parameters listed as CO_2 (mg/l)/pH

Sampling month	Growth		Small fish	
	Biofilter inlet	Biofilter outlet	Biofilter inlet	Biofilter outlet
April	20/6,3	10/6,6	24/6,3	10/6,4
May	25/6,2	9/6,5	24/6,3	8/6,7
June	28/6,1	12/6,5	20/6,3	11/6,6
July	18/6,1	10/6,4	19/6,3	10/7,1
August	29/6,2	10/6,6	27/6,2	9/6,7
September	20/6,4	10/6,7	27/6,1	10/6,7

Appendix C: Sample Overview

Table C-1: Sample information including the sample ID, sampling date, sampling type, tank, and fish weight (g) for all 432 samples.

Sample-ID	Sampling date	Sample type	Tank	Fish weight [g]
NFFT001	08.04.2021	SW	-	-
NFFT002	08.04.2021	SW	-	-
NFFT003	08.04.2021	SW	-	-
NFFT004	08.04.2021	BB	16	-
NFFT005	08.04.2021	BB	16	-
NFFT006	08.04.2021	BB	16	-
NFFT007	08.04.2021	TW	16	30-45
NFFT008	08.04.2021	TW	16	30-45
NFFT009	08.04.2021	TW	16	30-45
NFFT010	08.04.2021	TB	16	30-45
NFFT011	08.04.2021	TB	16	30-45
NFFT012	08.04.2021	TB	16	30-45
NFFT013	08.04.2021	SKM	16	30-45
NFFT014	08.04.2021	GIM	16	30-45
NFFT015	08.04.2021	GUM	16	30-45
NFFT016	08.04.2021	SKM	16	30-45
NFFT017	08.04.2021	GIM	16	30-45
NFFT018	08.04.2021	GUM	16	30-45
NFFT019	08.04.2021	SKM	16	30-45
NFFT020	08.04.2021	GIM	16	30-45
NFFT021	08.04.2021	GUM	16	30-45
NFFT022	08.04.2021	SKM	16	30-45
NFFT023	08.04.2021	GIM	16	30-45
NFFT024	08.04.2021	GUM	16	30-45
NFFT025	08.04.2021	SKM	16	30-45
NFFT026	08.04.2021	GIM	16	30-45
NFFT027	08.04.2021	GUM	16	30-45
NFFT028	08.04.2021	TW	17	180
NFFT029	08.04.2021	TW	17	180
NFFT030	08.04.2021	TW	17	180
NFFT031	08.04.2021	TB	17	180
NFFT032	08.04.2021	TB	17	180

NFFT033	08.04.2021	TB	17	180
NFFT034	08.04.2021	SKM	17	180
NFFT035	08.04.2021	GIM	17	180
NFFT036	08.04.2021	GUM	17	180
NFFT037	08.04.2021	SKM	17	180
NFFT038	08.04.2021	GIM	17	180
NFFT039	08.04.2021	GUM	17	180
NFFT040	08.04.2021	SKM	17	180
NFFT041	08.04.2021	GIM	17	180
NFFT042	08.04.2021	GUM	17	180
NFFT043	08.04.2021	SKM	17	180
NFFT044	08.04.2021	GIM	17	180
NFFT045	08.04.2021	GUM	17	180
NFFT046	08.04.2021	SKM	17	180
NFFT047	08.04.2021	GIM	17	180
NFFT048	08.04.2021	GUM	17	180
NFFT049	08.04.2021	TW	S1	550
NFFT050	08.04.2021	TW	S1	550
NFFT051	08.04.2021	TW	S1	550
NFFT052	08.04.2021	TB	S1	550
NFFT053	08.04.2021	TB	S1	550
NFFT054	08.04.2021	TB	S1	550
NFFT055	08.04.2021	SKM	S1	550
NFFT056	08.04.2021	GIM	S1	550
NFFT057	08.04.2021	GUM	S1	550
NFFT058	08.04.2021	SKM	S1	550
NFFT059	08.04.2021	GIM	S1	550
NFFT060	08.04.2021	GUM	S1	550
NFFT061	08.04.2021	SKM	S1	550
NFFT062	08.04.2021	GIM	S1	550
NFFT063	08.04.2021	GUM	S1	550
NFFT064	08.04.2021	SKM	S1	550
NFFT065	08.04.2021	GIM	S1	550
NFFT066	08.04.2021	GUM	S1	550
NFFT067	08.04.2021	SKM	S1	550
NFFT068	08.04.2021	GIM	S1	550

NFFT069	08.04.2021	GUM	S1	550
NFFT070	08.04.2021	BB	17	-
NFFT071	08.04.2021	BB	17	-
NFFT072	08.04.2021	BB	17	-
NFFT073	05.05.2021	SW	-	-
NFFT074	05.05.2021	SW	-	-
NFFT075	05.05.2021	SW	-	-
NFFT076	05.05.2021	BB	16	-
NFFT077	05.05.2021	BB	16	-
NFFT078	05.05.2021	BB	16	-
NFFT079	05.05.2021	TW	16	-
NFFT080	05.05.2021	TW	16	-
NFFT081	05.05.2021	TW	16	-
NFFT082	05.05.2021	TB	16	-
NFFT083	05.05.2021	TB	16	-
NFFT084	05.05.2021	TB	16	-
NFFT085	05.05.2021	SKM	16	74
NFFT086	05.05.2021	GIM	16	74
NFFT087	05.05.2021	GUM	16	74
NFFT088	05.05.2021	SKM	16	66
NFFT089	05.05.2021	GIM	16	66
NFFT090	05.05.2021	GUM	16	66
NFFT091	05.05.2021	SKM	16	92
NFFT092	05.05.2021	GIM	16	92
NFFT093	05.05.2021	GUM	16	92
NFFT094	05.05.2021	SKM	16	38
NFFT095	05.05.2021	GIM	16	38
NFFT096	05.05.2021	GUM	16	38
NFFT097	05.05.2021	SKM	16	32
NFFT098	05.05.2021	GIM	16	32
NFFT099	05.05.2021	GUM	16	32
NFFT100	05.05.2021	BB	17	-
NFFT101	05.05.2021	BB	17	-
NFFT102	05.05.2021	BB	17	-
NFFT103	05.05.2021	TW	17	-
NFFT104	05.05.2021	TW	17	-

NFFT105	05.05.2021	TW	17	-
NFFT106	05.05.2021	TB	17	-
NFFT107	05.05.2021	TB	17	-
NFFT108	05.05.2021	TB	17	-
NFFT109	05.05.2021	SKM	17	402
NFFT110	05.05.2021	GIM	17	402
NFFT111	05.05.2021	GUM	17	402
NFFT112	05.05.2021	SKM	17	232
NFFT113	05.05.2021	GIM	17	232
NFFT114	05.05.2021	GUM	17	232
NFFT115	05.05.2021	SKM	17	202
NFFT116	05.05.2021	GIM	17	202
NFFT117	05.05.2021	GUM	17	202
NFFT118	05.05.2021	SKM	17	302
NFFT119	05.05.2021	GIM	17	302
NFFT120	05.05.2021	GUM	17	302
NFFT121	05.05.2021	SKM	17	258
NFFT122	05.05.2021	GIM	17	258
NFFT123	05.05.2021	GUM	17	258
NFFT124	05.05.2021	TW	S1	-
NFFT125	05.05.2021	TW	S1	-
NFFT126	05.05.2021	TW	S1	-
NFFT127	05.05.2021	TB	S1	-
NFFT128	05.05.2021	TB	S1	-
NFFT129	05.05.2021	TB	S1	-
NFFT130	05.05.2021	SKM	S1	926
NFFT131	05.05.2021	GIM	S1	926
NFFT132	05.05.2021	GUM	S1	926
NFFT133	05.05.2021	SKM	S1	1010
NFFT134	05.05.2021	GIM	S1	1010
NFFT135	05.05.2021	GUM	S1	1010
NFFT136	05.05.2021	SKM	S1	794
NFFT137	05.05.2021	GIM	S1	794
NFFT138	05.05.2021	GUM	S1	794
NFFT139	05.05.2021	SKM	S1	796
NFFT140	05.05.2021	GIM	S1	796

NFFT141	05.05.2021	GUM	S1	796
NFFT142	05.05.2021	SKM	S1	708
NFFT143	05.05.2021	GIM	S1	708
NFFT144	05.05.2021	GUM	S1	708
NFFT145	11.06.2021	SW	-	-
NFFT146	11.06.2021	SW	-	-
NFFT147	11.06.2021	SW	-	-
NFFT148	11.06.2021	BB	16	-
NFFT149	11.06.2021	BB	16	-
NFFT150	11.06.2021	BB	16	-
NFFT151	11.06.2021	TW	16	-
NFFT152	11.06.2021	TW	16	-
NFFT153	11.06.2021	TW	16	-
NFFT154	11.06.2021	TB	16	-
NFFT155	11.06.2021	TB	16	-
NFFT156	11.06.2021	TB	16	-
NFFT157	11.06.2021	SKM	16	129
NFFT158	11.06.2021	GIM	16	129
NFFT159	11.06.2021	GUM	16	129
NFFT160	11.06.2021	SKM	16	125
NFFT161	11.06.2021	GIM	16	125
NFFT162	11.06.2021	GUM	16	125
NFFT163	11.06.2021	SKM	16	83
NFFT164	11.06.2021	GIM	16	83
NFFT165	11.06.2021	GUM	16	83
NFFT166	11.06.2021	SKM	16	81
NFFT167	11.06.2021	GIM	16	81
NFFT168	11.06.2021	GUM	16	81
NFFT169	11.06.2021	SKM	16	102
NFFT170	11.06.2021	GIM	16	102
NFFT171	11.06.2021	GUM	16	102
NFFT172	11.06.2021	BB	17	-
NFFT173	11.06.2021	BB	17	-
NFFT174	11.06.2021	BB	17	-
NFFT175	11.06.2021	TW	17	-
NFFT176	11.06.2021	TW	17	-

NFFT177	11.06.2021	TW	17	-
NFFT178	11.06.2021	TB	17	-
NFFT179	11.06.2021	TB	17	-
NFFT180	11.06.2021	TB	17	-
NFFT181	11.06.2021	SKM	17	286
NFFT182	11.06.2021	GIM	17	286
NFFT183	11.06.2021	GUM	17	286
NFFT184	11.06.2021	SKM	17	322
NFFT185	11.06.2021	GIM	17	322
NFFT186	11.06.2021	GUM	17	322
NFFT187	11.06.2021	SKM	17	317
NFFT188	11.06.2021	GIM	17	317
NFFT189	11.06.2021	GUM	17	317
NFFT190	11.06.2021	SKM	17	218
NFFT191	11.06.2021	GIM	17	218
NFFT192	11.06.2021	GUM	17	218
NFFT193	11.06.2021	SKM	17	342
NFFT194	11.06.2021	GIM	17	342
NFFT195	11.06.2021	GUM	17	342
NFFT196	11.06.2021	TW	S1	-
NFFT197	11.06.2021	TW	S1	-
NFFT198	11.06.2021	TW	S1	-
NFFT199	11.06.2021	TB	S1	-
NFFT200	11.06.2021	TB	S1	-
NFFT201	11.06.2021	TB	S1	-
NFFT202	11.06.2021	SKM	S1	434
NFFT203	11.06.2021	GIM	S1	434
NFFT204	11.06.2021	GUM	S1	434
NFFT205	11.06.2021	SKM	S1	606
NFFT206	11.06.2021	GIM	S1	606
NFFT207	11.06.2021	GUM	S1	606
NFFT208	11.06.2021	SKM	S1	690
NFFT209	11.06.2021	GIM	S1	690
NFFT210	11.06.2021	GUM	S1	690
NFFT211	11.06.2021	SKM	S1	628
NFFT212	11.06.2021	GIM	S1	628

NFFT213	11.06.2021	GUM	S1	628
NFFT214	11.06.2021	SKM	S1	816
NFFT215	11.06.2021	GIM	S1	816
NFFT216	11.06.2021	GUM	S1	816
NFFT217	09.07.2021	SW	-	-
NFFT218	09.07.2021	SW	-	-
NFFT219	09.07.2021	SW	-	-
NFFT220	09.07.2021	BB	16	-
NFFT221	09.07.2021	BB	16	-
NFFT222	09.07.2021	BB	16	-
NFFT223	09.07.2021	TW	16	-
NFFT224	09.07.2021	TW	16	-
NFFT225	09.07.2021	TW	16	-
NFFT226	09.07.2021	TB	16	-
NFFT227	09.07.2021	TB	16	-
NFFT228	09.07.2021	TB	16	-
NFFT229	09.07.2021	SKM	16	90
NFFT230	09.07.2021	GIM	16	90
NFFT231	09.07.2021	GUM	16	90
NFFT232	09.07.2021	SKM	16	100
NFFT233	09.07.2021	GIM	16	100
NFFT234	09.07.2021	GUM	16	100
NFFT235	09.07.2021	SKM	16	120
NFFT236	09.07.2021	GIM	16	120
NFFT237	09.07.2021	GUM	16	120
NFFT238	09.07.2021	SKM	16	100
NFFT239	09.07.2021	GIM	16	100
NFFT240	09.07.2021	GUM	16	100
NFFT241	09.07.2021	SKM	16	90
NFFT242	09.07.2021	GIM	16	90
NFFT243	09.07.2021	GUM	16	90
NFFT244	09.07.2021	BB	17	-
NFFT245	09.07.2021	BB	17	-
NFFT246	09.07.2021	BB	17	-
NFFT247	09.07.2021	TW	17	-
NFFT248	09.07.2021	TW	17	-

NFFT249	09.07.2021	TW	17	-
NFFT250	09.07.2021	TB	17	-
NFFT251	09.07.2021	TB	17	-
NFFT252	09.07.2021	TB	17	-
NFFT253	09.07.2021	SKM	17	185
NFFT254	09.07.2021	GIM	17	185
NFFT255	09.07.2021	GUM	17	185
NFFT256	09.07.2021	SKM	17	140
NFFT257	09.07.2021	GIM	17	140
NFFT258	09.07.2021	GUM	17	140
NFFT259	09.07.2021	SKM	17	85
NFFT260	09.07.2021	GIM	17	85
NFFT261	09.07.2021	GUM	17	85
NFFT262	09.07.2021	SKM	17	300
NFFT263	09.07.2021	GIM	17	300
NFFT264	09.07.2021	GUM	17	300
NFFT265	09.07.2021	SKM	17	210
NFFT266	09.07.2021	GIM	17	210
NFFT267	09.07.2021	GUM	17	210
NFFT268	09.07.2021	TW	S1	-
NFFT269	09.07.2021	TW	S1	-
NFFT270	09.07.2021	TW	S1	-
NFFT271	09.07.2021	TB	S1	-
NFFT272	09.07.2021	TB	S1	-
NFFT273	09.07.2021	TB	S1	-
NFFT274	09.07.2021	SKM	S1	430
NFFT275	09.07.2021	GIM	S1	430
NFFT276	09.07.2021	GUM	S1	430
NFFT277	09.07.2021	SKM	S1	485
NFFT278	09.07.2021	GIM	S1	485
NFFT279	09.07.2021	GUM	S1	485
NFFT280	09.07.2021	SKM	S1	595
NFFT281	09.07.2021	GIM	S1	595
NFFT282	09.07.2021	GUM	S1	595
NFFT283	09.07.2021	SKM	S1	545
NFFT284	09.07.2021	GIM	S1	545

NFFT285	09.07.2021	GUM	S1	545
NFFT286	09.07.2021	SKM	S1	930
NFFT287	09.07.2021	GIM	S1	930
NFFT288	09.07.2021	GUM	S1	930
NFFT289	09.08.2021	SW	-	-
NFFT290	09.08.2021	SW	-	-
NFFT291	09.08.2021	SW	-	-
NFFT292	09.08.2021	BB	16	-
NFFT293	09.08.2021	BB	16	-
NFFT294	09.08.2021	BB	16	-
NFFT295	09.08.2021	TW	16	-
NFFT296	09.08.2021	TW	16	-
NFFT297	09.08.2021	TW	16	-
NFFT298	09.08.2021	TB	16	-
NFFT299	09.08.2021	TB	16	-
NFFT300	09.08.2021	TB	16	-
NFFT301	09.08.2021	SKM	16	159
NFFT302	09.08.2021	GIM	16	159
NFFT303	09.08.2021	GUM	16	159
NFFT304	09.08.2021	SKM	16	100
NFFT305	09.08.2021	GIM	16	100
NFFT306	09.08.2021	GUM	16	100
NFFT307	09.08.2021	SKM	16	118
NFFT308	09.08.2021	GIM	16	118
NFFT309	09.08.2021	GUM	16	118
NFFT310	09.08.2021	SKM	16	37
NFFT311	09.08.2021	GIM	16	37
NFFT312	09.08.2021	GUM	16	37
NFFT313	09.08.2021	SKM	16	94
NFFT314	09.08.2021	GIM	16	94
NFFT315	09.08.2021	GUM	16	94
NFFT316	09.08.2021	BB	17	-
NFFT317	09.08.2021	BB	17	-
NFFT318	09.08.2021	BB	17	-
NFFT319	09.08.2021	TW	17	-
NFFT320	09.08.2021	TW	17	-

NFFT321	09.08.2021	TW	17	-
NFFT322	09.08.2021	TB	17	-
NFFT323	09.08.2021	TB	17	-
NFFT324	09.08.2021	TB	17	-
NFFT325	09.08.2021	SKM	17	179
NFFT326	09.08.2021	GIM	17	179
NFFT327	09.08.2021	GUM	17	179
NFFT328	09.08.2021	SKM	17	59
NFFT329	09.08.2021	GIM	17	59
NFFT330	09.08.2021	GUM	17	59
NFFT331	09.08.2021	SKM	17	210
NFFT332	09.08.2021	GIM	17	210
NFFT333	09.08.2021	GUM	17	210
NFFT334	09.08.2021	SKM	17	103
NFFT335	09.08.2021	GIM	17	103
NFFT336	09.08.2021	GUM	17	103
NFFT337	09.08.2021	SKM	17	219
NFFT338	09.08.2021	GIM	17	219
NFFT339	09.08.2021	GUM	17	219
NFFT340	09.08.2021	TW	S1	-
NFFT341	09.08.2021	TW	S1	-
NFFT342	09.08.2021	TW	S1	-
NFFT343	09.08.2021	TB	S1	-
NFFT344	09.08.2021	TB	S1	-
NFFT345	09.08.2021	TB	S1	-
NFFT346	09.08.2021	SKM	S1	613
NFFT347	09.08.2021	GIM	S1	613
NFFT348	09.08.2021	GUM	S1	613
NFFT349	09.08.2021	SKM	S1	672
NFFT350	09.08.2021	GIM	S1	672
NFFT351	09.08.2021	GUM	S1	672
NFFT352	09.08.2021	SKM	S1	736
NFFT353	09.08.2021	GIM	S1	736
NFFT354	09.08.2021	GUM	S1	736
NFFT355	09.08.2021	SKM	S1	599
NFFT356	09.08.2021	GIM	S1	599

NFFT357	09.08.2021	GUM	S1	599
NFFT358	09.08.2021	SKM	S1	513
NFFT359	09.08.2021	GIM	S1	513
NFFT360	09.08.2021	GUM	S1	513
NFFT361	13.09.2021	SW	-	-
NFFT362	13.09.2021	SW	-	-
NFFT363	13.09.2021	SW	-	-
NFFT364	13.09.2021	BB	16	-
NFFT365	13.09.2021	BB	16	-
NFFT366	13.09.2021	BB	16	-
NFFT367	13.09.2021	TW	16	-
NFFT368	13.09.2021	TW	16	-
NFFT369	13.09.2021	TW	16	-
NFFT370	13.09.2021	TB	16	-
NFFT371	13.09.2021	TB	16	-
NFFT372	13.09.2021	TB	16	-
NFFT373	13.09.2021	SKM	16	133
NFFT374	13.09.2021	GIM	16	133
NFFT375	13.09.2021	GUM	16	133
NFFT376	13.09.2021	SKM	16	162
NFFT377	13.09.2021	GIM	16	162
NFFT378	13.09.2021	GUM	16	162
NFFT379	13.09.2021	SKM	16	189
NFFT380	13.09.2021	GIM	16	189
NFFT381	13.09.2021	GUM	16	189
NFFT382	13.09.2021	SKM	16	89
NFFT383	13.09.2021	GIM	16	89
NFFT384	13.09.2021	GUM	16	89
NFFT385	13.09.2021	SKM	16	50
NFFT386	13.09.2021	GIM	16	50
NFFT387	13.09.2021	GUM	16	50
NFFT388	13.09.2021	BB	17	-
NFFT389	13.09.2021	BB	17	-
NFFT390	13.09.2021	BB	17	-
NFFT391	13.09.2021	TW	17	-
NFFT392	13.09.2021	TW	17	-

NFFT393	13.09.2021	TW	17	-
NFFT394	13.09.2021	TB	17	-
NFFT395	13.09.2021	TB	17	-
NFFT396	13.09.2021	TB	17	-
NFFT397	13.09.2021	SKM	17	220
NFFT398	13.09.2021	GIM	17	220
NFFT399	13.09.2021	GUM	17	220
NFFT400	13.09.2021	SKM	17	137
NFFT401	13.09.2021	GIM	17	137
NFFT402	13.09.2021	GUM	17	137
NFFT403	13.09.2021	SKM	17	232
NFFT404	13.09.2021	GIM	17	232
NFFT405	13.09.2021	GUM	17	232
NFFT406	13.09.2021	SKM	17	323
NFFT407	13.09.2021	GIM	17	323
NFFT408	13.09.2021	GUM	17	323
NFFT409	13.09.2021	SKM	17	349
NFFT410	13.09.2021	GIM	17	349
NFFT411	13.09.2021	GUM	17	349
NFFT412	13.09.2021	TW	S1	-
NFFT413	13.09.2021	TW	S1	-
NFFT414	13.09.2021	TW	S1	-
NFFT415	13.09.2021	TB	S1	-
NFFT416	13.09.2021	TB	S1	-
NFFT417	13.09.2021	TB	S1	-
NFFT418	13.09.2021	SKM	S1	603
NFFT419	13.09.2021	GIM	S1	603
NFFT420	13.09.2021	GUM	S1	603
NFFT421	13.09.2021	SKM	S1	609
NFFT422	13.09.2021	GIM	S1	609
NFFT423	13.09.2021	GUM	S1	609
NFFT424	13.09.2021	SKM	S1	490
NFFT425	13.09.2021	GIM	S1	490
NFFT426	13.09.2021	GUM	S1	490
NFFT427	13.09.2021	SKM	S1	658
NFFT428	13.09.2021	GIM	S1	658

NFFT429	13.09.2021	GUM	S1	658
NFFT430	13.09.2021	SKM	S1	424
NFFT431	13.09.2021	GIM	S1	424
NFFT432	13.09.2021	GUM	S1	424

Appendix D: DNA Isolation Protocol and Content

Content of ZymoBIOMICS™ 96 MagBead DNA Kit.

ZymoBIOMICS™ 96 MagBead DNA Kit (Kit Size)	**D4302** (2x 96 preps.)	**D4306** (2x 96 preps.)	**D4308** (2x 96 preps.)	**Storage Temperature**
ZymoBIOMICS™ Lysis Solution	150 ml	-	150 ml	Room Temp.
DNA/RNA Shield	50 ml x 3	-	50 ml x 3	Room Temp.
ZymoBIOMICS™ MagBinding Buffer	250 ml	250 ml	250 ml	Room Temp.
ZymoBIOMICS™ MagWash 1	100 ml x 2	100 ml x 2	100 ml x 2	Room Temp.
ZymoBIOMICS™ MagWash 2	200 ml x 3	200 ml x 3	200 ml x 3	Room Temp.
ZymoBIOMICS™ DNase/RNase Free Water	50 ml	50 ml	50 ml	Room Temp.
ZymoBIOMICS™ MagBinding Beads	12 ml	12 ml	12 ml	Room Temp.
ZR BashingBead™ Lysis Rack (0.1 & 0.5 mm)	2	-	-	Room Temp.
ZR BashingBead™ Lysis Tubes (0.1 & 0.5 mm)	-	-	200	Room Temp.
Instruction Manual	1	1	1	-

For automated scripts and **Technical Assistance** regarding generation of scripts for automated platforms, contact **Zymo Research's Technical Department** at 1-888-882-9682 or E-mail to techi@zymoresearch.com.

[1]For water samples, filter using desired filter (not provided). Cut the filter into small pieces and place into ZR BashingBead™ Lysis Tubes (0.1 & 0.5 mm).

[2]Swabs can also be cut or broken and placed directly in bead beating tube. For more information on processing swab samples, see Appendix B.

[3] See Appendix A for additional information on sample collection in DNA/RNA Shield™.

[4] For validated bead beating devices and conditions, refer to the Optimized Lysis Protocols on the website product page under Documents.

[5] For optimal lysis efficiency and unbiased profiling all bead beater devices beyond those validated by Zymo Research should be calibrated using the ZymoBIOMICS™ Microbial Community Standard. See Appendix C.

Protocol

Sample Lysis

For all mixing steps: pipette mix or shake at max speed.

Note: Shaking speed will depend on sample volume and plate well depth. Use of shaker plates will require user optimization.

1. Add sample to the **ZR BashingBead™ Module** using the table below.
   a. If using **ZR BashingBead™ Lysis Tubes (0.1 & 0.5 mm)**, add 750 µl ***ZymoBIOMICS Lysis Solution.***
   b. If using **ZR BashingBead™ Lysis Rack (0.1 & 0.5 mm)**, add 650 µl ***ZymoBIOMICS Lysis Solution.***

   Note: DNA/RNA Shield *has been provided to optionally replace* ***ZymoBIOMICS Lysis Solution*** *to improve DNA integrity.*

Sample Type	Maximum Input
Feces	100 mg
Soil	200 mg
Liquid Samples[1] and Swab Collections[2]	250 µl
Cells (Suspended in DNA/RNA Shield™ or isotonic buffer, *e.g.* PBS)	5-20 mg (wet weight) (2×10^8 bacterial or 2×10^7 yeast cells)
Samples in DNA/RNA Shield™ (10% v/v Sample)[3]	250 µl

2. Secure in a bead beater fitted with the appropriate holder assembly for your bead beating module and process using optimized bead beating conditions (speed and time) for your device[4,5].
3. Centrifuge the ZR BashingBead™ Lysis Module:
   a. If using **ZR BashingBead™ Lysis Tubes (0.1 & 0.5 mm),** centrifuge at ≥10,000 x g for 1 minute.
   b. If using **ZR BashingBead™ Lysis Rack (0.1 & 0.5 mm),** centrifuge at ≥4,000 x g for 5 minutes.

Sample Purification

4. Transfer 200 µl supernatant to the deep-well block (not provided). Add 600 µl **ZymoBIOMICS™ MagBinding Buffer.**

   Note: *For samples with excessive amounts of solid particulate, centrifuge at 4,000 x g for 5 minutes to reduce clogging.*

5. Dispense 25 µl of **ZymoBIOMICS™ MagBinding Beads** to each well. Mix well by pipette or shaker plate for 10 minutes.

   Note: *ZymoBIOMICS MagBinding Beads settle quickly, ensure that beads are kept in suspension while dispensing.*

Sample Purification (Continued)

6. Transfer the 96-well block to a magnetic stand until beads pellet, then aspirate and discard the supernatant. Remove the 96-Well Block from the magnetic stand.
7. Dispense 500 µl of **ZymoBIOMICS™ MagBinding Buffer** and mix well by pipette or shaker plate for 1 minute.
8. Transfer the 96-well block to a magnetic stand until beads pellet, then aspirate and discard the supernatant. Remove the 96-Well Block from the magnetic stand.
9. Dispense 500 µl of **ZymoBIOMICS™ MagWash 1** and mix well by pipette or shaker plate for 1 minute.
10. Transfer the 96-well block to a magnetic stand until beads pellet, then aspirate and discard the supernatant. Remove the 96-Well Block from the magnetic stand.
11. Dispense 900 µl **ZymoBIOMICS™ MagWash 2** and mix well by pipette or shaker plate for 1 minute.

    Note: *If high speed shaker plates are used, dispense 500 µl ZymoBIOMICS™ MagWash 2.*
12. Transfer the deep-well block to a magnetic stand until beads pellet, then aspirate and discard the supernatant. Remove the 96-Well Block from the magnetic stand.
13. Repeat the wash (Steps 11-12) twice.
14. Transfer the 96-Well Block onto a heating element (55°C) until beads dry (approximately 10 minutes). If no heating element is available, air dry for approximately 20-30 minutes.
15. Dispense 50 µl of **ZymoBIOMICS™ DNase/RNase Free Water** to each well and re-suspend beads. Mix the beads well for 10 minutes and then transfer the plate onto the magnetic stand for 2-3 minutes until the beads pellet[6].
16. Transfer the supernatant (containing the eluted DNA) to a clean elution plate or tube[7].

    The eluted DNA can be used immediately for molecular based applications or stored ≤ -20°C for future use.

[6] See Appendix D for additional elution information.

[7] For optimal spectrophotometric quantification, eluate may be centrifuged at max speed to pellet magbeads.

Appendix E: NanoDrop and Qubit measurements

Table E-1: Sample ID, NanoDrop 1000 concentration, and DNA purity ratios, as well as total DNA concentration measured with Qubit.

		NanoDrop			Qubit
Sample-ID	**Sample Type**	**DNA Concentration**	**260/280**	**260/230**	**DNA concentration**
NFFT001	SW	1.3	1.92	1.03	0.0025
NFFT002	SW	2	1.54	0.82	0.028
NFFT003	SW	1.8	0.98	0.89	0.026
NFFT004	BB	11.5	1.94	1.95	12.1
NFFT005	BB	13	2.19	2.25	13.8
NFFT006	BB	13.4	1.84	2.1	14.5
NFFT007	TW	4.6	2	1.21	3.86
NFFT008	TW	4.4	1.7	1.4	3.87
NFFT009	TW	8.7	1.96	1.1	4.36
NFFT010	TB	40.3	1.98	2.32	55
NFFT011	TB	20.2	1.74	2.36	21.9
NFFT012	TB	46.8	1.8	1.61	47
NFFT013	SKM	5.8	1.82	1.71	4.6
NFFT014	GIM	40.3	1.99	2.47	59
NFFT015	GUM	39.2	1.82	2.36	51
NFFT016	SKM	3.4	9	3.27	2.34
NFFT017	GIM	43.8	1.99	2.45	58
NFFT018	GUM	18.3	1.86	2.29	18.4
NFFT019	SKM	4.1	1.22	1.37	2.52
NFFT020	GIM	25.8	1.76	2.08	25.1
NFFT021	GUM	21.8	1.63	1.72	17.5
NFFT022	SKM	3.3	0.99	0.96	1.6
NFFT023	GIM	21.9	1.71	1.9	20.2
NFFT024	GUM	26.4	1.59	1.52	16.3
NFFT025	SKM	3.4	1.09	1.05	1.06
NFFT026	GIM	30.9	1.71	1.59	22.7
NFFT027	GUM	52.6	1.77	1.99	51

NFFT028	TW	5.4	1.83	2.14	4.76
NFFT029	TW	8.5	2.29	0.97	5.6
NFFT030	TW	12	1.67	1.05	5.02
NFFT031	TB	39.8	1.83	1.78	36.4
NFFT032	TB	22.9	1.66	1.9	20.1
NFFT033	TB	17.9	1.64	1.95	16.4
NFFT034	SKM	6	1.44	1.16	3.4
NFFT035	GIM	39.5	1.71	1.76	33.6
NFFT036	GUM	18.7	1.7	1.91	16.5
NFFT037	SKM	10	1.51	1.4	6.75
NFFT038	GIM	31.1	1.62	1.98	24.3
NFFT039	GUM	27.9	1.75	1.94	26
NFFT040	SKM	8	1.27	1.48	6.07
NFFT041	GIM	62.9	1.85	1.95	61
NFFT042	GUM	9	1.47	1.02	3.74
NFFT043	SKM	11.7	1.35	1.39	8.33
NFFT044	GIM	89.6	1.83	2.32	41
NFFT045	GUM	8.8	1.41	1.25	4.42
NFFT046	SKM	9.6	2.04	1.9	7.4
NFFT047	GIM	32.4	1.8	2.39	28.6
NFFT048	GUM	21.4	1.68	2.13	22.4
NFFT049	TW	10.4	1.62	1.19	6.34
NFFT050	TW	6.7	1.62	1.64	6
NFFT051	TW	7.4	2.08	1.72	6.2
NFFT052	TB	21.4	1.83	2.24	26
NFFT053	TB	21.3	2.01	2.28	20.7
NFFT054	TB	27.2	1.85	1.74	21.8
NFFT055	SKM	10.6	1.71	1.92	12
NFFT056	GIM	63.6	1.83	2.19	61.2
NFFT057	GUM	47.4	1.83	2.19	42.7
NFFT058	SKM	9.9	1.49	1.3	4.36
NFFT059	GIM	44.1	1.91	2.43	43.9
NFFT060	GUM	26.9	1.74	2.21	24.4
NFFT061	SKM	17.4	2.09	2.18	13.8
NFFT062	GIM	22.3	1.8	2.43	19.3
NFFT063	GUM	23.3	1.9	2.28	19.4

NFFT064	SKM	6.4	1.87	2.08	58.2
NFFT065	GIM	34.9	1.75	1.9	29
NFFT066	GUM	12.4	1.83	1.96	9.37
NFFT067	SKM	23.9	1.71	1.98	18.3
NFFT068	GIM	43.7	1.87	2.3	39.3
NFFT069	GUM	12	1.91	1.97	7.58
NFFT070	BB	40.7	1.88	2.23	34.3
NFFT071	BB	46.1	1.82	1.77	33
NFFT072	BB	10	1.5	1.7	6.01
NFFT073	SW	3.1	0.94	0.69	0.035
NFFT074	SW	7.2	1.82	0.77	0.032
NFFT075	SW	3.3	0.89	0.66	0.038
NFFT076	BB	22.3	1.81	2.03	22.6
NFFT077	BB	27.5	1.74	1.6	23.5
NFFT078	BB	13.9	1.79	2.13	13.5
NFFT079	TW	14	2.07	1.87	11.4
NFFT080	TW	11.8	2.11	1.84	11.2
NFFT081	TW	14.9	1.62	1.3	9.98
NFFT082	TB	24	1.68	1.76	20.5
NFFT083	TB	14.4	1.95	1.86	13.8
NFFT084	TB	31.5	1.85	1.93	34.4
NFFT085	SKM	7.5	1.36	1.61	6.28
NFFT086	GIM	23.1	1.78	1.83	21.1
NFFT087	GUM	66.1	1.83	2.04	31.3
NFFT088	SKM	12.6	1.66	1.98	11.5
NFFT089	GIM	30.1	1.86	2.3	33.2
NFFT090	GUM	93.1	1.85	2.31	51
NFFT091	SKM	3.2	3.98	1.01	0.636
NFFT092	GIM	20	2	1.88	17.8
NFFT093	GUM	321.5	1.91	2.28	53
NFFT094	SKM	3.8	2.11	0.79	0.572
NFFT095	GIM	5.9	2.2	1.23	2.18
NFFT096	GUM	315.2	1.89	2.27	56
NFFT097	SKM	3.8	3.82	1.17	0.952
NFFT098	GIM	7.6	2.2	1.5	4.12
NFFT099	GUM	141.4	1.91	2.21	33.7

NFFT100	BB	35.8	1.96	1.98	30.8
NFFT101	BB	21.9	1.95	2.17	18.5
NFFT102	BB	19	1.75	0.89	12.9
NFFT103	TW	7.7	1.42	1.19	4.76
NFFT104	TW	9.5	1.32	1.07	4.29
NFFT105	TW	6.6	1.52	1.47	4.16
NFFT106	TB	23.3	2.05	1.87	19.7
NFFT107	TB	47.4	1.92	1.67	40.2
NFFT108	TB	23.8	2.08	1.88	18.4
NFFT109	SKM	9.7	2.36	1.01	3.29
NFFT110	GIM	43.1	2.01	2.05	40.7
NFFT111	GUM	317.9	1.89	2.16	51
NFFT112	SKM	8	2.18	1.37	4.69
NFFT113	GIM	23.3	1.96	1.42	14.4
NFFT114	GUM	186.3	1.94	2.27	42.8
NFFT115	SKM	9.7	2.33	1.17	3.79
NFFT116	GIM	46.8	1.95	2.1	43.8
NFFT117	GUM	267.9	1.91	2.32	48.7
NFFT118	SKM	12	1.92	1.54	9.13
NFFT119	GIM	66.3	1.89	1.75	93
NFFT120	GUM	513.7	1.88	2.13	55
NFFT121	SKM	20.6	2	1.28	13.9
NFFT122	GIM	95.4	1.87	2.13	56
NFFT123	GUM	438.5	1.88	2.26	59.4
NFFT124	TW	15.9	1.58	1.52	12.1
NFFT125	TW	27.1	1.89	2.02	27.3
NFFT126	TW	20.1	1.87	1.99	20.9
NFFT127	TB	32.7	1.93	1.49	25.7
NFFT128	TB	33.2	1.92	1.66	31.5
NFFT129	TB	36.3	2.03	1.87	35.4
NFFT130	SKM	9.6	2.16	1.21	4.36
NFFT131	GIM	46	1.82	1.95	45.2
NFFT132	GUM	526.8	1.83	1.82	50.6
NFFT133	SKM	18.1	1.99	1.26	11.9
NFFT134	GIM	74.9	1.89	1.72	34.6
NFFT135	GUM	847.6	1.94	1.92	65.2

NFFT136	SKM	15.7	2.4	1.01	4.95
NFFT137	GIM	62.3	1.93	2.01	60.2
NFFT138	GUM	582.4	1.82	2.12	65
NFFT139	SKM	15	1.99	1.33	7.87
NFFT140	GIM	38.1	2.04	1.58	34.1
NFFT141	GUM	347.6	1.91	2.11	59
NFFT142	SKM	9.6	2.14	1.07	3.21
NFFT143	GIM	57.7	1.93	2.01	57.4
NFFT144	GUM	574.3	1.84	2.17	81.8
NFFT145	SW	11.5	1.33	0.93	0.037
NFFT146	SW	10.5	1.45	0.85	0.037
NFFT147	SW	9.5	1.42	0.9	0.036
NFFT148	BB	26.7	1.73	1.58	20.6
NFFT149	BB	31.3	1.82	1.43	22.8
NFFT150	BB	20.6	1.68	1.33	11.7
NFFT151	TW	20.1	1.69	1.17	9.13
NFFT152	TW	22.5	1.63	1.24	13.1
NFFT153	TW	17.6	1.58	1.06	5.58
NFFT154	TB	48.4	1.86	1.78	46.8
NFFT155	TB	39.1	1.78	1.68	32.2
NFFT156	TB	62	1.85	1.96	60.6
NFFT157	SKM	14.8	1.8	1.37	7.54
NFFT158	GIM	58	1.8	1.77	54.8
NFFT159	GUM	711.2	1.88	2.18	59.4
NFFT160	SKM	13	1.42	1.21	5.77
NFFT161	GIM	55	1.89	2.04	57.6
NFFT162	GUM	312.7	1.87	2.24	57
NFFT163	SKM	14.3	1.57	1.02	5.42
NFFT164	GIM	60.4	1.84	1.93	61.6
NFFT165	GUM	192.3	1.9	2.19	36
NFFT166	SKM	21.4	1.77	1.24	8.95
NFFT167	GIM	55.5	1.87	1.9	57
NFFT168	GUM	282.7	1.89	2.17	65.6
NFFT169	SKM	17.6	1.72	1.25	8.5
NFFT170	GIM	47.6	1.78	1.86	45
NFFT171	GUM	748.3	1.89	2.15	73

NFFT172	BB	82.7	1.86	1.92	10.9
NFFT173	BB	40.9	1.69	1.39	24.8
NFFT174	BB	36.6	1.69	1.39	24.8
NFFT175	TW	15.8	1.56	1.02	4.32
NFFT176	TW	20	1.45	0.98	4.78
NFFT177	TW	17.2	1.56	1.14	5.16
NFFT178	TB	25.3	1.85	1.34	16
NFFT179	TB	37.1	1.81	1.48	27.8
NFFT180	TB	42.5	1.78	1.59	34.6
NFFT181	SKM	22.1	1.76	1.47	14
NFFT182	GIM	51.2	1.79	1.84	50.8
NFFT183	GUM	225.4	1.87	2.02	21.7
NFFT184	SKM	26.1	1.77	1.58	11.9
NFFT185	GIM	40.5	1.79	1.82	39.6
NFFT186	GUM	960.8	1.86	205	57.6
NFFT187	SKM	50.1	1.7	1.62	15.9
NFFT188	GIM	61.3	1.88	1.95	67.4
NFFT189	GUM	1059	1.87	2.09	57.2
NFFT190	SKM	23	1.83	1.41	17.4
NFFT191	GIM	74.5	1.89	1.88	36.3
NFFT192	GUM	1210.1	1.92	2.25	57.4
NFFT193	SKM	20.6	1.65	1.25	13.5
NFFT194	GIM	72.2	1.84	2.02	34.2
NFFT195	GUM	551.2	1.81	2.05	48.2
NFFT196	TW	14.1	1.56	0.93	1.35
NFFT197	TW	13.2	1.44	0.93	1.69
NFFT198	TW	14.4	1.49	1.03	3.22
NFFT199	TB	31.5	1.89	1.35	20.6
NFFT200	TB	41.7	1.87	1.31	29.8
NFFT201	TB	38	1.82	1.36	28.9
NFFT202	SKM	24.8	1.76	1.44	15.7
NFFT203	GIM	56.6	1.85	1.93	61.2
NFFT204	GUM	969.5	1.88	2.16	56.2
NFFT205	SKM	30	1.58	1.3	19.9
NFFT206	GIM	82.8	1.82	1.85	41.8
NFFT207	GUM	479.4	1.87	2.12	55.6

NFFT208	SKM	28.7	1.71	1.35	20.2
NFFT209	GIM	90.5	1.86	2.05	47.6
NFFT210	GUM	1002.2	1.92	1.99	72.6
NFFT211	SKM	30.1	1.8	1.46	22.7
NFFT212	GIM	94.2	1.88	1.98	48
NFFT213	GUM	317	1.89	2.11	42.5
NFFT214	SKM	27.1	1.78	1.38	18.2
NFFT215	GIM	96.8	1.9	2.08	63.8
NFFT216	GUM	936.2	1.89	1.98	53.8
NFFT217	SW	13.9	1.58	0.81	0.039
NFFT218	SW	15.8	1.83	0.85	0.028
NFFT219	SW	14.4	1.38	0.78	0.034
NFFT220	BB	30.8	1.64	1.16	16.1
NFFT221	BB	32.4	1.7	1.17	15.5
NFFT222	BB	25.2	1.64	1.02	8.28
NFFT223	TW	18	1.49	0.84	1.51
NFFT224	TW	16.2	1.53	0.82	1.13
NFFT225	TW	20.7	1.68	0.79	1.34
NFFT226	TB	34.6	1.8	1.18	17.6
NFFT227	TB	43.7	1.78	1.29	29.4
NFFT228	TB	39.7	1.76	1.19	23.8
NFFT229	SKM	24.3	1.63	1.13	11.8
NFFT230	GIM	69.8	1.8	1.88	68
NFFT231	GUM	251.5	1.86	2.1	67
NFFT232	SKM	30.3	1.55	1.32	14.8
NFFT233	GIM	37.7	1.84	1.67	33.8
NFFT234	GUM	543.6	1.85	2.16	36.8
NFFT235	SKM	23	1.78	1.13	10.5
NFFT236	GIM	52.4	1.75	1.59	42
NFFT237	GUM	434.3	1.85	2.11	51.8
NFFT238	SKM	35.2	1.79	1.29	10.4
NFFT239	GIM	52.5	1.8	1.57	45
NFFT240	GUM	335.2	1.88	2.12	40.4
NFFT241	SKM	26.8	1.68	1.04	13.1
NFFT242	GIM	70.1	1.9	1.81	30
NFFT243	GUM	198.4	1.88	2.14	28.1

NFFT244	BB	27.9	1.76	1.11	14.1
NFFT245	BB	32.8	1.72	1.24	20.6
NFFT246	BB	30.6	1.83	1.19	16.4
NFFT247	TW	17.9	1.5	0.88	1.85
NFFT248	TW	17.9	1.56	0.75	1.22
NFFT249	TW	18.6	1.57	0.83	1.39
NFFT250	TB	44.5	1.72	0.93	27.8
NFFT251	TB	49.5	1.84	0.37	37.4
NFFT252	TB	43	1.77	1.13	28.8
NFFT253	SKM	25	1.88	1.38	18.1
NFFT254	GIM	58.8	1.82	1.73	56
NFFT255	GUM	161.9	1.86	2.02	64.8
NFFT256	SKM	33.2	1.71	1.38	23.7
NFFT257	GIM	75.1	1.88	1.62	30
NFFT258	GUM	184.6	1.89	2.03	34
NFFT259	SKM	21.2	1.69	1.01	8.29
NFFT260	GIM	85.9	1.84	1.81	40.4
NFFT261	GUM	142.6	1.86	2	47.6
NFFT262	SKM	15.5	1.74	0.98	4.22
NFFT263	GIM	60.6	1.81	1.62	53
NFFT264	GUM	497.3	1.86	2.1	51.6
NFFT265	SKM	23.8	1.85	1.12	11.2
NFFT266	GIM	41.2	1.85	1.56	31.4
NFFT267	GUM	392.7	1.88	2.08	37.9
NFFT268	TW	20.2	1.58	0.82	1.38
NFFT269	TW	18.5	1.46	0.83	1.69
NFFT270	TW	19	1.46	0.84	1.95
NFFT271	TB	40.4	1.75	1.25	21.4
NFFT272	TB	33.8	1.79	1.15	16.6
NFFT273	TB	36.2	1.71	1.2	17.5
NFFT274	SKM	24.5	1.75	1.13	9.62
NFFT275	GIM	43.2	1.75	1.51	32
NFFT276	GUM	988.6	1.88	2.25	54
NFFT277	SKM	39.3	1.82	1.43	6.8
NFFT278	GIM	54.8	1.83	1.63	41.8
NFFT279	GUM	176.9	1.91	2.16	39.4

NFFT280	SKM	19.4	1.51	0.86	2.44
NFFT281	GIM	36.7	1.87	1.39	27.3
NFFT282	GUM	281.2	1.87	1.98	36.3
NFFT283	SKM	20.3	1.76	0.95	2.72
NFFT284	GIM	42.4	1.72	1.34	24.4
NFFT285	GUM	234	1.88	2.11	22.4
NFFT286	SKM	30.3	1.74	1.27	15.6
NFFT287	GIM	58.3	1.79	1.57	48.6
NFFT288	GUM	35	1.87	2.14	32
NFFT289	SW	9.5	2.04	0.68	0.037
NFFT290	SW	12.1	2.01	0.67	0.042
NFFT291	SW	9.4	2.5	0.63	0.041
NFFT292	BB	43.8	1.86	1.24	27.4
NFFT293	BB	72.7	1.85	1.37	27.7
NFFT294	BB	45	1.86	1.19	25.8
NFFT295	TW	28.1	1.69	0.78	2.37
NFFT296	TW	21.6	1.72	0.8	2.29
NFFT297	TW	35.9	1.75	0.8	2.48
NFFT298	TB	62.5	1.76	1.28	40.2
NFFT299	TB	44	1.85	1.19	25.2
NFFT300	TB	49.2	1.87	1.27	35.2
NFFT301	SKM	20.6	1.88	0.89	5.35
NFFT302	GIM	51.5	1.78	1.34	41.2
NFFT303	GUM	731.8	1.88	2.02	48.4
NFFT304	SKM	27.9	1.75	0.93	7
NFFT305	GIM	51.9	1.8	1.3	37
NFFT306	GUM	272.3	1.85	1.92	31.8
NFFT307	SKM	26.7	1.76	0.93	6.7
NFFT308	GIM	57	1.83	1.37	534
NFFT309	GUM	105.1	1.85	1.59	25.8
NFFT310	SKM	29.1	1.74	1	1.63
NFFT311	GIM	62.8	1.8	1.46	25.5
NFFT312	GUM	72.5	1.85	1.45	29.1
NFFT313	SKM	25.5	1.67	0.9	4.4
NFFT314	GIM	89.1	1.87	1.67	39.6
NFFT315	GUM	90.6	1.84	1.56	41

NFFT316	BB	32.6	1.71	1.03	12.6
NFFT317	BB	33.9	1.67	1.05	13.8
NFFT318	BB	30.5	1.72	0.99	11.5
NFFT319	TW	19.8	1.73	0.82	4.57
NFFT320	TW	16.6	2.24	0.9	4.36
NFFT321	TW	16.2	2.06	0.85	4.32
NFFT322	TB	54.8	1.76	1.24	35.8
NFFT323	TB	38.1	1.64	1.01	13.2
NFFT324	TB	34.2	1.83	1.06	16
NFFT325	SKM	36.7	1.71	1.18	19.7
NFFT326	GIM	72.2	1.8	1.6	30
NFFT327	GUM	407.7	1.89	2.11	40.6
NFFT328	SKM	33.2	1.67	1.14	18
NFFT329	GIM	45	1.76	1.3	29
NFFT330	GUM	76.7	1.8	1.61	22.5
NFFT331	SKM	26.3	1.71	1.13	12.5
NFFT332	GIM	52.6	1.73	1.32	41.4
NFFT333	GUM	688	1.87	2.06	42.6
NFFT334	SKM	33.2	1.64	1.06	16.1
NFFT335	GIM	73.9	1.74	1.47	29.5
NFFT336	GUM	204.2	1.83	1.85	17.7
NFFT337	SKM	34.9	1.81	1.15	21.2
NFFT338	GIM	53.1	1.77	1.33	38.2
NFFT339	GUM	311.6	1.88	1.99	31.9
NFFT340	TW	12.5	2.14	0.81	1.64
NFFT341	TW	13.7	1.98	0.77	2.09
NFFT342	TW	16.3	1.85	0.78	2.12
NFFT343	TB	43.7	1.73	1.16	25
NFFT344	TB	35.8	1.68	1.04	14.7
NFFT345	TB	39.3	1.73	1.04	19.4
NFFT346	SKM	27.1	1.56	0.91	6.79
NFFT347	GIM	70.9	1.79	1.5	26.5
NFFT348	GUM	485.1	1.84	2.12	61
NFFT349	SKM	36.6	1.67	0.96	10.3
NFFT350	GIM	62.6	1.76	1.52	50.8
NFFT351	GUM	384.3	1.85	1.89	32.5

NFFT352	SKM	41.8	1.68	1.18	17.6
NFFT353	GIM	90.3	1.81	1.79	29.8
NFFT354	GUM	581.4	1.81	2.05	58.2
NFFT355	SKM	45.1	1.7	1.13	17.4
NFFT356	GIM	76.8	1.81	1.52	26.1
NFFT357	GUM	840.5	1.89	2.1	48
NFFT358	SKM	34.1	1.58	1.03	12.3
NFFT359	GIM	100.3	1.82	1.74	34.8
NFFT360	GUM	543.1	1.79	1.91	50.8
NFFT361	SW	21.5	1.52	0.73	0.05
NFFT362	SW	19.6	1.46	0.73	0.045
NFFT363	SW	18.3	1.48	0.75	0.035
NFFT364	BB	39.8	1.75	1.01	15.4
NFFT365	BB	25.8	1.68	0.89	4.96
NFFT366	BB	28.2	1.72	0.91	5.47
NFFT367	TW	34	1.7	0.78	5.07
NFFT368	TW	40.1	1.53	0.83	6.82
NFFT369	TW	37.9	1.55	0.79	4.59
NFFT370	TB	48.9	1.79	1.26	31.8
NFFT371	TB	70	1.84	1.51	28
NFFT372	TB	50.7	1.78	1.16	30
NFFT373	SKM	20.7	1.76	0.83	1.5
NFFT374	GIM	56.1	1.84	1.44	47.2
NFFT375	GUM	368.9	1.88	1.99	38.3
NFFT376	SKM	29.9	1.66	1.07	9.09
NFFT377	GIM	80.2	1.71	1.16	28.4
NFFT378	GUM	301.8	1.82	1.84	28.6
NFFT379	SKM	34.5	1.63	1.07	16.4
NFFT380	GIM	57	1.77	1.4	50.4
NFFT381	GUM	394.3	1.83	1.95	45
NFFT382	SKM	45	1.73	1.25	7.12
NFFT383	GIM	68.9	1.8	1.53	27.8
NFFT384	GUM	382.6	1.82	1.95	45
NFFT385	SKM	25.2	1.68	0.89	4.26
NFFT386	GIM	64	1.83	1.5	27.4
NFFT387	GUM	185.4	1.86	1.83	18.1

NFFT388	BB	37.8	1.73	1.21	21.4
NFFT389	BB	40.9	1.74	1.18	25
NFFT390	BB	38.8	1.79	1.18	23.4
NFFT391	TW	31.8	1.52	0.81	3.79
NFFT392	TW	33.7	1.53	0.87	8.21
NFFT393	TW	32.8	1.57	0.82	5.15
NFFT394	TB	37.1	1.98	1.01	13.8
NFFT395	TB	36.8	1.67	1.05	14.6
NFFT396	TB	56	1.78	1.29	23.6
NFFT397	SKM	32.4	1.65	1.06	12
NFFT398	GIM	66.6	1.77	1.23	19.6
NFFT399	GUM	842.3	1.9	2.05	41.4
NFFT400	SKM	60.7	1.74	1.45	12.4
NFFT401	GIM	53.7	1.81	1.39	41.4
NFFT402	GUM	869	1.9	2.04	43
NFFT403	SKM	33.4	2.02	1.37	18.7
NFFT404	GIM	88.4	1.9	1.85	39.6
NFFT405	GUM	385.7	1.87	1.91	41.4
NFFT406	SKM	33.3	1.8	0.94	7.53
NFFT407	GIM	81.4	1.88	1.61	31
NFFT408	GUM	374.6	1.88	2	44.2
NFFT409	SKM	39.8	1.81	1.18	22.5
NFFT410	GIM	100.5	1.87	1.86	41
NFFT411	GUM	232.5	1.88	2.12	29.5
NFFT412	TW	21.8	1.63	0.74	1.02
NFFT413	TW	25.6	1.59	0.71	1.61
NFFT414	TW	30.4	1.64	0.8	2.38
NFFT415	TB	41.5	1.77	1.05	15.8
NFFT416	TB	42.7	1.73	1.02	15.8
NFFT417	TB	36.7	1.88	1.03	12.4
NFFT418	SKM	24.1	1.73	1.02	7
NFFT419	GIM	93.9	1.91	1.83	40.8
NFFT420	GUM	1289.2	1.87	2.07	52.6
NFFT421	SKM	36.3	1.75	1.07	15.3
NFFT422	GIM	122.6	1.86	1.83	38.6
NFFT423	GUM	567.8	1.88	1.92	72

NFFT424	SKM	40.5	1.69	1.15	17.8
NFFT425	GIM	67	1.77	1.55	27.2
NFFT426	GUM	443	1.82	2.07	44.8
NFFT427	SKM	40	1.86	1.48	31.8
NFFT428	GIM	80.6	1.88	1.75	35.6
NFFT429	GUM	898.7	1.88	2.17	50.2
NFFT430	SKM	29.6	1.61	0.96	9.04
NFFT431	GIM	73.5	1.8	1.6	30.5
NFFT432	GUM	1349.8	1.88	2.18	61

Appendix F: Qubit 1X dsDNA HS Assay Kit

Material	Amount		Concentration	Storage*
	Q33230 (100 assays)	Q33231 (500 assays)		
Qubit™ 1X dsDNA HS Working Solution (Component A)	50 mL	250 mL	1X	• 2–8°C • Protect from light
Qubit™ 1X dsDNA HS Standard #1 (Component B)	1 mL	5 mL	0 ng/µL in TE buffer	• 2–8°C
Qubit™ 1X dsDNA HS Standard #2 (Component C)	1 mL	5 mL	10 ng/µL in TE buffer	
* When stored as directed, the kits are stable for at least 6 months from the date of receipt.				

Appendix G: Qubit Flex Fluorometer Protocol

Prepare standards and samples

This protocol assumes that you are preparing standards for calibrating the Qubit™ Fluorometer. If you plan to use the last calibration performed on the instrument (see "Qubit™ Fluorometer calibration", page 2), you need fewer tubes (step 1.1) and less working solution (step 1.3).

1.1 Set up the required number of assay tubes (or tube strips) for standards and samples. The Qubit™ 1X dsDNA HS Assay requires 2 standards.

Note: Use thin-wall, clear, 0.5-mL PCR tubes (Cat. No. Q32856) for the Qubit™ 4 Fluorometer and 8 × 200 µL tube strips (Cat. No. Q33252) for the Qubit™ Flex Fluorometer.

1.2 Label the tube lids.

Note: Do not label the side of the tube as this could interfere with the sample read. Label the lid of each standard tube correctly. Calibration of the Qubit™ Fluorometer requires the standards to be inserted into the instrument in the right order.

1.3 Add 10 µL of each Qubit™ standard to the appropriate tube.

1.4 Add 1–20 µL of each user sample to the appropriate tube.

Note: If you are adding 1–2 µL of sample, use a P-2 pipette for best results.

1.5 Add the Qubit™ 1X dsDNA working solution to each tube such that the final volume is 200 µL.

Note: The final volume in each tube must be 200 µL. Each standard tube requires 190 µL of Qubit™ working solution, and each sample tube requires anywhere from 180–199 µL. Ensure that you have sufficient Qubit™ working solution to accommodate all standards and samples.

Note: To avoid any cross-contamination, we recommend that you remove the total amount of working solution required for your samples and standards from the working solution bottle and then add the required volume to the appropriate tubes instead of pipetting directly from the bottle to each tube.

1.6 Mix each sample vigorously by vortexing for 3–5 seconds.

1.7 Allow all tubes to incubate at room temperature for 2 minutes, then proceed to "Read standards and samples". Follow the procedure appropriate for your instrument:

Read standards and samples

Qubit™ Flex Fluorometer

2.1 On the **Home** screen of the Qubit™ Flex Fluorometer, press the **1X dsDNA High Sensitivity (HS)** assay icon. The "Read standards" screen is displayed. Press **Read Standards & run samples** to proceed.

Note: If you have already performed a calibration for the selected assay, the instrument prompts you to choose between reading new standards and running samples using the previous calibration. If you want to use the previous calibration, press **Run samples** and skip to step 2.4. Otherwise, continue with step 2.2.

2.2 Insert the tube strip containing Standard #1 into the sample chamber, close the lid, then press **Run standards**. When the reading is complete (~3 seconds), remove Standard #1.

2.3 Insert the tube strip containing Standard #2 into the sample chamber, close the lid, then press **Read standards**. When the reading is complete, remove Standard #2.

The instrument displays the graphical results on the **Standards complete** screen. For information on interpreting the calibration results, refer to the *Qubit™ Flex Fluorometer User Guide*, available for download at **thermofisher.com/qubit**.

2.4 Press **Next** from the **Standards complete** screen. When prompted, load the tubes as shown in the **Insert samples** screen. If you have fewer than 8 samples, press to deselect the tube positions that do not contain a sample. Select the units for the output sample concentration, then select **Next**.

Note: *(Optional)* Select **More Options** to add the assay kit lot number, Tags, or sample IDs. For information on using these options, refer to the *Qubit™ Flex Fluorometer User Guide*.

2.5 In the **Sample volume** screen, enter the sample volume added to the assay tube (from 1-20 µL). Enter the volume directly in the sample volume text box, use the + or – buttons or adjust the sample volume wheel to select the sample volume added to the assay tube.

Note: The sample volume used (1-20 µL) changes the assay accuracy range. A different sample volume or assay may be required if the sample concentration is outside of what the assay can accurately quantify.

2.6 Insert a sample tube strip into the sample chamber, close the lid, then press **Run samples**. When the reading is complete (~3 seconds), remove the sample tube.

Standards and samples are displayed on a graph with the results in a list below. Select the graph icon only to view the results list. The value listed is the concentration of the original sample. For more information on interpreting the sample results, refer to the *Qubit™ Flex Fluorometer User Guide*.

2.7 Select **Add samples** to read more samples and repeat step 2.6.

Note: *(Optional)* Select **Calculators** to access the Molarity and Normalization calculators. For information on the calculators, refer to the *Qubit™ Flex Fluorometer User Guide*.

Appendix H: QIIME2 Workflow

Importing MiSeq demultiplexed pair-end reads into qiime artefacts:

```
qiime tools import --type 'SampleData[PairedEndSequencesWithQuality]' --input-path filenames-NFFT.txt --output-path 2_demux-paired-end.qza --input-format PairedEndFastqManifestPhred33
```

Summarize to view the output:

```
qiime demux summarize --i-data 2_demux-paired-end.qza --o-visualization 2_demux-paired-end.qzv
```

Quality check and trimming (DADA2 step):

```
qiime dada2 denoise-paired --i-demultiplexed-seqs 2_demux-paired-end.qza --p-trim-left-f 20 --p-trunc-len-f 287 --p-trim-left-r 20 --p-trunc-len-r 215 --o-representative-sequences 3_rep-seqs.qza --o-table 3_table.qza --p-n-threads 6 --output-dir dada2
```

Align sequences and create phylogenetic tree:

```
qiime phylogeny align-to-tree-mafft-fasttree \
  --i-sequences 3_rep-seqs.qza \
  --o-alignment 4_aligned-rep-seqs.qza \
  --o-masked-alignment 5_masked-aligned-rep-seqs.qza \
  --o-tree 6_unrooted-tree.qza \
  --o-rooted-tree 7_rooted-tree.qza
```

Assigning taxonomy to the reads:

```
qiime feature-classifier classify-sklearn --i-classifier /home/storage/QIIME2_taxonomic-classifier/silva-138-pro341_806-classifier.qza --i-reads 3_rep-seqs.qza --o-classification 9_taxonomy.qza
```

Appendix I: PCoA Plot of Environment Samples

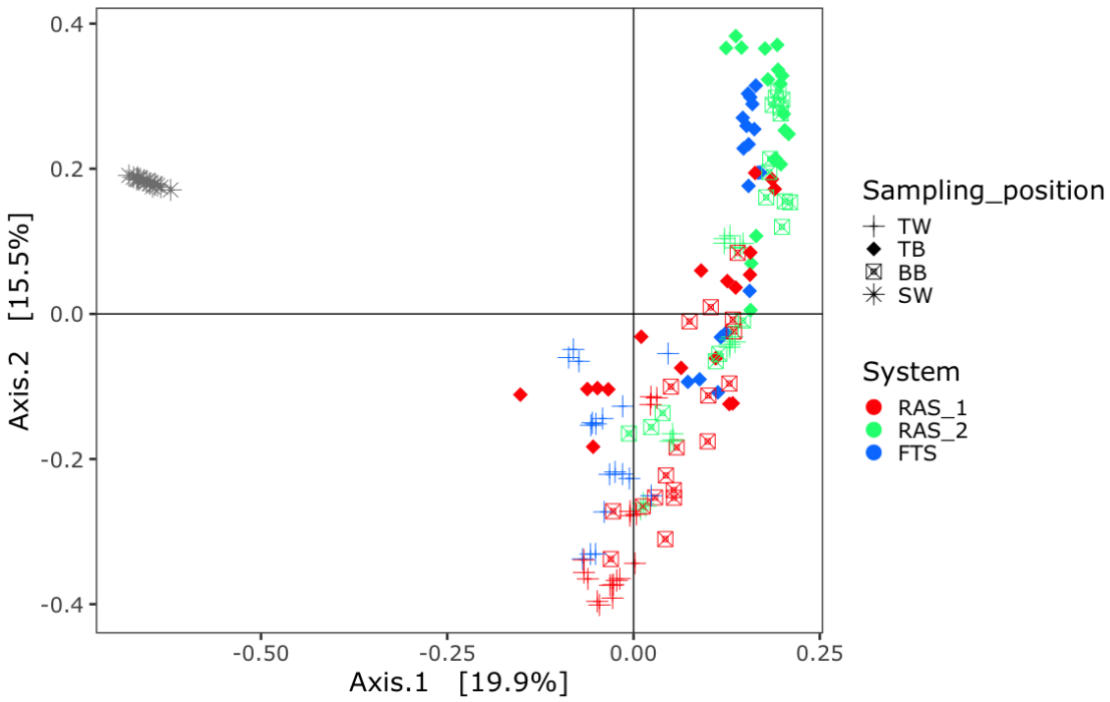

Figure I-1: PCoA plot based on Bray-Curtis dissimilarities on ASV level for comparison of the microbial communities present in the environment samples (TW = tank water, TB = tank biofilm, BB = biofilter biofilm and SW = source water) from the three different systems (RAS_1, RAS_2 and FTS) over a period of 6 months.

Appendix J: Temporal PCoA Plot of Environment Samples

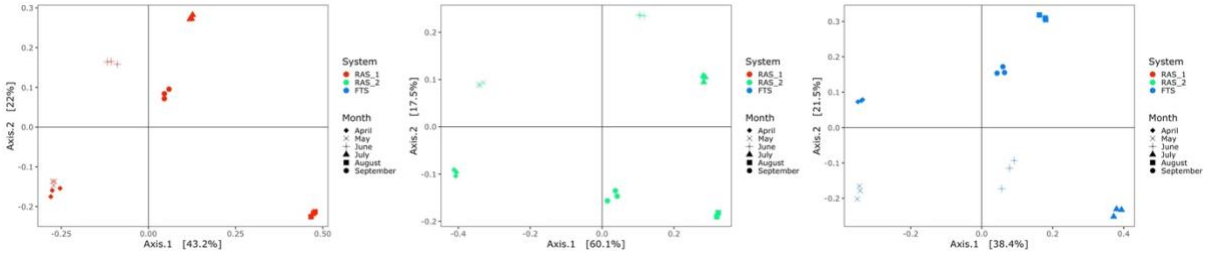

Figure J-1: PCoA plots based on Bray Curtis dissimilarities for investigation of temporal differences in microbial composition in tank water samples from production system RAS_1 (A), RAS_2 (B) and FTS (C).

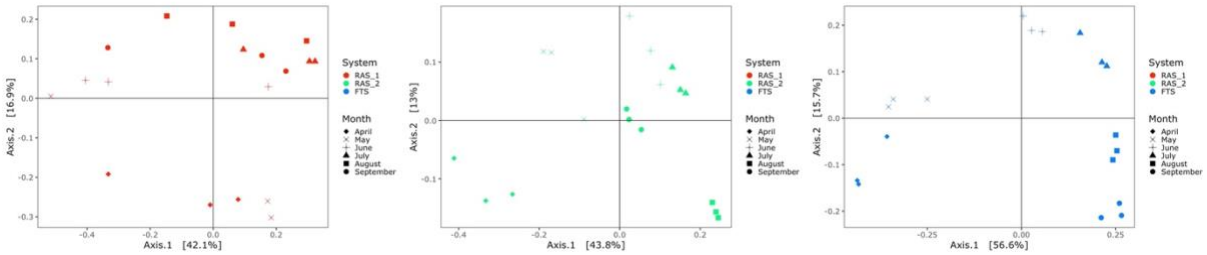

Figure J-2: PCoA plots based on Bray Curtis dissimilarities for investigation of temporal differences in microbial composition in tank biofilm samples from production system RAS_1 (A), RAS_2 (B) and FTS (C).

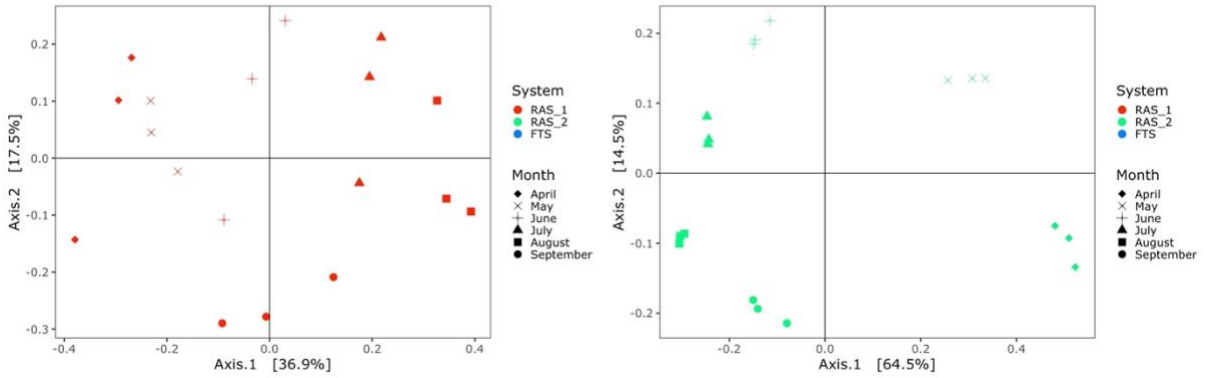

Figure J-3: PCoA plots based on Bray Curtis dissimilarities for investigation of temporal differences in microbial composition in biofilter biofilm samples from production system RAS_1 (A) and RAS_2 (B). The FTS did not have a biofilter in connection to it and is therefore not present.

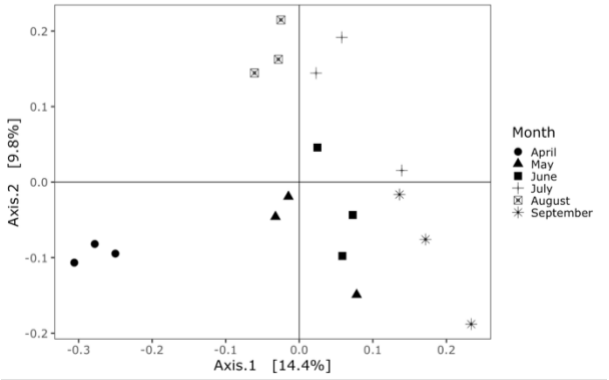

Figure J-4: PCoA plot based on Bray Curtis dissimilarities for investigation of temporal differences in microbial composition in source water samples.

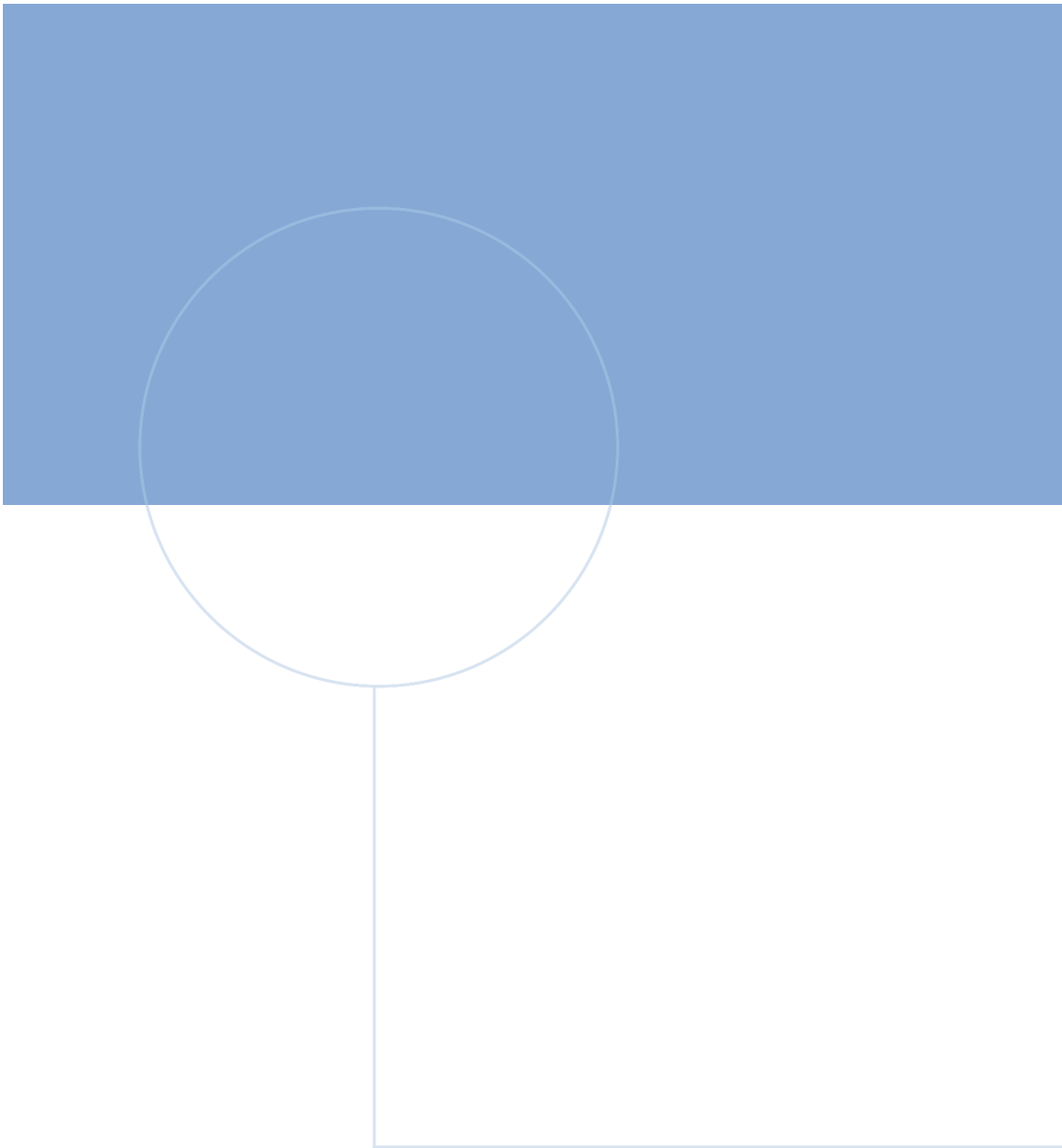

NTNU
Norwegian University of
Science and Technology

SINTEF